

The Colour of Tropical Woods Influenced by Brown Rot

Zuzana Vidholdová * and Ladislav Reinprecht

Technical University in Zvolen, Faculty of Wood Sciences and Technology, T. G. Masaryka 24, Zvolen, SK 96001, Slovakia; reinprecht@tuzvo.sk

* Correspondence: zuzana.vidholdova@tuzvo.sk; Tel.: +421-45-520-6389

Received: 26 February 2019; Accepted: 2 April 2019; Published: 10 April 2019

Abstract: Interesting aesthetic properties of tropical woods, like surface texture and colour, are rarely impaired due to weathering, rotting and other degradation processes. This study analyses the colour of 21 tropical woods before and after six weeks of intentional attack by the brown-rot fungus *Coniophora puteana*. The CIEL*a*b* colour system was applied for measuring the lightness, redness and yellowness, and from these parameters the hue tone angle and colour saturation were calculated. Lighter tropical woods tended to appear a less red and a more yellow, and had a greater hue tone angle. However, for the original woods was not found dependence between the lightness and colour saturation. Tropical woods at attack by *C. puteana* lost a weight from 0.08% to 6.48%. The lightest and moderately light species—like okoumé, iroko, ovengol and sapelli—significantly darkened, while the darkest species—wengé and ipé—significantly lightened. The majority of tropical woods obtained a brighter shade of yellow, typically wengé, okoumé and blue gum, while some of them also a brighter shade of green, typically sapelli, padouk and macaranduba. *C. puteana* specifically affected the hue tone angle and colour saturation of tested tropical woods, but without an apparent changing the tendency of these colour parameters to lightness. The total colour difference of tested tropical woods significantly increased in connection with changes of their lightness ($\Delta E_{ab}^* = 5.92 - 0.50 \cdot \Delta L^*$; $R^2 = 0.37$), but it was not influenced by the red and yellow tint changes, and weight losses.

Keywords: tropical woods; brown rot; *Coniophora puteana*; colour; CIEL*a*b* system

1. Introduction

The surface appearance of wood is often evaluated by examining its texture, roughness, and colour [1–3]. The colour of an individual wood species is predetermined by the type and amount of extractives, by the surface roughness and moisture, and by the direction of light irradiation [4].

The CIE 1976 L*a*b* colour system classifies the temperate and tropical wood species into the positive octant with the lightness (L^*) from 20 to 90, the redness index ($+a^*$) from 0 to 20, and the yellowness index ($+b^*$) from 10 to 30 [1,5]. The CIE 1976 L*a*b* colour system also allows visualisation of the cylindrical parameters of wood, the colour saturation—chromaticity (C_{ab}^*) and the hue tone angle (h_{ab}) [6]. The tropical wood species occupy a much greater portion of the colour space in comparison with temperate (for example European) species [7,8].

Within a defined wood species, the colour variations can be influenced by more factors, mainly by its chemical and anatomical structure [9] and specific genetic parameters [10], and also by environmental conditions at growth [11,12], atmospheric effects at exposure in exteriors or interiors [13,14], and biodeterioration processes [15–17].

Wooden products having a higher moisture content—usually above 20%–30%—are no rarely damaged by biodeterioration processes in presence of wood decaying fungi, staining fungi, moulds, or bacteria.

Generally, brown-rot fungi cause firstly yellowing and gradually browning of woods in a connection with decomposition of whiter hemicelluloses and cellulose, while darker lignin is less evidently damaged [18,19]. Wood extractives, which give to different wood species a characteristic colour, are specifically resistant to individual species of brown-rot fungi [20–22]. Therefore, the accidental or deliberate exposures of wood products to brown-rot fungi can lead to typical changes in their colour and aesthetic parameters.

The rotting of damp wooden products is common not only outdoors, but also inside of buildings. In interiors, the rotting of wood is first of all caused by brown-rot fungi [23–25]. The genus *Coniophora* comprises about 20 species frequently occurring in buildings. Gabriel and Švec [26] listed the species abundance of seven indoor wood decay basidiomycetes reported in Europe, when the brown-rot fungi *Serpula lacrymans* and *Coniophora puteana* (*C. puteana*) were most frequent. *C. puteana* causes—already in the early period of wood attack—a disruption of linkages between hemicelluloses and lignin, decomposition of polysaccharides, while lignin is oxidative modified and partly damaged [27]. Rot of wood with *C. puteana* is not usually homogenous and its specific parts can be more damaged [15].

In the literature, it is also noted that wood-inhabiting fungi are able add colour to wood due to a pigment residues left by fungi in wood (called as spalting) [17,28–34]. Spalting occurs in growing tree in form of zone lines formation or pigmentation. Also bleaching is marked as kinds of wood spalting [17,29,31]. Bleaching is caused by the breakdown of coloured lignin from the wood cell wall, generally by fungi classified as white-rotting, which results in a lightening of the natural wood colour and structural integrity of the wood. A lightening in colour can also be due to a build-up of white mycelium [18,20,35]. Wood with zone lines (thin and winding lines of dark melanin) are formed due to inter- or intra- fungal antagonism for example a pairing of the white-rot fungi *Trametes versicolor*/*Bjerkadera adusta* or by solitary isolates of *Xylaria polymorpha* ascomycete that causes soft rot [31]. Also, the brown-rot fungus *Fistulina hepatica* stains oaks and some other woods from light gold, yellow brown to reddish brown shades [36,37]. Pigment-type spalting fungi are a select group of soft-rotting ascomycetes with extracellular pigments production into wood, for example fungi from genera *Chlorocibolia*, *Ceratocystis*, *Ophiostoma*, *Scytalidium* and others [32,33]. Pigment penetration into wood depends on moisture content, the digestive capabilities of the fungus, the permeability of the wood structure, differences between heartwood and sapwood, and the type of pigment produced [29]. Mold fungi, such as *Trichoderma* spp., are not considered to be spalting fungi, as their hyphae do not colonize the wood internally and they do not produce the enzymes necessary to digest the wood cell wall components.

From several tropical woods are manufactured various products for interiors, for example, furniture, flooring, stairs, windows, doors, claddings or structural elements—using usually massive, glued timbers, veneers or plywood [38]. For more of these products, both strength and aesthetic are important. The interesting aesthetic and specific colours of the individual tropical wood species, existing in the natural state as well as in the primarily fungal-pigmented state, can be changed or even worsened at additional rotting processes. In interiors, the degree and range of rotting is influenced mainly by: (1) the natural durability of wood to decaying fungi (e.g., [39] classifies woods into five classes of durability), and (2) the enough moisture of wood above 20%, depending on presence of condensed, capillary, plumbing or rain water.

The aim of this study was to determine the colour changes of 21 tropical woods when exposed to the brown-rot fungus *C. puteana*, which can cause an important deterioration of wood products in the interiors of buildings.

2. Materials and Methods

2.1. Woods and Specimens

Twenty-one tropical woods, in a form of naturally dried and conditioned boards with a moisture content of $13 \pm 2.5\%$, was bought from the trading company JAF Holz, Ltd., Slovakia (Table 1).

Table 1. Tropical wood species used in the experiment.

Family	Species Common Name ¹⁾	Species	Density at MC 12% (kg·m ^{−3})	
		Scientific Name	“Literature” [40]	“Experiment”
Bignoniaceae	Ipé	<i>Handroanthus serratifolius</i> (Vahl) S.O.Grose ³⁾ ⁴⁾	960–1100	968 (26)
Burseraceae	Okoumé	<i>Aucoumea klaineana</i> Pierre ²⁾	370–560	566 (27)
Cunoniaceae	Tineo	<i>Weinmannia trichosperma</i> Cav.	570–650	646 (31)
Dipterocarpaceae	Dark red meranti	<i>Shorea curtisii</i> Dyer ex King ²⁾	590–890	592 (10)
	Yellow balau ⁵⁾	<i>Shorea laevis</i> Ridl. ²⁾	900–1100	925 (55)
Ebenaceae	Macassar ebony	<i>Diospyros celebica</i> Bakh. ²⁾	1100–1200	1 013 (82)
Fabaceae	Doussié	<i>Afzelia bipindensis</i> Harms ²⁾	750–950	889 (18)
	Cerejeira	<i>Amburana cearensis</i> A. C. Sm. ²⁾	550–650	651 (10)
	Bubinga	<i>Guibourtia demeusei</i> J. Léonard	830–950	830 (13)
	Ovengol	<i>Guibourtia elie</i> J. Léonard ²⁾	700–910	755 (27)
	Merbau	<i>Intsia bijuga</i> O. Ktze. ²⁾	830–900	837 (50)
	Santos	<i>Machaerium scleroxylon</i> Tul. ²⁾	900–1000	904 (6)
	rosewood	<i>Microberlinia brazzavillensis</i> Chev. ²⁾	700–850	718 (23)
	Zebrano	<i>Millettia laurentii</i> De Wild. ²⁾	810–950	823 (37)
	Wengé	<i>Pterocarpus soyauxii</i> Taub.	650–850	647 (37)
	Padouk	<i>Entandrophragma cylindricum</i> Sprague ²⁾	510–750	631 (38)
Meliaceae	Sapelli	<i>Milicia excelsa</i> C. C. Berg ²⁾	550–850	551 (16)
Moraceae	Iroko	<i>Eucalyptus diversicolor</i> F. Muell.	800–870	804 (30)
Myrtaceae	Karri	<i>Eucalyptus globulus</i> Labill.	720–770	760 (59)
Sapotaceae	Maçaranduba ⁶⁾	<i>Manilkara bidentata</i> A. Chev.	900–1000	916 (19)
	Makoré	<i>Tieghemella heckelii</i> Pierre ²⁾	530–720	570 (25)

Notes: ¹⁾ by Association Technique Internationale des Bois Tropicaux (ATIBT) in France; ²⁾ registered in The IUCN Red List of Threatened Species™ [41]; ³⁾ name by EN 350 [39]; ⁴⁾ previous name by [40] was *Tabebuia serratifolia*; ⁵⁾ its other name is Bangkirai; ⁶⁾ its other name is Massaranduba; Mean values of experimental densities are from 16 specimens (4 of those were used in this experiment) and standard deviations are in italic and parentheses.

From the heart-zone of each wood species were prepared and tested four specimens 25 mm × 25 mm × 3 mm (longitudinal × radial × tangential)—without biological damage, knots or other defects. Before the fungal attack, the top surfaces of specimens were sanded along fibres using 240-grit sandpaper. Subsequently, the specimens were conditioned on a moisture content of 12 ± 1%, weighted with an accuracy of 0.001 g, sterilized with 30 W germicidal lamp (Chirana, Slovakia) at a temperature of 22 ± 2 °C per 20 min for each side, and finally their top surfaces submitted in sterilized room to colour analyses (point 2.3).

After fungal attack (point 2.2), the specimens were carefully cleaned from surface fungal mycelia, slowly dried in a laboratory, conditioned on a moisture content of 12 ± 1%, weighted with an accuracy of 0.001 g, the top surfaces sanded along fibres with 240-grit sandpaper, and finally the top surfaces again submitted to colour analyses (point 2.3).

At sanding of the top surfaces of tested specimens, performed before and after fungal attack, in both cases the thickness of specimens declined about approximately 10 micrometers.

2.2. Fungal Attack of Woods

The specimens of tropical woods were exposed to the brown-rot fungus *Coniophora puteana* (Schumacher ex Freist) Karsten, strain BAM Ebw. 15 (Bundesanstalt für Materialforschung und—prüfung, Berlin) in glass Petri dishes with a diameter of 100 mm. Two replicates of the same wood species were placed into one dish on plastic mats under which a fungal mycelium was already grown on an autoclave sterilized and solidified 3–4 mm thick layer of 4.5 wt.% malt agar medium (HiMedia, Ltd., India). Fungal attacks lasted 6 weeks at a temperature of 24 ± 2 °C and a relative humidity of $90 \pm 5\%$.

The weight loss Δm (%) of specimens was calculated from their weights in conditioned state before and after fungal attack. This method may have caused some inaccuracies in Δm (due to sorption hysteresis and differential water sorption by healthy and rotten woods), but it was preferred to the method evaluating specimens in absolute dry state when colour change could be manifested at drying temperature of 103 °C.

2.3. Colour Analyses of Woods

The colour analyses were performed for each specimen before and after fungal attack on the sanded top surfaces (point 2.1) in the same four places (Figure 1). The colour measurements were performed with the Color Reader CR-10 (Konica Minolta, Japan), having a CIE 10° standard observer, CIE standard illuminate D65, sensor head with a diameter of 8 mm (i.e., the measuring area was 50 mm²), and a detector with 6 silicon photocells.

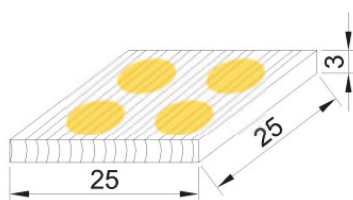


Figure 1. The same four places on the top surface of specimen in which colour measurements were performed in its original and fungal-attacked state.

The colourimetric parameters of each specimen were analysed according to the CIE 1976 $L^*a^*b^*$ colour system. A larger value of L^* , a^* , or b^* means a lighter, redder, or yellower colour, respectively.

Based on the L^* , a^* , and b^* colour coordinates, following the colour saturation—chromacity C_{ab}^* and the hue tone angle h_{ab} were calculated according to the [42] by Equations (1) and (2):

$$C_{ab}^* = \sqrt{a^{*2} + b^{*2}}, \quad (1)$$

$$h_{ab} = \tan^{-1}(b^*/a^*), \quad (2)$$

From the relative colour changes ΔL^* , Δa^* , and Δb^* , namely differences between colour coordinates of the fungal-attacked and the original wood specimens, the total colour difference ΔE_{ab}^* was calculated by Equation (3) [42]:

$$\Delta E_{ab}^* = \sqrt{\Delta L^{*2} + \Delta a^{*2} + \Delta b^{*2}}, \quad (3)$$

Selected colourimetric parameters of tropical woods determined in the original state (a^* , b^* , C_{ab}^* , h_{ab}), as well as in the fungal-attacked state (a_F^* , b_F^* , C_{abF}^* , h_{abF}), were finally analysed in relation to their lightness (L^* or L_F^*) by linear correlations using Equation (4):

$$\text{Colourimetric parameter} = A + B \cdot L^*, \quad (4)$$

Equation (4) was used as well as for searching relations between the ΔE^*_{ab} and the relative colour changes ΔL^* , Δa^* , Δb^* , and the weight loss Δm , respectively.

Conversion of average value of the colourimetric coordinates L^* , a^* and b^* of the fungal-attacked and the original wood specimens was generated their colour (Pantone) swatch.

The t -test statistically analysed the colour changes of individual tropical woods due to the brown-rot fungus *C. puteana*.

3. Results and Discussion

3.1. Colour of Original Tropical Woods

Table 2 documents colour characteristics of 21 tropical woods in the original state—a visualisation (colour and surface structure), and the colourimetric parameters L^* , a^* , b^* , C^*_{ab} and h_{ab} .

Table 2. Visualisations and colorimetric parameters of 21 tropical woods.



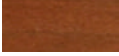








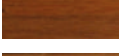








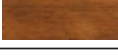
Wood Species	Visual	Lightness L^*	Redness $+a^*$	Yellowness $+b^*$	Colour Saturation C^*_{ab}	Hue Tone Angle h_{ab}
Ipé		42.59 (0.79)	8.87 (0.55)	16.46 (1.01)	18.70 (2.59)	61.66 (1.22)
Okoumé		75.36 (1.13)	5.61 (0.61)	16.89 (0.57)	17.81 (0.65)	71.66 (1.69)
Tineo		47.69 (4.98)	14.56 (1.81)	16.23 (0.99)	21.83 (1.77)	48.26 (2.83)
Darkred meranti		62.03 (1.52)	11.76 (0.81)	16.35 (0.64)	20.15 (0.87)	54.30 (1.56)
Yellow balau		54.59 (0.92)	13.22 (0.83)	21.92 (0.88)	25.60 (1.12)	58.93 (1.02)
Macassar ebony		59.40 (0.80)	13.86 (0.68)	21.29 (0.81)	25.41 (0.91)	56.93 (1.23)
Doussié		60.57 (6.61)	10.28 (1.89)	25.42 (2.09)	27.50 (1.81)	67.93 (4.80)
Cerejeira		49.93 (3.34)	10.85 (1.52)	18.19 (1.34)	21.22 (1.59)	59.24 (3.46)
Bubinga		46.81 (1.23)	17.50 (0.89)	16.98 (1.17)	24.40 (1.20)	44.11 (2.00)
Ovengol		53.56 (4.65)	8.08 (1.07)	19.63 (4.38)	21.27 (4.33)	67.36 (2.69)
Merbau		46.92 (1.57)	15.43 (0.53)	18.97 (1.12)	24.46 (1.09)	50.83 (1.37)
Santos rosewood		50.79 (3.39)	14.68 (1.31)	22.49 (3.13)	26.88 (3.23)	56.63 (2.44)
Zebrano		55.85 (4.91)	10.09 (1.06)	19.18 (1.49)	21.68 (1.63)	62.24 (2.18)
Wengé		34.88 (1.68)	7.89 (0.64)	10.33 (1.30)	13.02 (1.24)	52.42 (3.38)

Table 2. Cont.

Wood Species	Visual	Lightness L^*	Redness $+a^*$	Yellowness $+b^*$	Colour Saturation C^*_{ab}	Hue Tone Angle h_{ab}
Padouk		43.78 (2.05)	31.42 (1.61)	26.72 (2.02)	41.26 (2.32)	40.34 (1.57)
Sapelli		53.04 (1.69)	13.88 (0.88)	18.34 (0.72)	23.01 (0.94)	52.90 (1.62)
Iroko		63.52 (6.78)	8.49 (0.88)	26.20 (5.69)	27.57 (5.59)	71.70 (2.54)
Karri		50.72 (2.07)	17.36 (1.13)	23.84 (1.59)	29.50 (1.83)	53.92 (1.32)
Blue gum		59.25 (3.37)	8.05 (0.74)	17.24 (1.23)	19.03 (1.27)	64.95 (1.98)
Maçaranduba		45.06 (2.16)	17.61 (2.39)	14.34 (0.99)	22.75 (2.23)	39.45 (3.79)
Makoré		49.85 (2.24)	12.08 (0.88)	18.95 (1.10)	22.49 (1.15)	57.47 (2.10)

Notes: Mean values are from 16 measurements. Standard deviations are in italic and parentheses.

The studied tropical woods differed mainly in the lightness L^* , which ranged between 34.88 (“very dark” wengé), 43.78 (“dark” padouk), 63.58 (“light” iroko) and 75.36 (“very light” okoumé). Achieved results are in an accordance with similar works disserting specific colour and texture characteristics of selected tropical woods [7,40,43].

All 21 tropical woods had the colour parameters a^* and b^* in a positive sphere of distribution. The redness index ($+a^*$) ranged from 5.61 (okoumé) to 31.42 (padouk), and the yellowness index ($+b^*$) from 10.33 (wengé) to 26.72 (padouk). This result suggests that woods coloured a brighter red or yellow, such as padouk, may belong also to darker species. When the values of a^* and b^* were for 21 tropical wood species evaluated in comparison to their lightness L^* , different tendencies of linear correlation were found. Value a^* had a negative correlation against the L^* (Figure 2A; $R^2 = 0.18$), while the b^* had a positive correlation against the L^* (Figure 2B; $R^2 = 0.10$). Nishino et al. [43] determined similar dependences between a^* or b^* and L^* for 97 wood species from French Guiana.

The colour saturation C^*_{ab} indicates the distance from the chromatic point ($a^* = 0, b^* = 0$) on the CIE 1976 $L^*a^*b^*$ colour space. For tropical woods the values of colour saturation ranged from 13.02 (wengé—characterized by a little intensive red-yellow shade) to 41.26 (padouk—characterized by a strong intensive red-yellow shade). Graphical analysis of the C^*_{ab} against the L^* for 21 tropical woods is present in Figure 2C. The C^*_{ab} exhibited only a minimal decrease at higher values of lightness L^* with zero coefficient of determination ($R^2 = 0.00$), i.e., was not found significant correlation.

The hue tone angle h_{ab} ranges for wood between 0° and 90° (the first quadrante), where 0° represents the red colour and 90° represents the yellow colour. The yellow shade prevailed to the red shade for a vast majority of tested tropical woods, typically for iroko and okoumé. On the contrary, for padouk, having the most red and yellow striking shades, a slightly more dominant was the red shade. A reasonable positive linear correlation between the hue tone angle h_{ab} and the lightness L^* of individual tropical woods is presented in Figure 2D ($R^2 = 0.46$).

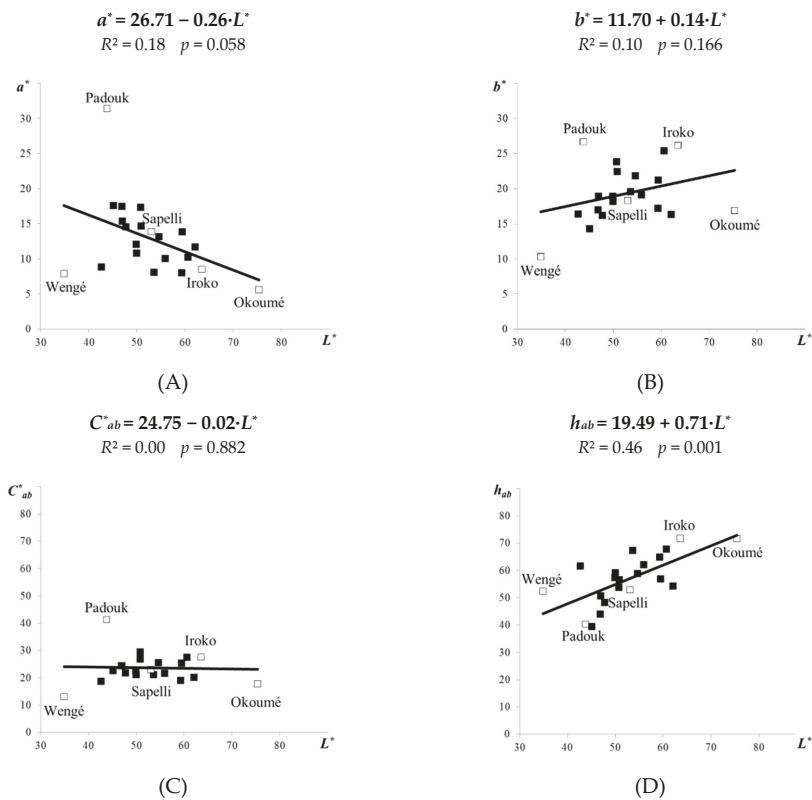


Figure 2. Linear correlations between the lightness L^* and the colour coordinates a^* , b^* (A, B), the colour saturation C^*_{ab} (C), and the hue tone angle h_{ab} (D)—for 21 original tropical wood species.

This result suggests that tropical woods with a dominant yellow shade are usually lighter. Németh [44] also found a linear correlation between the lightness L^* and the hue angle h_{ab} examining the colour co-ordinates of different temperate wood species.

3.2. Colour of Tropical Woods Exposed to the Fungus *Coniophora puteana*

Woods attacked by the brown-rot fungi gradually acquire deeper shades of brown of yellow [15,22,27,37,45]. However, specific colour changes during action of the brown-rot fungi can also occur, depending on the wood species [37,46], the history of wood ageing before fungal attack [15], the degree and uniformity of decay [47], or the specific enzymes, Fenton and other low-molecular degradation systems, and pigments produced by fungal mycelia [45].

Weight losses of 21 tropical woods attacked for 6 weeks by the brown-rot fungus *C. puteana* ranged from 0.08% to 6.48% (Table 3). The differences of the lightness ΔL^* and other colourimetric parameters Δa^* , Δb^* , ΔC^*_{ab} , Δh_{ab} and ΔE^*_{ab} , determined as a difference between the fungal-attacked and the original tropical wood, are documented in Table 3. Visualization, together with the pantone swatches, of the top surfaces of selected tropical woods before and after their exposure to *C. puteana* is shown in Figure 3.



Figure 3. Visualization and pantone swatches of the top surfaces of selected tropical woods before and after exposure to *C. puteana*.

After exposition to the brown-rot fungus *C. puteana*, the top surfaces of the darkest tropical woods wengé and ipé (Table 2) developed significantly lighter shades with the lightness increase ΔL^* +10.46 and +2.47 (Table 3). This “unexpected” result can be explained by a washout or deterioration of dark extractives present in darker wood species during the mycological test performed in humid environment in Petri dishes. On the contrary, the most noticeable darkening was observed in the top surfaces of the lightest and medium light tropical woods sapelli, okoumé, iroko and ovengol with the ΔL^* from -21.54 to -11.08 (Table 3). This “expected” result can be explained by degradation of white cellulose and hemicelluloses in presence of hydrolases and Fenton agent produced by *C. puteana* [45]. Previous studies have also reported a darkening of lighter European woods (beech and pine) due to decay processes [15,16].

A pronounced shade of the red due to *C. puteana* obtained only wengé, with Δa^* +4.98. A lighter shade of red obtained okoumé, zebrano, iroko, and blue gum, with Δa^* from +0.31 to +2.53 (Table 3). Conversely, the other tropical woods developed a greener shade, with Δa^* from -0.22 to -7.76 , the most markedly sapelli, padouk and macaranduba, with $\Delta a^* \geq -5.68$ (Table 3). The significant greening of padouk may be justified by its intensive red shade in the original state (Table 2).

The majority of tropical woods attacked by *C. puteana* obtained a more yellow shade, typically wengé, okoumé and blue gum, with Δb^* from +4.42 to +10.05. However, three tropical woods—padouk, sapelli, and yellow balau—showed a significant tendency to become bluer, with Δb^* from -3.08 to -8.74 (Table 3).

After fungal attack, a significant positive change in the colour saturation ΔC_{ab}^* had wengé +11.16, okoumé +5.93, and blue gum +5.15 (Table 3). It is an interesting knowledge, because the original wengé was the darkest species and okoumé the lightest one (Table 2). On the contrary, an evident negative change in ΔC_{ab}^* had sapelli, padouk, and yellow balau, with ΔC_{ab}^* from -4.04 to -10.84 (Table 3). However in a summary, the colour saturation of the tested original or fungal-attacked tropical woods had no significance to their lightness (Figure 2C, Figure 4C).

The positive differences in the hue tone angle Δh_{ab} indicate that the wood surfaces changed due to the brown-rot fungus more towards yellowish as to reddish. The largest positive change in Δh_{ab} was observed for macaranduba, bubinga, dark red meranti, and sapelli in range from +13.46 to +7.21 (Table 3). A significantly negative Δh_{ab} , connected with more evident redness as yellowing, obtained padouk -5.49 , and iroko -4.30 . Statistically insignificant redness occurred for blue gum, ovengol, and zebrano, with Δh_{ab} from -0.99 to -0.09 (Table 3).

Table 3. Weight loss and relative change of colourimetric parameters of 21 tropical woods caused by *C. puteana*.

Wood species	Δm	ΔL^*		Δa^*		Δb^*		ΔC^*_{ab}		Δh_{ab}		ΔE^*_{ab}
Ipé	0.20 (0.03)	2.47 (1.32)	a	−0.59 (0.50)	c	0.01 (0.31)	d	−0.26 (0.29)	d	1.68 (1.56)	b	2.63 (1.26)
Okoumé	6.48 (2.98)	−15.74 (1.55)	a	1.20 (0.23)	b	5.80 (0.50)	a	5.93 (0.49)	a	1.70 (0.51)	d	16.84 (1.34)
Tineo	5.38 (3.71)	−3.59 (1.63)	d	−1.88 (1.12)	b	1.41 (0.43)	c	−0.11 (0.92)	d	6.03 (2.10)	a	4.44 (1.68)
Dark red meranti	0.22 (0.09)	−8.44 (0.96)	a	−2.29 (0.27)	a	3.28 (1.04)	a	1.71 (0.94)	a	9.90 (1.70)	a	9.43 (0.70)
Yellow balau	0.40 (0.08)	−8.61 (1.06)	a	−2.77 (1.00)	a	−3.08 (0.95)	a	−4.04 (1.17)	a	2.04 (1.77)	b	9.59 (1.47)
Macassar ebony	0.52 (0.30)	−3.48 (1.87)	a	−1.88 (0.31)	a	−1.76 (0.84)	a	−2.49 (0.86)	a	1.57 (0.49)	a	4.73 (0.81)
Doussié	1.63 (1.51)	−2.51 (1.68)	d	−0.91 (0.76)	d	−0.76 (0.66)	d	−1.23 (0.84)	d	1.36 (1.07)	d	3.05 (1.60)
Cerejeira	0.30 (0.15)	−3.51 (2.26)	b	−2.89 (1.57)	b	−1.86 (1.28)	b	−2.89 (1.67)	b	5.73 (2.12)	c	4.98 (2.93)
Bubinga	0.96 (0.13)	−3.81 (1.24)	a	−3.87 (0.85)	a	1.89 (0.47)	a	−1.11 (0.90)	c	10.29 (1.10)	a	5.96 (0.15)
Ovengol	0.61 (1.02)	−11.08 (1.28)	a	−0.46 (0.48)	d	−1.81 (0.84)	a	−1.83 (0.87)	b	−0.84 (1.10)	d	11.28 (1.24)
Merbau	0.48 (0.32)	−4.29 (1.71)	a	−0.22 (1.71)	d	−1.01 (1.25)	d	−0.88 (1.95)	d	−1.16 (1.99)	d	4.87 (1.78)
Santos rosewood	1.28 (0.31)	−0.83 (0.66)	d	−1.49 (1.67)	c	−1.48 (2.55)	d	−2.49 (0.86)	d	1.57 (0.49)	d	3.36 (1.89)
Zebrano	1.65 (0.62)	−9.14 (1.01)	a	0.82 (1.04)	d	1.26 (1.18)	d	1.52 (1.46)	d	−0.09 (1.69)	d	9.39 (1.08)
Wengé	0.67 (0.35)	10.46 (2.17)	a	4.98 (0.72)	a	10.05 (1.87)	a	11.16 (1.50)	a	4.69 (2.60)	b	15.54 (1.55)
Padouk	0.95 (1.69)	−6.18 (1.32)	a	−5.91 (0.96)	a	−8.74 (1.93)	a	−9.93 (1.46)	a	−5.49 (2.70)	a	12.41 (1.41)
Sapelli	3.12 (1.15)	−21.54 (0.92)	a	−7.76 (1.26)	a	−7.87 (1.52)	a	−10.84 (1.99)	a	7.21 (1.11)	a	24.26 (1.52)
Iroko	0.20 (0.97)	−15.08 (3.76)	a	1.07 (0.57)	c	−2.89 (1.41)	c	−2.37 (1.49)	d	−4.30 (0.71)	a	15.44 (3.89)
Karri	0.69 (0.47)	−3.83 (1.37)	a	0.31 (1.23)	d	0.89 (1.41)	d	0.91 (1.81)	d	0.54 (0.89)	d	4.43 (1.17)
Blue gum	0.38 (0.21)	−6.27 (2.54)	a	2.53 (1.46)	a	4.42 (0.88)	a	5.15 (1.52)	a	−0.99 (1.35)	d	8.42 (1.91)
Maçaranduba	0.08 (0.05)	−1.99 (1.21)	b	−5.68 (0.40)	a	1.66 (0.40)	b	−2.81 (0.38)	a	13.46 (1.08)	a	6.35 (0.64)
Makoré	1.78 (1.84)	−9.43 (1.69)	a	−2.44 (1.37)	a	−2.45 (1.65)	b	−3.33 (2.09)	b	2.35 (1.28)	c	10.19 (2.10)

Note: Mean values of colourimetric parameters are from 16 measurements, and of weight losses from 4 specimens. Standard deviations are in italics and parentheses. The t-test analysed the colour changes in relation to the original wood at the 99.9% significance level (a), the 99% significance level (b), the 95% significance level (c), and without an evident significant difference at $p \geq 0.05$ (d).

The linear correlations between the colourimetric parameters a^*_F , $C^*_{ab\ F}$ or $h_{ab\ F}$ versus the lightness L^*_F for the 21 fungal-attacked tropical woods (Figure 4A,C,D) remained almost the same as were determined for the 21 original tropical woods (Figure 2A,C,D).

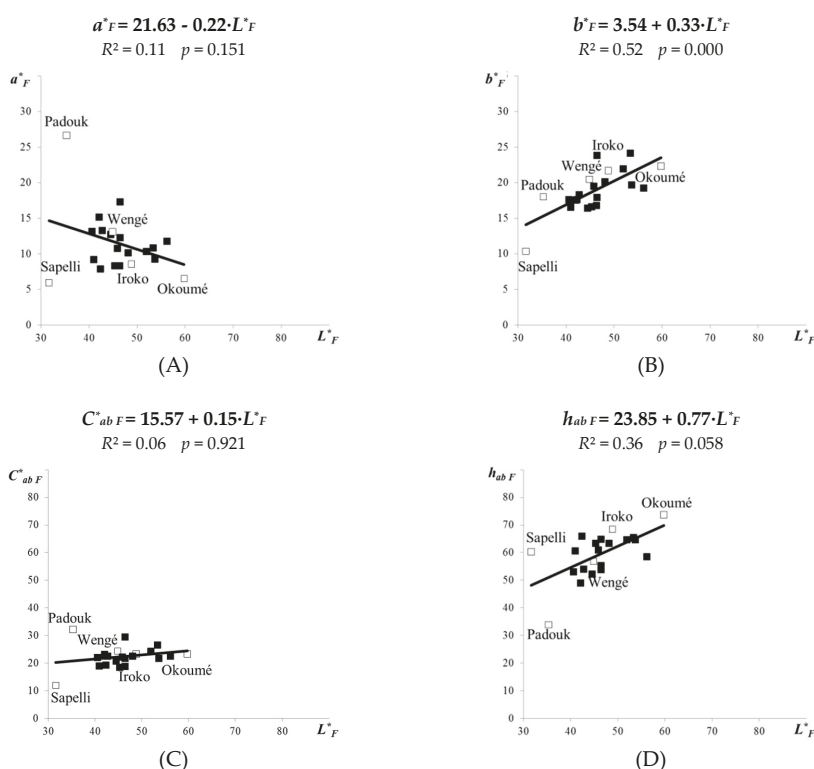


Figure 4. Linear correlations between the lightness L^* and the colour coordinates a^* , b^* (A,B), the colour saturation C^*_{ab} (C), and the hue tone angle h^*_{ab} (D)—for 21 tropical wood species attacked by the brown-rot fungus *C. puteana*.

In the fungal-attacked tropical woods, again no evident relationships were found between the lightness and redness ($R^2 = 0.11$), or the lightness and colour saturation ($R^2 = 0.06$). Indirectly, it can be stated that fungal attack did not have an apparent effect on these relationships. However, due to *C. puteana* the relationship between lightness and hue tone angle evidently decreased ($R^2 = 0.36$ for h^*_{abF} —Figure 4D; while previously $R^2 = 0.46$ for h^*_{ab} —Figure 2D).

Conversely, the b^*_F coordinate, which indicates yellowing, grew more evidently with L^*_F for the 21 fungal-attacked tropical woods. It is evident from comparing the slope trend B and the coefficient of determination R^2 in Figure 2B ($b^* = 11.70 + 0.14 \cdot L^*$; $B = 0.14$; $R^2 = 0.10$) with the same parameters in Figure 4B ($b^*_F = 3.54 + 0.33 \cdot L^*_F$; $B = 0.33$; $R^2 = 0.52$). As the slope trend B increased more evidently only for the yellow colour coordinate b^* , from 0.14 to 0.33, there indirectly was confirmed that at brown rot some lighter tropical woods (such as okoumé, or dark red meranti) obtain a more yellow shade.

The total colour differences ΔE^*_{ab} of the fungal-attacked tropical woods were significantly similar to their lightness changes ΔL^* (Figure 5A), however, values of ΔE^*_{ab} were greater as ΔL^* in an accordance with Equation (3) (Table 3). Usually, the lightest and medium light tropical woods okoumé, sapelli, iroko and ovengol had the highest ΔE^*_{ab} values from 11.28 to 24.26. This result is in an accordance with other works dealing with the durability and colour changes of tropical woods due to biological deterioration [48,49]. However, it was simultaneously observed that after attack by *C. puteana* the top surfaces of wengé and padouk (darker tropical woods—Table 2) also had high values of ΔE^*_{ab} 15.80 and 12.41 (Table 3, Figure 5A). This result can be explained by washout of dark extractives presented in darker wood species during the mycological test, similarly mentioned for the

lightness changes. On the contrary, effects of the Δa^* and Δb^* values of all tropical species on the ΔE^*_{ab} value were not significant (Figure 5B,C).

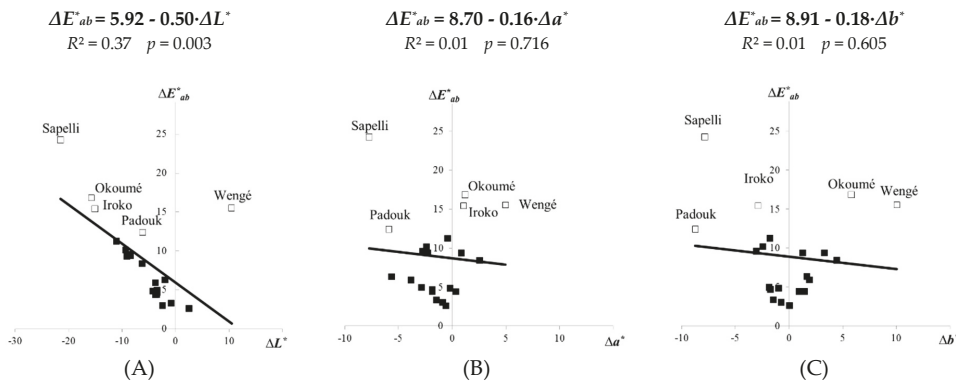


Figure 5. Linear correlations between the total colour difference ΔE^*_{ab} and changes of other colour parameter ΔL^* (A), Δa^* (B), Δb^* (C)—for 21 tropical woods attacked with the brown-rot fungus *C. puteana*.

Several studies have shown that there are some relationships between the colour parameters of wood and its decay resistance [15,16,46–50]. The relationship between the colour and weight loss of decayed wood is based on the type and amount of wood extractives, which have effect on the colour, and on its decay resistance. Such relationships could be encouraging but not always sufficient for predicting decay resistance of tested woods. Specifically, from our experiment it is evident that for 21 tropical woods no dependency was found between the total colour difference ΔE^*_{ab} and the decay resistance determined as weight loss Δm (Figure 6; $R^2 = 0.10$).

Generally, the intensity and specificity of colour changes in woods attacked by brown rot—when browning can be connected with yellowing or bluing and also with reddening or greening—are influenced not only by the enzymatic and pigment specification of the individual brown-rot fungus, but also by the wood species (e.g., presence of specific extracts), the degree of its decay, and the environmental factors. Therefore, some of tested tropical woods at exposition to *C. puteana* had a more yellowish shade while other ones a more reddish shade, when all the colour changes depended probably on their molecular structure and natural durability. In future experiments, we would like to analyse these factors in more detail.

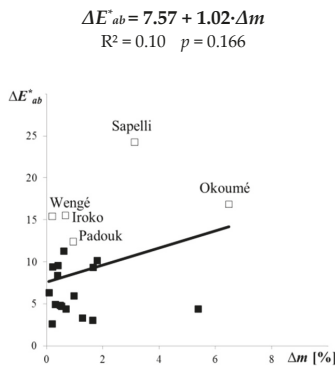


Figure 6. Linear correlations between the total colour differences ΔE^*_{ab} and the weight losses Δm of 21 tropical woods exposed 6 weeks to *C. puteana*.

Colour changes of tropical woods exposed in interiors of buildings are unwanted. Brown-rot fungi decrease their strength and can worsen their colour and aesthetic. On the contrary, some benefits of rotting can be interesting for claddings and other decorative products, but in this situation the intentional decay has to be performed before they are installed. By processing spalted wood artists can create decorative material, such as fine art mosaics, furniture, and dishes, which have been used for centuries [51] and also hold an interesting niche modern market in decorative veneers or other decorative materials in North America and Europe [17].

4. Conclusions

Several tropical woods have positive surface characteristics, such as interesting texture and colour, and high natural durability, which is an essential requisite for wooden constructions exposed to the environment with a high risk of biodeterioration by fungi and insects. For architects, changes in their original colour at biodeterioration processes are important. The colour analyses of 21 tropical woods before and after intentional attack by the brown rot-fungus *C. puteana* led to the following conclusions:

- For the original tropical woods, the a^* coordinate (redding) declined with increase of the lightness L^* , while the b^* (yellowing) and h^*_{ab} (hue ton angle) coordinates grew with the lightness. No significance was found between C^*_{ab} (colour saturation) and L^* .
- For the fungal-attacked tropical woods, the linear correlations between the colour coordinates a^* , C^*_{ab} or h^*_{ab} and the lightness L^* remained almost the same as for the original tropical woods, and only the b^* coordinate grew more evidently in relation to L^* .
- The total discoloration ΔE^*_{ab} values were highest for the top surfaces of the lighter species (sapelli, okoumé, iroko) and the darkest species (wengé), when the ΔE^*_{ab} were justified by the marked change of the lightness ΔL^* .
- Significant changes in the lightness and colouration of the fungal-attacked tropical woods indicated these colour changes could be caused not only by the biodegradation of polysaccharides, but also by biodegradation or leaching of some extractives during laboratory mycological tests.

Author Contributions: For research articles with several authors, a short paragraph specifying their individual contributions must be provided. The following statements should be used “conceptualization, Z.V. and L.R.; methodology, Z.V. and L.R.; software, Z.V. and L.R.; validation, Z.V. and L.R.; formal analysis, Z.V. and L.R.; investigation, Z.V. and L.R.; resources, Z.V. and L.R.; data curation, Z.V. and L.R.; writing—original draft preparation, Z.V. and L.R.; writing—review and editing, Z.V. and L.R.; visualization, Z.V.; supervision, L.R.; project administration, L.R.

Acknowledgments: This work was supported by the Slovak Research and Development Agency under the contract No. APVV-17-0583, and the VEGA project 1/0729/18.

Conflicts of Interest: The authors declare no conflicts of interest.

References

1. Janin, G.; Gonçalves, J.C.; Ananías, R.A.; Charrier, B.; Silva, G.F.D.; Dilem, A. Aesthetics appreciation of wood colour and patterns by colorimetry. Part 1. Colorimetry theory for the CIE Lab system. *Maderas Cienc. Tecnol.* **2001**, *3*, 14.
2. Tolvaj, L.; Persze, L.; Lang, E. Correlation between hue angle and lightness of wood species grown in Hungary. *Wood Res.* **2013**, *58*, 141–145.
3. Slabejová, G.; Šmidriaková, M.; Fekiač, J. Gloss of transparent coating on beech wood surface. *Acta Fac. Xylologiae Zvolen* **2016**, *58*, 37–44.
4. Hon, D.N.-S.; Minemura, N. Color and discoloration. In *Wood and Cellulosic Chemistry*, 2nd ed.; Hon, D.N.-S., Shiraishi, N., Eds.; CRC Press: New York, USA, 2000; pp. 385–442.
5. Babiak, M.; Kubovský, I.; Mamoňová, M. Color space of the selected domestic species. In *Interaction of Wood with Various Forms of Energy*, 1st ed.; Kurjatko, S., Kúdela, J., Eds.; Technical University in Zvolen: Zvolen, Slovakia, 2004; pp. 113–117.

6. Katuščák, S.; Kucera, J. CIE orthogonal and cylindrical color parameters and the color sequences of the temperate wood species. *Wood Res.* **2000**, *45*, 9–21.
7. da Silva, R.A.F.; Setter, C.; Mazette, S.S.; de Melo, R.R.; Stangerlin, D.M. Colorimetry of wood from thirty tropical species. *Ciênc. Madeira* **2017**, *8*, 36–41.
8. Meints, T.; Teischinger, A.; Stingl, R.; Hansmann, C. Wood colour of central European wood species: CIE Lab characterisation and colour intensification. *Eur. J. Wood Wood Prod.* **2017**, *75*, 499–509. [[CrossRef](#)]
9. Klement, I.; Vilkovská, T. Color characteristics of red false heartwood and mature wood of beech (*Fagus sylvatica* L.) determining by different colour saturation city coordinates. *Sustainability* **2019**, *11*, 690. [[CrossRef](#)]
10. Mosedale, J.R.; Charrier, B.; Janin, G. Genetic control of wood colour, density and heartwood ellagitannin content of European oak (*Quercus petraea* and *Quercus robur*). *Forestry* **1996**, *69*, 111–124. [[CrossRef](#)]
11. Phelps, J.E.; McGinnes, E.A.; Garret, H.E.; Cox, G.S. Growth quality evaluation of black walnut wood. II. Color analyses of veneer produced on different sites. *Wood Fiber Sci.* **1982**, *15*, 177–185.
12. Derkyi, N.S.A.; Bailleres, H.; Chaix, G.; Thevenon, M.F. Colour variation in teak (*Tectona grandis*) wood from plantations across the ecological zones of Ghana. *Ghana J. For.* **2009**, *25*, 40–48. [[CrossRef](#)]
13. Kržišnik, D.; Lesar, B.; Thaler, N.; Humar, M. Influence of natural and artificial weathering on the colour change of different wood and wood-based materials. *Forests* **2018**, *9*, 488. [[CrossRef](#)]
14. Reinprecht, L.; Mamoňová, M.; Pánek, M.; Kačík, F. The impact of natural and artificial weathering on the visual, colour and structural changes of seven tropical woods. *Eur. J. Wood Wood Prod.* **2018**, *76*, 175–190. [[CrossRef](#)]
15. Reinprecht, L.; Hulla, M. Colour changes in beech wood modified with essential oils due to fungal and ageing-fungal attacks with *Coniophora puteana*. *Drewno* **2015**, *58*, 37–48.
16. Vidholdová, Z.; Slabejová, G.; Polomský, J. Colour changes of Scots pine wood due to action of the white-rot fungus *Trametes versicolor*. In *Protecting Trees and Wood*, 1st ed.; Hlaváč, P., Vidholdová, Z., Eds.; Technical University in Zvolen: Zvolen, Slovakia, 2016; pp. 61–66.
17. Van Court, R.C.; Robinson, S.C. Stimulating Production of Pigment-Type Secondary Metabolites from Soft Rotting Wood Decay Fungi (“Spalting” Fungi). In *Advances in Biochemical Engineering/Biotechnology*, 1st ed.; Springer Nature: Basel, Switzerland, 2019; p. 16.
18. Rayner, A.D.; Boddy, L. *Fungal Decomposition of Wood. Its Biology and Ecology*; Antony Rowe Ltd.: Chippenham, UK, 1997; p. 587.
19. Pandey, K.K.; Pitman, A.J. FTIR studies of the changes in wood chemistry following decay by brown-rot and white-rot fungi. *Int. Biodeter. Biodegr.* **2003**, *52*, 151–160. [[CrossRef](#)]
20. Zabel, R.A.; Morrell, J.J. *Wood Microbiology: Decay and Its Prevention*; Academic Press: London, UK, 2012; p. 476.
21. Nascimento, M.S.; Santana, A.L.B.D.; Maranhão, C.A.; Oliveira, L.S.; Bieber, L. Phenolic extractives and natural resistance of wood. In *Biodegradation-Life of Science*; Chamy, R., Rosenkranz, F., Eds.; InTech: Rijeka, Croatia, 2013; pp. 349–370.
22. Sablík, P.; Giagli, K.; Pařil, P.; Baar, J.; Rademacher, P. Impact of extractive chemical compounds from durable wood species on fungal decay after impregnation of nondurable wood species. *Eur. J. Wood Wood Prod.* **2016**, *74*, 231–236. [[CrossRef](#)]
23. Schmidt, O. Indoor wood-decay basidiomycetes: Damage, causal fungi, physiology, identification and characterization, prevention and control. *Mycol. Prog.* **2007**, *6*, 261–279. [[CrossRef](#)]
24. Frankl, J. Wood-damaging fungi in truss structures of baroque churches. *J. Perform. Constr. Facil.* **2015**, *29*, 04014138. [[CrossRef](#)]
25. Hyde, K.D.; Al-Hatmi, A.M.S.; Andersen, B.; Boekhout, T.; Buzina, W.; Dawson, T.L.; Eastwood, D.C.; Jones, E.B.G.; Hoog, S.; Kang, Y.; et al. The world’s ten most feared fungi. *Fungal Divers.* **2018**, *93*, 161–194. [[CrossRef](#)]
26. Gabriel, J.; Švec, K. Occurrence of indoor wood decay basidiomycetes in Europe. *Fungal Biol. Rev.* **2017**, *31*, 212–217. [[CrossRef](#)]
27. Irbe, I.; Andersone, I.; Andersons, B.; Noldt, G.; Dizhbite, T.; Kurnosova, N.; Nuopponen, M.; Stewart, D. Characterisation of the initial degradation stage of Scots pine (*Pinus sylvestris* L.) sapwood after attack by brown-rot fungus *Coniophora puteana*. *Biodegradation* **2011**, *22*, 719–728. [[CrossRef](#)]

28. Robinson, S.C.; Laks, P.E. Wood species and culture age affect zone line production of *Xylaria polymorpha*. *Open Mycol. J.* **2010**, *4*, 18–21. [CrossRef]
29. Robinson, S.C.; Tudor, D.; Cooper, P.A. Wood preference of spalting fungi in urban hardwood species. *Int. Biodeter. Biodegr.* **2011**, *65*, 1145–1149. [CrossRef]
30. Robinson, S.C.; Tudor, D.; Cooper, P.A. Feasibility of using red pigment producing fungi to stain wood for decorative applications. *Can. J. For. Res.* **2011**, *41*, 1722–1728. [CrossRef]
31. Robinson, S.C. Developing fungal pigments for “painting” vascular plants. *Appl. Microbiol. Biotechnol.* **2012**, *93*, 1389–1394. [CrossRef]
32. Robinson, S.C.; Tudor, D.; Cooper, P.A. Utilizing pigment-producing fungi to add commercial value to American beech (*Fagus grandifolia*). *Appl. Microbiol. Biotechnol.* **2012**, *93*, 1041–1048. [CrossRef]
33. Beck, H.G.; Freitas, S.; Weber, G.; Robinson, S.C.; Morrell, J.J. Resistance of fungal derived pigments to ultraviolet light exposure. In *International Research Group in Wood Protection; IRG/WP*: St. George, UT, USA, 2014.
34. Vega Gutierrez, S.; Robinson, S.C. Microscopic analysis of pigments extracted from spalting fungi. *J. Fungi* **2017**, *3*, 15. [CrossRef]
35. Blanchette, R.A. Screening wood decayed by white rot fungi for preferential lignin degradation. *Appl. Environ. Microbiol.* **1984**, *48*, 647–653.
36. Stalpers, J.A.; Vlug, I. Confitulina, the anamorphs of *Fistulina hepatica*. *Can. J. Bot.* **1983**, *61*, 1660–1666. [CrossRef]
37. Hillis, W.E. *Heartwood and Tree Exudates*; Springer: Berlin/Heidelberg, Germany, 1987; p. 267.
38. Coulson, J. *Wood in Construction—How to Avoid Costly Mistakes*; John Wiley & Sons Ltd.: Chichester, UK, 2012; p. 208.
39. EN 350. *Durability of Wood and Wood-Based Products. Testing and Classification of the Durability to Biological Agents of Wood and Wood-Based Materials*; European Committee for Standardization: Brussels, Belgium, 2016.
40. Wagenführ, R. *Holzatlas*; Fachbuchverlag Leipzig, Carl Hanser Verlag: München, Germany, 2007; p. 816.
41. URL 1. The IUCN Red List of Threatened Species. Version 2017-2. Available online: www.iucnredlist.org (accessed on 16 November 2017).
42. CIE. *Colorimetry—Part 4: CIE 1976 L*a*b Colour Space*; CIE DS 014-4.3/E:2007; CIE Central Bureau: Vienna, Austria, 2007.
43. Nishino, Y.; Janin, G.; Chanson, B.; Détienné, P.; Gril, J.; Thibaut, B. Colorimetry of wood specimens from French Guiana. *J. Wood Sci.* **1998**, *44*, 3–8. [CrossRef]
44. Németh, K. The colour of wood in CIE Lab system. *Az Erdészeti és Faipari Egyetem Tudományos Közleményei* **1982**, *2*, 125–135.
45. Eriksson, K.-E.L.; Blanchett, R.A.; Ander, P. *Microbial and Enzymatic Degradation of Wood and Wood Components*; Springer Series in Wood Science: Berlin/Heidelberg, Germany; New York, NY, USA, 1990; p. 407.
46. Gierlinger, N.; Jacques, D.; Grabner, M.; Wimmer, R.; Schwanninger, M.; Rozenberg, P.; Pâques, L.E. Colour of larch heartwood and relationships to extractives and brown-rot decay resistance. *Trees* **2004**, *18*, 102–108. [CrossRef]
47. Kokutse, A.D.; Stokes, A.; Baillères, H.; Kokou, K.; Baudasse, C. Decay resistance of Togolese teak (*Tectona grandis* Lf) heartwood and relationship with colour. *Trees* **2006**, *20*, 219–223. [CrossRef]
48. Costa, M.D.A.; Costa, A.F.D.; Pastore, T.C.M.; Braga, J.W.B.; Gonçalves, J.C. Characterization of wood decay by rot fungi using colorimetry and infrared spectroscopy. *Ciência Florestal* **2011**, *21*, 567–577.
49. Amusant, N.; Fournier, M.; Beauchene, J. Colour and decay resistance and its relationships in *Eperua grandiflora*. *J. Ann. For. Sci.* **2008**, *65*, 1–6. [CrossRef]
50. Stangerlin, D.M.; Costa, A.F.D.; Gonçalves, J.C.; Pastore, T.C.M.; Garlet, A. Monitoring of biodeterioration of three Amazonian wood species by the colorimetry technique. *Acta Amazon.* **2013**, *43*, 429–438. [CrossRef]
51. Blanchette, R.A.; Wilmering, A.M.; Baumeister, M. The use of green-stained wood caused by the fungus *Chlorociboria* in intarsia masterpieces from the 15th century. *Holzforschung* **1992**, *46*, 225–232. [CrossRef]



Analysis of Economic Feasibility of Ash and Maple Lamella Production for Glued Laminated Timber

Philipp Schlotzhauer ^{1,*}, Andriy Kovryga ², Lukas Emmerich ¹, Susanne Bollmus ¹, Jan-Willem Van de Kuilen ^{2,3} and Holger Militz ¹

¹ Dept. Wood Biology and Wood Products, Faculty of Forest Sciences and Forest Ecology, Georg-August-University of Göttingen, 37077 Lower Saxony, Germany

² Holzforschung München, Technical University of Munich, 80797 Bavaria, Germany

³ Faculty of Civil Engineering and Geosciences, Delft University of Technology, 2628 CN Delft, The Netherlands

* Correspondence: philipp.schlotzhauer@uni-goettingen.de; Tel.: +49-551/39-33562

Received: 28 May 2019; Accepted: 24 June 2019; Published: 26 June 2019

Abstract: *Background and Objectives:* In the near future, in Europe a raised availability of hardwoods is expected. One possible sales market is the building sector, where medium dense European hardwoods could be used as load bearing elements. For the hardwood species beech, oak, and sweet chestnut technical building approvals already allow the production of hardwood glulam. For the species maple and ash this is not possible yet. This paper aims to evaluate the economic feasibility of glulam production from low dimension ash and maple timber from thinnings. Therefore, round wood qualities and the resulting lumber qualities are assessed and final as well as intermediate yields are calculated. *Materials and Methods:* 81 maple logs and 79 ash logs cut from trees from thinning operations in mixed (beech) forest stands were visually graded, cant sawn, and turned into strength-graded glulam lamellas. The volume yield of each production step was calculated. *Results:* The highest volume yield losses occur during milling of round wood (around 50%) and “presorting and planning” the dried lumber (56%–60%). Strength grading is another key process in the production process. When grading according to DIN 4074-5 (2008), another 40%–50% volume loss is reported, while combined visual and machine grading only produces 7%–15% rejects. *Conclusions:* Yield raise potentials were identified especially in the production steps milling, presorting and planning and strength grading.

Keywords: volume yield; European hardwoods; low quality round wood; strength grading; glulam

1. Introduction

The share of hardwoods in the wood stock of Central European forests is steadily increasing [1]. The higher availability of hardwoods requires the development of new markets and new value chains for an overall increase in use. A possible, large sales market is the application in load-bearing structures.

Medium dense hardwoods have preferable mechanical properties compared to softwood. The higher tensile strength of hardwoods leads to either smaller member dimensions or higher load carrying capacities. The high bending strength for hardwood glulam (up to 48 MPa) has been reported by Blaß et al. [2] and Frühwald et al. [3] for beech glulam and by Van de Kuilen and Torno [4] for ash glulam. In recent years, a number of technical approvals for hardwood glulam have been issued:

Beech glulam [5],
VIGAM oak glulam [6],
Schiller oak glulam [7], and
SIEROLAM glulam of chestnut [8].

Despite the attractive mechanical properties, the use of hardwoods in structural applications remains minor. According to Frühwald et al. [3] and Mack [9], more than 90% of the glulam products in Europe are made of softwood (mainly spruce). The survey by Ohnesorge et al. [10] on glulam producers in Germany, Switzerland, and Austria revealed that in the year 2005 out of 900,000 m³ of glued rod-shaped solid wood products only 1% contained hardwood.

A number of technological reasons as well as historical and silvicultural reasons has led to the fact that mainly softwood is used in wood construction. The use of softwood has been favored over decades because the physical properties are quite predictable and differences between the different softwood species are small. Furthermore, softwood is characterized by long, straight logs with low degrees of taper, homogeneous assortments, and few knots that are usually evenly distributed [11]. There are several further technological constraints for the use of hardwoods in structural applications, such as lack of knowledge of the long-term behavior of hardwood gluing, or the less number of certified grading machines compared to softwood, non-harmonized standardization and production processes not optimized for hardwood species.

One major aspect for the broader use of hardwoods in construction (especially glulam) is the economic feasibility of the production. For hardwoods, at present, no calculated data from a production facility is available. Torno et al. [12] estimated the production cost of ash lamellas to be three times higher as of spruce lamellas. Thus, besides the higher load-bearing capacity of hardwood glulam, the cost-efficient use of the resource hardwood is required, in order to reduce this cost difference. This includes both the optimization of the production process and of the resources used. Processing cheap, particularly small diameter hardwood logs, which are usually used for energy recovery in Europe [12], is one of the frequently discussed issues. Exploiting small diameter hardwoods for material utilization, e.g., sawing, is an important issue in Northern America as well [13].

It is the aim of this paper to contribute to the overall goal of an effective use of the available hardwood resources by minimizing the waste of each production step (of glulam lamellas) separately and for the entire production. The use of small diameter logs from thinnings as a poor-quality resource is the focus of this yield analysis. In the current study, the yield analysis from log sections to planed and graded glulam lamellas is performed using state of the art processing technology. Moreover, the achieved yields are linked to the mechanical properties relevant for glulam lamellas and measured for the investigated samples. Doing so, the economic feasibility of lamella production out of small diameter logs of the rare hardwood species maple and ash can be estimated. The single production steps and technologies of the production of glulam from low-dimension maple and ash logs are analyzed and described.

2. Conversion Efficiency of Hardwoods

In literature, different terms exist to measure the conversion efficiency. In Northern America, the recovery rates with measures like lumber overrun, lumber recovery factor (LRF) and cubic lumber recovery (CLR) are used. In Europe, the term yield is most commonly used. All these definitions have in common that they calculate the volume ratio between the output sawn product and the input logs. The term yield goes even beyond that and can be determined for each production step separately. It can include final, as well as intermediate, products. This allows revealing and analyzing the weakest points of the production process. The use of waste material as side product or for energy production can also be considered. A higher lumber volume does not necessarily lead to higher lumber value. That is why it is important to distinguish between lumber volume recovery and lumber value recovery. For sawmill owners or managers, the latter is decision relevant [14].

Due to the low production volumes of hardwood glulam, yield values are known to only a very small extent. Studies on European hardwoods analyzing the yield from log to planed (dry-dressed) lumber are rare. Torno et al. [12] performed an extensive study on the production of beech lamellas and Van de Kuilen and Torno [15] on beech and ash lamellas. For lamellas sorted according to the German visual grading standard DIN 4074-5 [16], volume yield values as high as 26% for beech and

22.7% for ash were attained. When sorting the lamellas according to the more stringent sorting rules of the German technical approval Z 9.1 679 [5], for the production of glulam the total yield starting at round wood (middle diameter classes 2b–6) ended at only 22% for beech and 26.9% for ash. In this case, however, higher mechanical properties are presumed. As shown by Torno et al. [12], the cutting pattern and the sawing technology affect the final yield. For graded beech lamellas those can drop to 10% or rise to 26%. The highest yield was attained with the grade sawing method, where a vertical bandsaw headrig cuts “around the log” until only a heart plank is left. In these studies, in addition to the cutting pattern and the sawing technology, the quality and the diameter of the round wood had a major influence on the final yield. Frühwald et al. [3] estimate the total yield of the production of high-quality beech glulam from good to medium round wood qualities (B and C) to be around 28.5%.

The reported final yields for hardwood lamellas are below the ones for softwoods. Final yields of the latter range from 24.5%–38.5% [17,18]. Even higher yield values of 40% are stated by Torno et al. [12] for a modern spruce profiling unit. Frühwald et al. [3] mention that the final yield depends greatly on the size (production volume) of the glulam producing company. Only looking at the production of spruce glulam from dried sawn lumber, big producers are able to attain yields between 69% and 75%, while little glulam producers only reach yields of 53%.

Studies like the ones presented by Torno et al. [12] and Van de Kuilen and Torno [15] on the yield from logs to planed and strength graded hardwood lamellas are scarce. A few studies describe the yields of only individual production steps. Their results are summarized below.

2.1. Sawing/Milling

According to Steele [19], the following factors influence the lumber recovery in sawing (milling):

- Log diameter, length, taper, and quality
- Kerf width
- Sawing variation, rough green-lumber size, and size of dry-dressed lumber
- Product mix
- Decision making by sawmill personnel
- Condition and maintenance of mill equipment
- Sawing method

In the study of Lin et al. [14] in small US hardwood sawmills the factors log grade, diameter, sweep, length, species and sawmill specifications had a significant influence on the lumber volume recovery. It is also stressed that interactions between different factors can have a significant influence on the lumber volume recovery. Further influencing factors like board edging and trimming are also introduced. Richards et al. [20] simulate the volume and value yield of sawing hardwood lumber depending on the above mentioned factors. In their simulation the volume yield of live sawing is always higher than that of any four-sided sawing pattern (quadrant, cant, and decision), when sawing the same size logs. When sawing small logs with large core defects the value yield, though, is higher when applying a four-sided sawing pattern. The authors also emphasize the importance of the rotational position on the carriage for the first cut.

Ehlebracht [17] compares volume yield values of four German sawmills for the sawing of square-edged sawn lumber (rough green) from low dimension beech logs. The highest yield value of 57% is attained by a gang saw headrig utilizing the cant sawing method [20]. The lowest yield value of 36% is produced by a circular saw headrig, which produces a comparatively wide kerf. These values are consistent with the values reported by Emhardt and Pfingstag [21] and Fronius [22] that, when combining their findings, present values that range from 42%–47% for the production of square-edged sawn lumber from low dimension beech logs (middle diameter classes 2b and 3a). The lower yield values of Ehlebracht [17] are comparable to the 35% yield reported by Fischer [23] for the production of parquet friezes and pallet boards from low dimension oak logs. For five small US hardwood mills, Lin et al. [14] report cubic recovery percentages (CRP) of 53.2% for red oak (*Quercus rubra* L.) and 57.5%

for yellow polar (*Liriodendron tulipifera* L.). The CRP expresses the volume of rough green lumber as percentage of cubic log scale volume and is therefore comparable to the yield of the production step “sawing” analyzed by Ehlebracht [17]. The mean small-end diameter (SED) of the input logs in the study of Lin et al. [14] was 33 cm, i.e., also low dimension logs were sawn. All five sawmills used the grade sawing method—two with circular saw headrigs and three with bandsaw headrigs. The simulations of Richards et al. [20] for US hardwood mills result in volume yield values, which range from 54%–76%. The high values, though, are only attainable, when live sawing large logs. According to Fronius [22], a further yield drop of 15%–20% (relative to the original round wood volume) is to be expected when square edging live sawn lumber.

2.2. Drying

Drying losses arise from volumetric shrinkage and the quality of the sawn lumber after drying. For hardwoods such as oak, improper drying results in staining, checking, splitting, and warp, which leads to a reduced sawn wood value [24,25]. Therefore, proper drying schedules are of high importance.

Generally, the higher the specific gravity of the wood is the higher is also the volumetric shrinkage [26]. It varies within a species and even for lumber from the same log. The volumetric shrinkage during technical drying of rough green lumber to a moisture content of 12% ranges from 14%–21% for beech, from 12.8%–13.6% for ash and from 11.5%–11.8% for maple [17,27]. Spruce shrinkage losses are around 12% [27]. The volumetric shrinkage in the production of hardwood lamellas for glulam lies between 11% and 17% for beech and at 9.8% for ash [15].

2.3. Planing

Planing losses depend on the chosen oversize, the final product and the drying quality (i.e., warping and bowing). The resulting losses present a combination of planing away the oversize and sorting out (presorting) boards with intensive bowing. For example, when trimming the lamellas to shorter lengths, the oversize can be reduced and thus the planing losses are also reduced. In similar studies to the presented one [12,15], planing and presorting losses (due to bowing) for the production of hardwood glulam lamellas vary from 18%–46%—a relatively wide range.

2.4. Grading

Grading is an important step within the production, as the quality of sawn wood is assessed in terms of appearance (i.e., cladding, furniture) or mechanical properties predicted. As a consequence, a discrete value is assigned to a lumber specimen. Both the quality of the produced lumber in terms of achieved mechanical properties and the yield are of interest. For grading, the yield is the share of dry-dressed lumber (dried, jointed, and planed), which is assigned to a certain quality class and not rejected.

Data on hardwood grading yield in general, and on strength grading in particular, is scarce, since hardwoods are rarely strength graded. Generally, the yield losses depend on the grading method (machine vs. visual grading), wood quality, growth region, cross-section, and sawing pattern selected. For European hardwoods, the effect the single mentioned factors have on the grading yield, are known to only a small extent. If lamellas are sawn pith free, the grading losses are lower compared to other sawing patterns. This is because the pith is a general rejection criterion for visually graded hardwood lumber after the German visual grading standard for structural timber DIN 4074-5 [16]. Thus, Glos and Torno [28] report for 324 ash boards and 459 maple boards graded according to DIN 4074-5 rules for joists rejection rates of as high as 21% and 37% due to pith and extreme grain deviation. It should be mentioned, though, that for that study the visual assessment of the boards is only being made for that part of each specimen, which is selected as free testing length. In Torno et al. [12] the loss values for beech lamellas range from 37%–62%, if graded visually in accordance with the German visual grading rules for structural lumber DIN 4074-5 [16]. If lamellas are graded in accordance with the German technical building approval for beech glulam Z 9.1 679 [5] the rejection rate increases to 47% and 69%.

3. Test material

The round wood used for this investigation came from thinnings in mixed forest stands (mixed beech forests) of the state forestry offices Leinefelde and Heiligenstadt (Central Germany). The wood was harvested in the winter of 2014/2015 with harvester technology. Until the milling in June 2015, the round wood sections (logs) with a length between 3.20 and 3.40 m remained on the log yard of the department sawmill. According to the transport invoice 14.89 m³ (79 logs) of ash (*Fraxinus excelsior* L.) and 16.25 m³ (81 logs) of maple (80 logs of *Acer platanoides* L. and 1 log of *Acer pseudoplatanus* L.) were delivered (with bark). For the yield analysis, round wood sections (logs) with the following characteristics were ordered:

- Round wood quality C or worse (according to the Framework Agreement on Raw Timber Trade in Germany-RVR [29]);
- Length ≥ 3.20 m; and
- Round wood diameter classes 2–3

4. Production Steps and Determination of Characteristics

4.1. Round Wood Sections (Logs)

On the log yard the round wood sections were trimmed uniformly to a length of 3.15 m in order to be able to determine the heartwood coloring (i.e., brown heart) on both ends. At the top (small) end of each trunk a slice of 1–2 cm thickness was cut off. The final cut was performed at the bottom of each trunk (large end) to a length of 3.15 m. Thus, total log volumes were reduced to 14.3 m³ for ash and 15.8 m³ for maple. For each round wood section the minimum and the maximum diameter was determined in the middle of every 25 cm section. The last section only had a length of 15 cm. Using the mean diameter for each 25 cm section and the one 15 cm section (d_{Mn}), the section volumes were calculated with Huber's formula. The single section's volumes were then added up resulting in Equation (1):

$$V_{\text{Sec.}} = \left(\sum_{i=1}^{12} \frac{\pi}{4} \times 0.25 \text{ m} \times d_{Mn}^2 \right) + \frac{\pi}{4} \times 0.15 \text{ m} \times d_{Mn}^2 \text{ [m}^3\text{]} \quad (1)$$

The logs were sorted into diameter classes according to their small-end (top-end) diameter (SED) and into quality classes according to the specifications of the RVR [29] and DIN 1316-3 [30]. Both standards allow the assignment to classes from A (highest quality) to D (lowest quality). The quality-determining characteristics of the round wood sections were determined and recorded in accordance with Annex VIII (Measurement of the characteristics) of the RVR [29]. The characteristics shrinkage cracks, insect holes, tree cancer and the so-called moon ring (light discoloration in heartwood) were not recorded and thus were not part of sorting.

The RVR [29] offers no separate quality grading for maple and ash logs. Thus, depending on the particular characteristic, the oak grading rules (e.g., for knots, star shake, twigs, etc.) or those for beech (only for width of brown heart and heart shake) were used.

4.2. Sawing/Milling

The logs were milled with a mobile horizontal bandsaw headrig (Montana ME 90 2.0 from SERRA, Rimsting, Germany) with a kerf width of 2.45 mm. The cant sawing patterns used are shown in Figure 1.

The sawing patterns and the distribution of board dimensions were chosen for each log separately, mainly depending on the small-end log diameter (d_z or SED). Thus, the maximum yield could be attained. The pattern A was used most. If side boards were produced (colored boards in pattern C), they were edged to square edged lumber on a circular saw. For maple, five different lumber dimensions were sawn, for ash three (see Table 1).

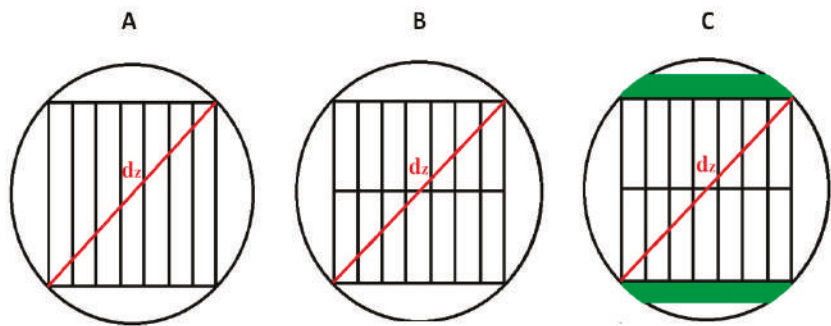


Figure 1. Cant sawing patterns of the milling.

Table 1. Nominal dimensions and quantities (*n*) of sawn green lumber and the resulting planed lamellas (dry-dressed lumber).

Sawn Green Lumber	Planed Lamellas	Maple	Ash
Width × height (mm) × (mm)	Width × height (mm) × (mm)	<i>n</i>	<i>n</i>
115 × 35	100 × 25	88	-
145 × 35	125 × 25	132	-
145 × 40	125 × 30	85	121
115 × 45	100 × 35	92	104
145 × 45	125 × 35	94	162

Only the main product glulam lamella was produced for this study. No side products, like trimming or baseboards, etc., were produced. The side products would raise the final yield. The final product—planed glulam lamellas—were subjected to destructive tensile testing after visual and machine strength grading (see sub sample “TH II” in Kovryga et al. [31]).

4.3. Drying

The technical drying took place in the in-house conventional dryer (HB Drying Systems, Almelo, The Netherlands). The drying parameters were chosen in order to ensure gentle drying of the boards. The drying process took 21 days. To determine the volumetric shrinkage, the dry lumber volume (at 12% moisture content) is subtracted from the sawn lumber (rough green) volume. For this purpose, for each dimension and wood species six lamellas were selected randomly. On these lamellas, the lengths (in mm) were determined with a tape measure on the rough green and the dry lumber. Lumber dimensions (in mm) were measured at intervals of 25 cm—starting and ending at the board ends.

4.4. Presorting and Planing

The dried boards were jointed and planed to glulam lamellas (dry-dressed lumber) with the nominal dimensions presented in Table 1. After the planing process, each lamella that could not attain the nominal dimension (cross-section) on the full length was sorted out (due to a combination of bowing and too little oversize). The volume of the remaining glulam lamellas was calculated by determining their lengths with a tape measure and using the nominal lamella dimensions.

4.5. Strength Grading of Planed Boards

4.5.1. Visual Strength Grading

To assess the quality of hardwood lamellas, different grading methods were used. First, each of the lamellas was visually classified according to the German visual strength grading standard DIN

4074-5 [16] over the entire length. The standard uses ten visual criteria to assign hardwood boards to visual strength grading classes. In the current study, the knottiness, presence of pith, bark inclusion, wane, and fiber deviation (grain angle) were considered.

All relevant grading criteria were measured as defined in DIN 4074-5 [16]. To assess the knottiness—one of the major parameters of strength grading—the criteria single knot (SK) and knot cluster (KC) were used. Single knot or *DIN Einzelast Brett (DEB)* relates the size of the single knot to the lamella width. For grading, the ratio (knot) with the highest value is indicative. Knot cluster (KC) or *DIN Astansammlung Brett (DAB)* is a multiple knot criterion, which considers all knots appearing in a (moving) window of 150 mm. Therefore, the spread of all knots over the 150 mm window is related to the width of the board. The edge knot criterion (E) or *Schmalseitenast* is an optional criterion for boards and represents the penetration depth of the knots appearing on the edge side only. A low value of these visual grading criteria stands for either rare occurrence or small size of the strength reducing knots and vice versa.

The only adjustment made concerns the measurement of the fiber deviation (grain angle). Fiber deviation is defined as an angle between the fibers and loading direction over a certain length and is measured in percent. The grain angle has a significant impact on strength [32]. Most grading standards indicate that the fiber deviation can be measured on drying checks or by the scribing method on the wood surface. Both methods are reported to have limited use for medium-dense hardwoods [33,34]. In the present study, the visible fiber deviation was detected on drying checks and, additionally, the surface was assessed qualitatively for fiber deviations exceeding the limits of DIN 4074-5 [16]. The specimens exceeding the limits are rejected.

Hardwood boards are assigned to the visual grades LS13 (highest quality), LS10 (medium quality) and LS7 (lowest quality) based on the boundary values listed in Table 2. To assign a lamella to a visual grade, all boundary values are to be met. Otherwise, the specimen is assigned to the next lower grade or rejected.

Table 2. Boundary values for grading of hardwood lamellas to visual grades (LS7 to LS13) after DIN 4074-5 [16].

	LS13	LS10	LS7
DEB (SK)	0.2	0.333	0.5
DAB (KC)	0.333	0.5	0.666
Edge knot (E)	—*	—*	—*
Pith	no	no	no
Fibre deviation	7%	12%	16%

* No requirements set.

Additionally, to estimate the effect of the grading parameters pith and DAB on the yield, two grading combinations—one without any requirements on pith and one without any requirements on pith and DAB—are applied to the lamellas.

4.5.2. Combined Visual and Machine Strength Grading

Additionally, the boards were graded using a combined visual and machine grading approach. The procedure was suggested by Frese and Blaß [35] and is used for beech glulam produced after the German technical building approval Z-9.1-679 [5]. This grading approach combines visual grading parameters (i.e., SK and KC) with the dynamic Modulus of Elasticity (MOE_{dyn}), a parameter used in most state of the art grading machines for softwoods. The MOE_{dyn} was determined using the “eigenfrequency” method (laboratory and grading machine ViSCAN by MiCROTEC, Bressanone/Brixen, Italy). In case of ViSCAN, the natural frequency (f) from longitudinal oscillation was combined with the density (ρ) measured by an X-ray source, and the length (l) of the measured specimen (Equation (2)).

In the laboratory, the density was determined using the gravimetric method. Both measurements provide comparable results in terms of R^2 value (0.972).

$$MOE_{dyn} = 4 \times l^2 \times \rho \times f^2 \times 10^6 \tag{2}$$

The combined approach uses separate boundary values for visual grading parameters (i.e., SK, KC) and MOE_{dyn} . The boundaries presented by Frese and Blaß [35] are fitted to beech lamellas. For the present study, the combined grading is optimized for ash and maple and presented by the paper Kovryga et al. [31]. Table 3 shows the combination of boundary values selected for the current study. As example, for maple the “Solution B” and for ash the “Solution C” proposed for combined grading by Kovryga et al. [31] is selected. The presented combination allows grading to three different grades plus reject group. The highest grade shows characteristic tensile strength values (above 38 N/mm²) fitting the tensile strength of finger jointed lamellas stated by Van de Kuilen and Torno [4].

Table 3. Optimized grading rules for combined visual and machine strength grading of ash and maple (according to Kovryga et al. [31]; maple: “Solution B”, ash: “Solution C”).

	Grade	Boundary Values				MOE_{dyn} (kN/mm ²)	Resulting Tensile-Classes
		DEB (SK) (–)	DAB (KC) (–)	Edge knot (E) (–)	Pith (–)		
Maple	1	0.1	0.1	–*	Allowed	13.9	DT38
	2	0.2	0.5	–*	Allowed	12.2	DT25
	3	0.3	0.6	–*	Allowed	10.9	T15
	Reject						
Ash	1	0.2	0.2	–*	Allowed	16.5	DT38
	2	0.3	0.3	–*	Allowed	15.5	DT34
	3	0.4	0.4	–*	Allowed	11.6	DT22
	Reject						

* No requirements set.

4.6. Yield Calculation

For the determination of the total yield, the yields of each single production step are added up. The yield of each production step is calculated by dividing the output product volume by the input volume. How volumes of each intermediate product are calculated and what assumptions are made for these calculations is described above for each production step separately.

5. Results and Discussion

5.1. Grading of Logs

Table 4 shows the sorting of the maple and ash logs into diameter and quality classes. Following the descriptions of Van de Kuilen and Torno [15], the diameter sorting was carried out by considering the small-end diameter (SED) inside bark. The supplied round wood sections mainly cover the diameter classes from 2a to 3b, with individual sections with diameters below 20 cm and over 40 cm. For maple and ash, the bark shows a mean thickness of 0.5 cm. Maple shows a higher number of logs graded to the higher quality classes (B and C) compared to ash.

Table 4. Number of logs per species sorted after small-end diameter (inside bark) class and quality class according to RVR [29].

Diameter Class	2a	2b	3b	4	1b	2a	2b	3a	3b	1b	2a	2b	3a	3b
Quality Class	B				C				D					
Quantity	Maple	3	2	1	4	18	11	9	3	5	14	5	2	3
	Ash	1				8	16	5	1	2	23	19	4	

Tables 5 and 6 show the results of the log quality sorting according to RVR [29] and DIN 1316 3 [30] in detail.

Table 5. Yields in % for quality sorting of logs according to RVR [29] separated after sorting criteria (log characteristics).

Log Characteristics	Maple				Ash			
	A	B	C	D	A	B	C	D
Callused knot (bump)	23	1	76		46		54	
Healthy knot	63	29	9		89	10	1	
Decayed knot	63	31	5	1	89	6	5	
Twigs	76	24			100			
Bump on group of broken of twigs	95	1	4		100			
Star shake/check	60	29	11		4	14	80	3
Heart shake/check	33	61	5	1	81	15	1	3
Frost crack	98		3		99		1	
Ring shake	98	3			99		1	
Bow (Sweep and crook)	48	14	6	33	38	1	5	56
Spiral (twisted) grain	98		3		100			
Rot	99			1	97			3
Log length	99		1		96		4	
Width of brown heart	86	14			25	46	29	
Final quality class of logs		8	56	36		1	38	61

Table 6. Yields in % for quality sorting of logs according to DIN 1316-3 [30] separated after sorting criteria (log characteristics).

Log characteristics	Maple				Ash			
	A	B	C	D	A	B	C	D
Length	99		1		96		4	
Mid-diameter	14	11	70	5		4	9 *	
Callused knot (bump)	25		34	41	47		42	11
Healthy knot	95		5		91	3	6	
Decayed knot	90		8	3	96		4	
Eccentricity of pith	88	13			80	20		
Star shake/check	60		5	35	4			96
Heart shake/check	40	14	46		87	4	9	
Brown heart	66		34		38	25	37	
Bow (Sweep and crook)	61	5	1	33	39	5		56
Rot	99			1	97			3
Final quality class of logs	1	1	26	71			4	96

* No requirements set.

Tables 5 and 6 present the final assignment of the round wood sections into the quality classes (the last row of both tables) based on the individual class assignment for each sorting criterion. Each single criterion's influence on the grading can be seen as well as the total distribution of quality classes per species. For example, according to DIN 1316-3 [30], 71% of the maple logs are graded into the lowest quality class D (see Table 6). The final percentage value is a result of all wood characteristics combined. It can be seen that for maple the grading into the D class is mainly due to the characteristics callused knot, star shake, and bow. When sorting according to the RVR [29] specifications, mainly log bowing is decisive for sorting into class D (see Table 5). Especially in the second lowest grade C, it is observable that the two different quality sorting schemes weigh the different characteristics differently, i.e., have different characteristic's boundary values for the same class. While grading into RVR class C of maple is mainly due to callused knots (76%), DIN 1316-3 [30] sorting into class C is due to a number of characteristics (mid diameter, callused knots, heart shake, and brown heart). Both grading schemes sort the majority of the studied logs into the classes C and D.

In general, the two sorting guidelines for round wood use different lists of characteristics. For example, Table 6 shows that in the case of sorting according to DIN 1316-3 [30] the criterion

mid-diameter leads to a classification into quality class C for 70% of the maple logs and for 96% of the ash logs. Compared to that, the diameter of the logs is not relevant, when sorting according to RVR [29]. The possible advantage of the absence of log size criteria is that the actual visible log quality can be assessed and used to qualify the logs for the production in addition to the diameter.

Looking at Tables 5 and 6, it also becomes obvious that—under the same storage conditions—ash logs tend to form more severe end cracks (star and heart shake) than maple. This cracking results in a serious deterioration of quality and leads to a reduced sawn lumber yield (mainly value yield). Thus, it is recommended to saw (mill) ash logs shortly after logging or adapt storage (e.g., water storage) to ensure the best possible lumber quality and highest yield. Short storage times’ respectively adjusted storage conditions are also advised for maple logs, since fungal discoloration starting from the log ends presents problems [27]. For an end use as construction material, though, these discolorations may be of low significance, since they do not affect the elasto-mechanic properties of the lumber.

5.2. Yields from Logs to Unsorted Glulam Lamellas

Table 7 summarizes the volume losses and the resulting yields for each production step. It can be seen that the major production losses arise from sawing the logs and presorting the dried boards. Both species do not differ considerably.

Table 7. Yield for each production step from logs to planed lamellas (unsorted).

Product	Production Step (PS)	Maple				Ash			
		Yield		Waste/Loss		Yield		Waste/Loss	
		in m ³	in %	in m ³	in % PS	in m ³	in %	in m ³	in % PS
Logs		15.8				14.3			
Boards (green)	Milling/sawing			7.6	48.2			7.1	49.5
		8.2	51.8			7.2	50.5		
Boards (dry)	Drying			0.7	8.7			0.8	10.7
		7.5	47.3			6.5	45.1		
	Presorting & planing			4.2	56.3			3.8	59.6
Planed lamellas		3.3	20.9			2.6	18.2		

5.2.1. Sawing/Milling

The mean volume yield of sawing the 81 maple logs by the cant sawing method to square-edged lumber is 51.8%. The mean volume yield of sawing the 79 ash logs is with 50.5% slightly lower. The log diameter strongly influences the volume yield of this production step. The effect the mid-diameter has on the sawing yield of this study can be observed in Figure 2.

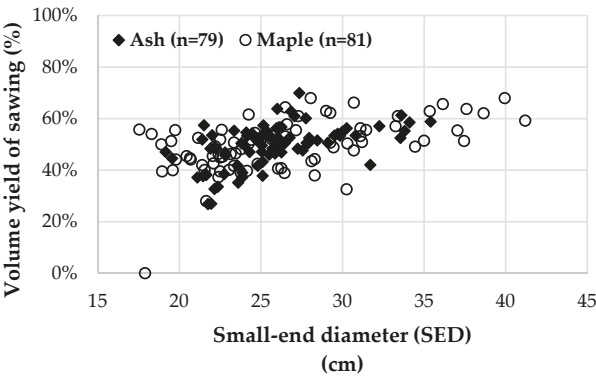


Figure 2. Volume yield of sawing ash and maple depending on the small-end log diameter (inside bark).

The higher the log diameter gets, the higher the yield gets. The variation in sawing yield values drops with increasing diameters, as the influence of the log grade (quality class) on the yield decreases. Compared to the log diameter, the quality class only has a minor influence. Wade et al. [36] analyzed data from 35 US hardwood mills and also concluded that a positive linear relationship between log diameter and sawing yield (in their case LRF) exists. In the simulation of Richards et al. [20] hardwood sawing yields of sawing low dimension logs (SED = 25 cm) by the cant sawing method start at 56.1%, while from logs with large diameters (SED = 71 cm) up to 67.2% rough green lumber can be produced. In Ehlebracht [17] only one of four hardwood mills attained a sawing yield of 57%, when cant sawing low-dimensional hardwood logs. Two mills achieved yields like this study (50% and 51%), while a mill with a circular saw headrig only reached 36% volume yield. All presented studies show that it is economically advantageous to sort out logs with diameters below a certain value. The boundary value for the diameter has to be determined for each production site and product separately. The results of Wiedenbeck et al. [13] give rise to the assumption that this boundary value also depends on the wood species sawn.

Lin et al. [14] prove that the log grade (quality class) has an effect on the hardwood volume recovery. In this study, this is only observed in the lower log diameter classes. The individual characteristics eccentricity of pith, ovality and taper show no significant influence on the yield of the first production step. The two latter characteristics are not part of the RVR [29] and DIN 1316-3 [30] sorting standards. Nonetheless, their influence on the yield during production is examined. For ash, the degree of bowing (in one direction) has no influence on the yield of milling. For maple, increased bowing (in one direction) leads to a decreased yield of milling. Multiple bows in one log (in one or more directions) decrease the yield of milling significantly. Comparing logs with one bow in only one direction with logs with multiple bows, the yield is reduced from 52.7% to 43.7% for maple and from 51.7% to 46.1% for ash. The same relationship—but less pronounced—can be found in so-called butt-cuts. In these first logs of trees taken above the stump, the milling process removes a high volume of wood from the large end of the log.

5.2.2. Drying

Drying of the green lumber was carried out for all dimensions and species with the same slow drying program, in order to avoid damages due to inadequate (i.e., too fast) drying. For maple, the volumetric shrinkage lies between 8.0% and 8.9% (average 8.7%), while for ash it lies between 9.6% and 11% (average 10.7%). For both species, these values lie in the lower range of the above-mentioned literature values. In some cases, the boards started warping (bowing, crooking, cupping, twisting, etc.) immediately after or even during the milling due to inherent tension in the trunks (eccentric pith, reaction wood, around big knots, etc.). Nonetheless, these boards were stacked and underwent drying.

5.2.3. Presorting and Planing

Before planing the dried boards, they were pre-sorted. Boards with extreme bowing were sorted out. If the infeed and outfeed rollers of the planer were able to press down the bow, resulting in fully planed board surfaces, the lamellas were not sorted out. Nevertheless, the volume loss of this production step is 56.3% for maple and 59.6% for ash. The resulting total yields of planed boards (unsorted glulam lamellas) are, thus, 20.9% for maple and 18.2% for ash. If the presorting was excluded from this calculation, i.e., if the bows were cut out (resulting in shorter lamella lengths) and thus all boards could be planed to the nominal dimensions, total yield values of 33.4% (maple) and 33.2% (ash) could be obtained. For future investigations, it is planned to evaluate the influence round wood quality has on presorting and planning losses. Especially for low-dimension logs of poor quality the question arises, how much of the resulting twisting and bowing in the dried lumber is due to the drying process and how much is already present in the rough green lumber.

5.3. Strength Grading of Glulam Lamellas (Planed Boards)

5.3.1. Grading Results

As explained in Section 4.5, the planed boards were graded visually according to the German visual strength grading standard DIN 4074-5 [16]. Furthermore, the result of two adjusted grading schemes were compared—when the criterion “pith” is excluded from visual strength grading according to DIN 4074-5 [16] and when only single knots (DEB) are evaluated according to DIN 4074-5 [16]. Additionally, the lamellas were graded following the combined visual and machine grading proposed by Kovryga et al. [31] and presented in Table 3.

Figure 3 shows the grading results for ash and maple, respectively. The second box of each diagram gives the results of visual grading according to DIN 4074-5 [16]. For both ash and maple, only few boards are sorted into the classes LS7 and LS10. The majority is either sorted into the highest quality class LS13 or rejected. When excluding the criterion pith from DIN 4074-5 [16] sorting (see third box), no ash lamellas and four maple lamellas were rejected. The majority of the lamellas is graded into LS13 (ash: 195; maple: 238). Only applying the DIN 4074-5 [16] boundary values for the criterion DEB (single knot) gives almost identical sorting results. The combined grading proposed and optimized by Kovryga et al. [31] for the here studied lamellas result in a relatively even distribution of lamellas over the three grades. For ash 6.8% and for maple 15.7% of the lamellas are rejected.

For grading according to DIN 4074-5 [16], a high effect of the pith criterion on the grade class assignment can be stated. Grading with pith as rejection criterion results in a reject rate of 48% for the ash boards and 38% for the maple boards. If the pith criterion is excluded from grading, none of the ash boards and only 1% of the maple boards are rejected. Similar results are reported by Torno et al. [12], who detected pith in 26% and 30% of the graded beech boards. Here the sawing pattern was similar to this study, but logs with larger diameters were sawn. Van de Kuilen and Torno [15] calculated for their study the ratio of pith containing board volume to initial round wood volume (inside bark) to be 0.2% for ash and 0.9% for beech. In this study, this ratio is 9.1% for ash and 8.0% for maple. This much higher appearance of pith can be explained by the fact that lower dimension logs were sawn and the overall log quality was poorer. Furthermore, the study of Van de Kuilen and Torno [15] used a special sawing pattern (“sawing around the log” or “grade sawing”) designed to produce boards without pith. Generally, it can be concluded that the sawing pattern and the low log dimensions chosen for this study resulted in a high amount of pith boards, which have to be sorted out, when sorting according to DIN 4074-5 [16]. Pith is also the main downgrading criterion in the grading of ash and maple lamellas studied by Glos and Torno [28]. The rest of the boards of this study show good quality for both species, resulting in a high proportion in LS13 grading.

One explanation for the higher amount of pith containing boards in the ash compared to the maple collective can be the fact that in ash trees the pith is typically “wandering”, which is due to crooked growth in early years [17,37]. Other reasons can be more severe bowing of the ash logs or littler log dimensions. Figure 4 proves that the small-end diameters are not severely different for the 81 maple and 79 ash log sections.

The bowing of the raw material was according to RVR [29] specifications only measured for log sections that had one bow over the entire log length. This criterion shows now difference between the species ash and maple as well (see Figure 4). Checking the number of logs with compound bowing (bowing into two or more directions) reveals a different picture, though. While only 55% of the maple log sections are characterized by compound bowing, 77% of the ash log sections have compound bows. This could be an explanation for the higher amount of pith containing boards in the ash collective. Since the collected data does not contain information on the degree of compound bowing, one cannot distinguish between the influence of the “wandering pith” and the log section bowing.

To finalize the discussion of the effect of the grading parameters on the yield, the effect of the knot cluster criterion (DAB) is observed. Comparing both visual grading options—for DIN 4074-5 [16] “without considering pith” and “only DEB (without considering pith and DAB)”—little to no changes

can be observed (see Figure 3). The added value (information) of DAB for grading is illustrated in Figure 5, which plots the maximum DEB against maximum DAB values for all ash and maple boards. The paired values (boards) on the bisector show those boards, where the maximum DEB is bigger than or equal to any found DAB. For all other boards a DAB greater then the DEB is reported. The grey area indicates those boards, for which the criterion DAB leads to a sorting class downgrading, when sorting according to for DIN 4074-5 [16]. This is the case for only twelve maple boards (3.7%) and three ash boards (1.4%). Therefore, the criterion knot cluster (DAB) is not decisive for downgrading into a lower sorting class, if graded after DIN 4074-5 [16].

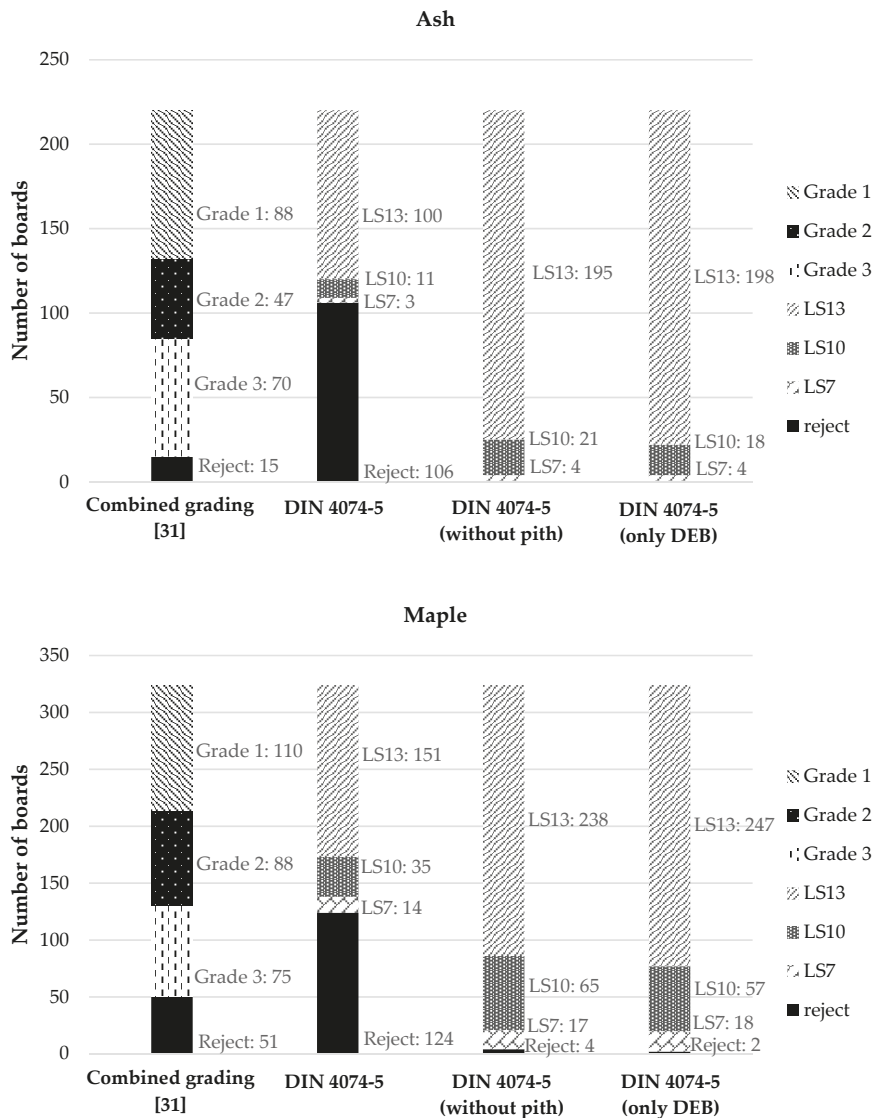


Figure 3. Yields for the combined (left bar) and visual grading (three right bars) of the planed ash and maple boards.

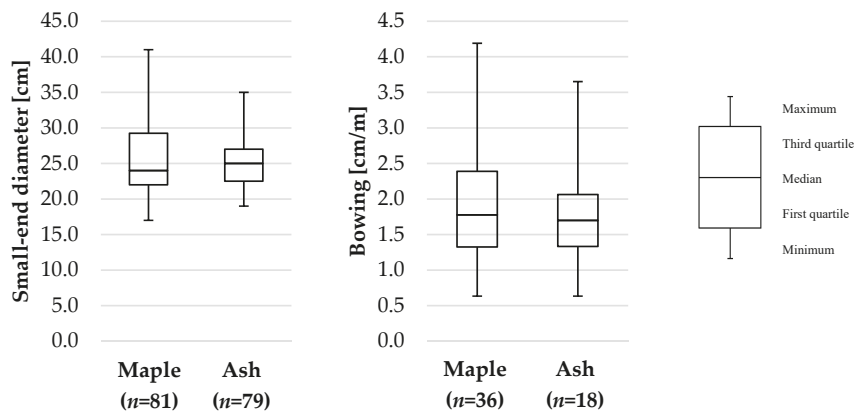


Figure 4. Boxplots for log section small-end diameter and bowing (only in one direction according to RVR instructions) separated after species (n = number of log sections).

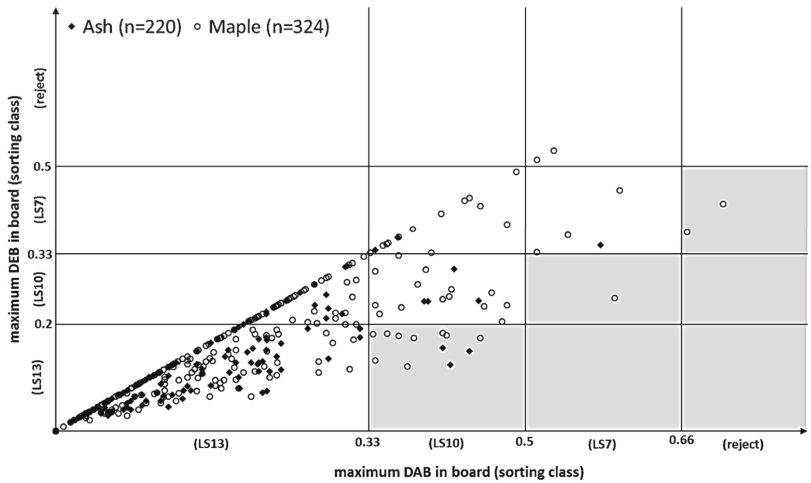


Figure 5. Maximum knot ratio of single knot (DEB) and knot cluster (DAB) for ash and maple boards. For all boards in grey area the criterion knot cluster (DAB) leads to downgrading into lower sorting class.

This confirms the findings made by other authors for the hardwood species beech. Frese and Riedler [38] postulate that for flat sawn beech lamellas (with lying annual rings) the sorting criterion DAB is not decisive for downgrading. Glos and Lederer [33] state that out of 219 beech boards only for one board the criterion DAB is sorting class determining. Blaß et al. [2] find similar results for a set of 350 beech boards (for 1.4% DAB decisive) and another set of 1888 beech boards (for 0.4% DAB decisive).

When applying stricter boundary values for the DAB than stated by the DIN 4074-5 [16], the DAB's influence on the grade rises. In the combined grading proposed by Kovryga et al. [31], the boundary values for DEB and DAB for ash were set to be identical—i.e., the strictest DAB setting possible. Thus, 13.6% of the ash lamellas of this study are downgraded due to the criterion DAB (cluster knot). For maple grading according to the settings proposed by Kovryga et al. [31] only 6.5% of the studied lamellas are downgraded due to the criterion DAB (cluster knot). This is because the proposed DAB boundary values for maple are not as strict as for ash. Regarding knot clusters (DAB), Figure 5 suggests that the investigated maple wood contains proportionally more knot clusters than the ash wood. Further analysis reveals only a difference of 6%, though. A total of 33% of the ash boards and 39%

of the maple boards contain knot clusters (greater than the max. DEB). Figure 6 shows that these maximum knot clusters are bigger in the maple collective than in the ash collective. The same holds for single knots. This leads to a higher proportion of LS7 and LS10 boards in the maple collective compared to the ash group (see Figure 3).

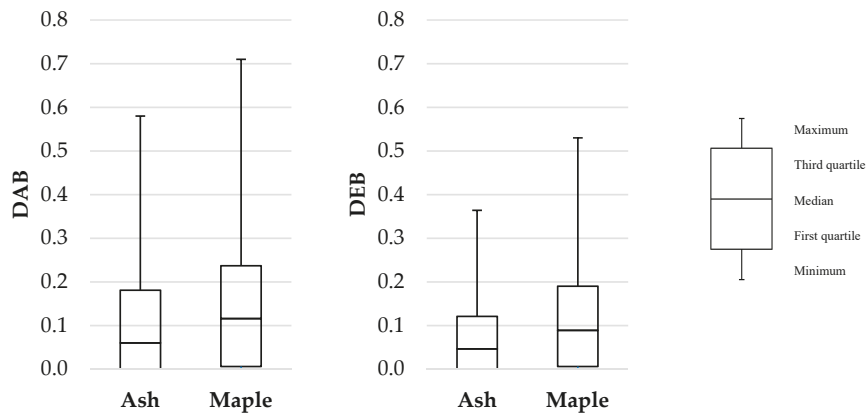


Figure 6. Boxplots separated after sorting criteria (maximum DEB and DAB in board) and species.

In general, special care must be taken when comparing grading results of different publications. The research material can be extremely diverse (i.e., species, origin, quality, sawing pattern, etc.), but also data acquisition for grading can be different. For example, Glos and Torno [28] grade the evaluated lumber only after the sorting criteria occurring within the tension test length, while for this study the entire board length is evaluated. Furthermore, the sorting criterion “grain angle” is a source of confusion, since its visual determination on unbroken boards is problematic [33,34].

5.3.2. Yields of Graded Lumber

The four sorting schemes presented in Figure 3 lead to different rates of so-called “rejects”, i.e., boards that have to be sorted out. Table 8 lists the relative and absolute losses for the production step “grading” for each grading scheme and the resulting overall yields (referring to the round wood volume).

Table 8. Volume yields for the production step grading (from planed board to graded lamella) for four different grading schemes.

Product	Options for Production Step Grading	Maple				Ash			
		Yield		Waste/Loss		Yield		Waste/Loss	
		in m ³	in %	in m ³	in % PS	in m ³	in %	in m ³	in % PS
Boards planed (unsorted lamellas)		3.3	20.9			2.6	18.2		
	Grading I (Combined grading according to Kovryga et al. [31])			0.5	15.7			0.2	6.8
Combined grading lamellas		2.8	17.8			2.4	17.0		
4074-5 lamellas	Grading II (4074-5)			1.3	39.0			1.3	49.8
	Grading III (4074-5 without pith)	2.0	12.7	0.04	1.3	1.3	9.1	0	0
4074-5 lamellas without pith		3.3	20.6			2.6	18.2		
4074-5 lamellas (only DEB)	Grading IV (4074-5, only DEB)			0.02	0.7			0	0
		3.3	20.8			2.6	18.2		

When grading the lamellas according to DIN 4074-5 [16], for ash yield values lie around 9%, for maple around 13%. When excluding the sorting criterion “pith”, total yields of ash are doubled (18.2%), those of maple rise to 20.6%. The difference between grading scheme III and IV is very little to none. This is due to the fact that the DAB (KC) has very little influence on the strength grading according to DIN 4074-5 [16].

As Table 8 shows, excluding the sorting criterion pith from the sorting scheme, raises the final yield considerably. Since board tension strength is the key influencing factor on glulam bending strength, tension testing of glulam lamellas has to show the effect the pith has on the board tension strength and stiffness (see [31]). If this influence is neglectable, the yield of grading can be raised extremely. It is important to state, though, that this does not hold equally for other strength properties. Glos and Torno [28], for example, prove for ash and maple that pith has a significant influence on the bending strength of square-edged lumber. They also stress the fact that the appearance of pith is often accompanied by bows, twists, and cracks. Similar results are presented by Glos and Lederer [33] for beech and oak square-edged lumber. Hübner [39] proves the pith’s significant influence on the tension strength perpendicular to grain of ash glulam.

Further research has to work towards a hardwood strength grading system that is based on the mechanical properties of the resulting glulam. Kovryga et al. [31] proposes different optimized grading schemes for ash and maple glulam lamellas. For this study, one optimized combined grading solution from Kovryga et al. [31] was chosen for each species (see Table 3) to show an example of resulting yield. The chosen grading scheme distinguishes between three grades resulting in three board tensile strength classes based on destructive tension testing. For ash, the lowest class is DT22 with a characteristic tensile strength higher than 22 N/mm². For hardwoods, Kovryga et al. [40] proposes no tensile strength class lower than DT18. For lower mechanical properties softwood T-classes can be used. Therefore, for maple the lowest class is T15 (softwood tensile strength class) with a characteristic tensile strength not lower than 15 N/mm² (see Table 3). In this study, the proposed strength grading results in 15.7% rejects for maple and 6.8% rejects for ash. The resulting yields of 17.8% and 17.0% are considerably higher compared to grading according to DIN 4074-5 [16].

The economic feasibility of the production of hardwood glulam is strongly influenced by the final yield of glulam lamellas. Torno et al. [12] calculated that the production of beech glulam lamellas costs at least three times as much as that of spruce lamellas, calculating with beech round wood prices of €53.50–€80.00 per cubic meter. Since final yield figures of this study and Torno et al. [12] lie in a similar range, these costs can also be assumed for the lamellas of this study. This makes raising the yield inevitable, if a competitive hardwood product shall be produced.

When evaluating the competitiveness of a product, not only the production cost, but also the added value should be considered. Following the proposed combined grading of Kovryga et al. [31], for this study strength classes with a characteristic tensile strength as high as 38 N/mm² can be produced. With ash lamellas of this characteristic strength, glulam with bending strength values of as high as 48 N/mm² can be achieved [4]. Via “upgrading”, i.e., cutting out large knots, the characteristic tensile strength of ash lamellas can be raised up to 54 N/mm² [31]. Using the combined grading approach for beech lamellas, Erhardt et al. [41] report tensile strength values of as high as 50 N/mm². This raised strength allows the production of more slender structures, which means material savings but also more construction possibilities for the architect and engineer. The listed benefits would yield obviously in higher reward for the producer. Although the present market situation has not led to a wide spread use of hardwood glulam, future changes in spruce availability, round wood prices (especially hardwood) and wood processing technology (etc.) might make the production lucrative.

6. Conclusions

For this study, the volume yields of the production of glulam lamellas from low quality and low dimension ash and maple log sections are investigated. For this purpose, 16.25 m³ of maple (81 log sections) and 14.89 m³ of ash (79 log sections) were harvested from natural forest stands (mixed beech

forests) in central Germany and were turned into dry-dressed lumber (unsorted lamellas) with state of the art technologies. The resulting board volumes amount for only 20.9% (maple) and 18.2% (ash) of the original log volumes. The most waste is produced in the production step “presorting and planing” (maple: 56%; ash: 60%), since here a high percentage of the boards has to be sorted out due to bowing. By trimming these boards to shorter lengths, the waste of this production step could be reduced considerably. In addition, the sawing (milling) of the boards produced in both cases around 50% waste, which is in line with the above-mentioned literature values for sawing low-quality hardwoods. Nonetheless, with an adjusted sawing technology, this waste can be reduced (e.g., through shorter log sections and optimized machine combinations). It is also advisable to define a minimum input log diameter, since the lower the log diameter is, the lower the volume yield of milling becomes. Another approach to a raised final volume and value yield is the diversification of final products. Thus, as an example, glulam lamellas could be produced as a low-quality co-product from the production of high quality lumber for furniture production.

Strength grading of lamellas lowers final volume yields even further. When sorting the lamellas according to DIN 4074-5 [16], final volume yields of 12.7% for maple and 9.1% for ash are attained. One way of raising the final volume and also value yield could be the adjustment of the sorting (grading) scheme. For example, by excluding the criterion “pith” from sorting, final yield values of 20.6% (maple) and 18.2% (ash) can be achieved. Generally, it is advisable to combine visual and machine sorting to an assortment and species adjusted combined grading, which is optimized after the criteria “desired tensile strength and stiffness” but also “yield”. The paper Kovryga et al. [31] is attempting this. Resulting total yields, when applying the selected optimized combined grading of Kovryga et al. [31] to this study’s lumber, lie between 17% and 18%. This yield is considerably lower than that obtained for softwood glulam lamellas. Factors like the higher attainable tensile strength, if compared to 30 N/mm² possible for softwoods [42], and the appealing appearance of hardwood glulam may make up for the yield disadvantages. In general, the economic feasibility of hardwood glulam is influenced by a serious of factors, which have to be analyzed in detail for each final product and production plant separately.

Author Contributions: Conceptualization, methodology, investigation, formal analysis, visualization, and writing—original draft preparation: P.S. and A.K.; data curation and investigation: L.E.; funding acquisition, project administration, supervision, and writing—review and editing: S.B.; resources, supervision, and writing—review, and editing: J.W.V.d.K. and H.M.

Funding: This study was funded by the German Federal Ministry of Food and Agriculture (grant number 22024211).

Acknowledgments: We thank Antje Gellerich for giving helpful advice during data acquisition.

Conflicts of Interest: The authors declare no conflict of interest.

References

1. Sauter, U. WP 1: Hardwood Resources in Europe—Standing Stock and Resource Forecasts. Presented at Workshop “European Hardwoods for the Building Sector”, Garmisch-Patenkirchen, Germany, 2016.
2. Blaß, H.J.; Denzler, J.; Frese, M.; Glos, P.; Linsenmann, P. *Biegefestigkeit Von Brettschichtholz Aus Buche [Bending Strength of Beech Glulam]*; Karlsruher Berichte zum Ingenieurholzbau, Band 1 Karlsruher Berichte zum Ingenieurholzbau; Universitätsverlag Karlsruhe: Karlsruhe, Germany, 2005.
3. Frühwald, A.; Ressel, J.B.; Bernasconi, A.; Becker, P.; Pitzner, B.; Wonnemann, R.; Mantau, U.; Sörgel, C.; Thoroe, C.; Dieter, M.; et al. *Hochwertiges Brettschichtholz Aus Buchenholz [High Quality Glulam Made of Beech Wood]*; Final Report; University of Hamburg: Hamburg, Germany, 2003.
4. Van de Kuilen, J.W.; Torno, S. *Materialkennwerte von Eschenholz Für Den Einsatz in Brettschichtholz [Material Properties of Ash Wood for the Use in Glulam]*; Final Report; Holzforschung München, Technische Universität München: Munich, Germany, 2014.
5. DIBt. BS-Holz aus Buche und BS-Holz Buche-Hybridträger [Glulam and hybrid glulam made of beech]; German technical building approval Z-9.1-679; holder of approval: Studiengemeinschaft Holzleimbau e.V., Germany; issued by Deutsches Institut für Bautechnik (DIBt), Germany; valid until 27.10.2019. 2014.

6. OiB. VIGAM—Glued laminated timber of oak; ETA-13/0642 European Technical Approval; holder of approval: Elaborados y Fabricados Gámiz, S.A., Spain; issued by Austrian Institute of Construction Engineering (OiB), Austria; valid until 27.06.2018. 2013.
7. DIBt. Holz Schiller Eiche-Pfosten-Riegel-Brettschichtholz [Timber Schiller oak post and beam glulam]; German technical building approval Z-9.1-821; holder of approval: Holz Schiller GmbH, Germany; issued by Deutsches Institut für Bautechnik (DIBt), Germany; valid until 02.03.2018. 2013.
8. OiB. Sierolam—Glued laminated timber of chestnut; ETA-13/0646 European Technical approval; holder of approval: Siero Lam, S.A., Spain; issued by Austrian Institute of Construction Engineering (OiB), Austria; valid until 27.06.2018. 2013.
9. Mack, H. The European Market for Glulam—Results of a Survey within the European Glued Timber Industry. In Proceedings of the “Wiener Leimholz Symposium 2006”, Vienna, Austria, 23–24 March 2006; pp. 35–50.
10. Ohnesorge, D.; Hennig, M.; Becker, G. Bedeutung von Laubholz bei der Brettschichtholzerstellung [Significance of hardwoods in glulam production]. *Holztechnologie* **2009**, *6*, 47–49.
11. Welling, J. Differences between hard—and softwoods and their influence on processing and use. In Proceedings of the “Gülzower Fachgespräche Stoffliche Nutzung von Laubholz”, Würzburg, Germany, 6–7 September 2012.
12. Torno, S.; Knorz, M.; Van de Kuilen, J.W. Supply of beech lamellas for the production of glued laminated timber. In Proceedings of the 4th International Scientific Conference on Hardwood Processing, Florence, Italy, 7–9 October 2013; pp. 210–217.
13. Wiedenbeck, J.; Scholl, M.S.; Blankenhorn, P.R.; Ray, C.D. Lumber volume and value recovery from small—diameter black cherry, sugar maple, and red oak logs. *BioResources* **2017**, *12*, 853–870. [[CrossRef](#)]
14. Lin, W.; Wang, J.; Wu, J.; DeVallance, D. Log Sawing Practices and Lumber Recovery of Small Hardwood Sawmills in West Virginia. *For. Prod. J.* **2011**, *61*, 216–224. [[CrossRef](#)]
15. Van de Kuilen, J.W.; Torno, S. *Untersuchungen Zur Bereitstellung von Lamellen Aus Buchen- Und Eschenholz Für Die Produktion von Brettschichtholz* [Studies on the Supply of Lamellas for the Production of Glulam from Beech and Ash Wood]; Final Report X37; Holzforschung München, Technische Universität München: Munich, Germany, 2014.
16. DIN 4074-5. *Strength Grading of Wood—Part 5: Sawn Hardwood*; German Institute for Standardization (DIN): Berlin, Germany, 2008.
17. Ehlebracht, V. *Untersuchung Zur Verbesserten Wertschöpfung Bei Der Schnittholzerzeugung Aus Schwachem Buchenstammholz (Fagus Sylvatica L.)* [Investigation on improved Added Value in the Production of Sawn Lumber from Low Dimension Beech Timber]. Dissertation, Georg-August-Universität Göttingen, Göttingen, Germany, 2000.
18. Eickers, A. *Verschnittuntersuchungen Bei Der Verarbeitung von Brettschichtholzlamellen* [Yield Loss in the Production of Glulam Lamellas]. Diploma Thesis, Fachhochschule Hildesheim/Holzminden, Hildesheim, Germany, 1997.
19. Steele, P.H. *Factors Determining Lumber Recovery in Sawmillin*; General Technical Report FPL-39; U.S. Department of Agriculture, Forest Service, Forest Products Laboratory: Madison, WI, USA, 1984.
20. Richards, D.B.; Adkins, W.K.; Hallock, H.; Bulgrin, E.H. *Lumber Values from Computerized Simulation of Hardwood Log Sawing*; Research Paper FPL-356; U.S. Department of Agriculture, Forest Service, Forest Products Laboratory: Madison, WI, USA, 1980.
21. Emhardt, M.; Pflingstag, S. *Schnittholzqualität und Ausbeute von Schwachem Buchenstammholz* [Sawn Lumber Quality and Yield Produced from Low Dimension Beech Logs]; Final Report; FVA Baden-Württemberg: Freiburg, Germany, 1993.
22. Fronius, K. *Arbeiten Und Anlagen Im Sägewerk—Spaner, Kreissäge, Bandsäge* [Work and Machines in a Sawmill—Chipper Canter, Circular Saw, Band Saw], 2nd ed.; DRW-Verlag Weinbrenner: Leinfelden-Echterdingen, Germany, 1989.
23. Fischer, H. *Neue Verwendungsmöglichkeiten von Laubschwachholz* [New Possible Uses for Low Dimensions Hardwood Timber]; Internal Report; Forstliche Versuchsanstalt Rheinland-Pfalz: Trippstadt, Germany, 1996.
24. Lamb, F.M.; Wengert, E.M. Techniques and procedures for the quality drying of oak lumber. In Proceedings of the 41st Meeting of the Western Dry Kiln Association, Corvallis, OR, USA, 1990.
25. Denig, J.; Wengert, E.M.; Simpson, W.T. *Drying Hardwood Lumber*; General technical Report FPL-GTR-118; U.S. Department of Agriculture, Forest Service, Forest Products Laboratory: Madison, WI, USA, 2000.

26. Kollmann, F.; Côté, W.A., Jr. *Principles of Wood Science and Technology, I. Solid Wood*; Springer: Berlin, Heidelberg, 1968.
27. Wagenführ, R. *Holzatlas*; Fachbuchverlag im Carl Hanser Verlag: Leipzig, Germany, 2007.
28. Glos, P.; Torno, S. *Aufnahme Der Einheimischen Holzarten Ahorn, Esche und Pappel in Die europäische Norm EN 1912: "Bauholz – Festigkeitsklassen— Zuordnung von Visuellen Sortierklassen und Holzarten"* [Inclusion of the Native Wood Species Maple, Ash and Poplar in the European Standard EN 1912: "Structural Timber—Strength Classes—Assignment of Visual Grades and Species"]; Final Report 06517; Holzforschung München, Technische Universität München: Munich, Germany, 2008.
29. RVR. *Rahmenvereinbarung Für Den Rohholzhandel in Deutschland (RVR) [Framework Agreement on Raw Timber Trade in Germany]*; Deutscher Forstwirtschaftsrat & Deutscher Holzwirtschaftsrat: Berlin, Germany, 2015.
30. DIN 1316-3. *Hardwood Round Timber—Qualitative Classification—Part 3: Ash and Maples and Sycamore*; German Institute for Standardization (DIN): Berlin, Germany, 1997.
31. Kovryga, A.; Schlotzhauer, P.; Stapel, P.; Miltitz, H.; Van de Kuilen, J.W. Visual and machine strength grading of European ash and maple for glulam application. *Holzforschung* **2019**, *0*. [[CrossRef](#)]
32. Hankinson, R.L. *Investigation of Crushing Strength of Spruce at Varying Angles of Grain*; Air Service Information Circular No. 259; U.S. Air Service: Washington, DC, USA, 1921.
33. Glos, P.; Lederer, B. *Sortierung von Buchen-Und Eichenschmitt Holz Nach Der Tragfähigkeit Und Bestimmung Der Zugehörigen Festigkeits-Und Steifigkeitskennwerte [Strength Grading of Beech and Oak Lumber and Determination of Characteristic Strength and Stiffness Values]*; Final Report; Institut für Holzforschung, Technische Universität München: Munich, Germany, 2000.
34. Frühwald, A.; Schickhofer, G. Strength grading of hardwoods. In Proceedings of the 14th International Symposium on Nondestructive Testing of Wood, Eberswalde, Germany, 2–4 May 2005.
35. Frese, M.; Bläß, H.J. Beech glulam strength classes. In Proceedings of the Meeting 38 of the International Council of Research and Innovation in Building and Construction, Working Commission W18—Timber Structures, Karlsruhe, Germany, 2005.
36. Wade, M.W.; Bullard, S.H.; Steele, P.H.; Araman, P.A. Estimating Hardwood Sawmill Conversion Efficiency Based on Sawing Machine and Log characteristics. *For. Prod. J.* **1992**, *42*, 21–26.
37. Torno, S.; Van de Kuilen, J.W. Esche für tragende Verwendungen—Festigkeitseigenschaften visuell sortierten Eschenholzes [Ash for load bearing use—Strength properties of visually graded ash lumber]. *LWF Aktuell* **2010**, *77*, 18–19.
38. Frese, M.; Riedler, T. Untersuchung von Buchenschmitt Holz (Fagus sylvatica L.) hinsichtlich der Eignung für Brettschichtholz [Examination of suitability of beech lumber for glulam]. *Eur. J. Wood Wood Prod.* **2010**, *68*, 445–453. [[CrossRef](#)]
39. Hübner, U. Mechanische Kenngrößen von Buchen-, Eschen- Und Robinienholz Für Lastabtragende Bauteile [Mechanical parameters of Beech, Ash and Locust Lumber for Load Bearing Members]. Ph.D. Thesis, Technische Universität Graz, Graz, Austria, 2013.
40. Kovryga, A.; Stapel, P.; Van De Kuilen, J.W. Tensile strength classes for hardwoods. In Proceedings of the 49th INTER & CIB Meeting, Graz, Austria, 2016.
41. Erhardt, T.; Fink, G.; Steiger, R.; Frangi, A. Strength grading of European beech lamellas for the production of GLT & CLT. In Proceedings of the 49th INTER & CIB Meeting, Graz, Austria, 2016.
42. EN 338. *Structural Timber—Strength Classes*; European Committee for Standardization: Brussels, Belgium, 2016.



© 2019 by the authors. Licensee MDPI, Basel, Switzerland. This article is an open access article distributed under the terms and conditions of the Creative Commons Attribution (CC BY) license (<http://creativecommons.org/licenses/by/4.0/>).

Construction of Wood-Based Lamella for Increased Load on Seating Furniture

Nadežda Langová, Roman Réh, Rastislav Igaz, Ľuboš Krišťák *, Miloš Hitka and Pavol Joščák

Faculty of Wood Sciences and Technology, Technical University in Zvolen, 960 01 Zvolen, Slovakia; langova@tuzvo.sk (N.L.); reh@tuzvo.sk (R.R.); igaz@tuzvo.sk (R.I.); hitka@tuzvo.sk (M.H.); joscak@tuzvo.sk (P.J.)

* Correspondence: kristak@tuzvo; Tel.: +421-4552-06836

Received: 9 May 2019; Accepted: 18 June 2019; Published: 25 June 2019

Abstract: The research on population shows that the count of overweight people has been constantly growing. Therefore, designing and modifying utility items, e.g., furniture should be brought into focus. Indeed, furniture function and safety is associated with the weight of a user. Current processes and standards dealing with the design of seating furniture do not meet the requirements of overweight users. The research is aimed at designing flexible chairs consisting of lamellae using the finite element method (FEM). Three types of glued lamellae based on wood with different number of layers and thickness were made and subsequently, their mechanical properties were tested. Values for modulus of elasticity and modulus of rupture were used to determine stress and deformation applying the FEM method for modelling flexible chairs. In this research, the methodology for evaluating the ultimate state of flexible chairs used to analyse deformation and stability was defined. The analysis confirms that several designed constructions meet the requirements of actual standards (valid for the weight of a user up to 110 kg) but fail to meet the requirements for weight gain of a population.

Keywords: glued lamella; flexible chair; weight of a user; ultimate state

1. Introduction

Requirements of the construction design of furniture for sitting arise from the needs to ensure that healthy sitting provides physical, mental and social comfort for users. Promoting correct posture with high quality lumbar support (total surface pressure is reduced as much as possible) and the ability to change positions while sitting are two ways to make users feel comfortable over long periods of usage. Correct sitting positions may prevent permanent spinal deformity or lower quality of life physiology, such as breathing, digestion, etc. [1]. Several requirements must be taken into consideration while designing seating furniture, but two of them are considered essential: Various measurements of the human body (especially height), and different weight and human body shapes must be taken into account.

Determining the appropriate single weight for all users is a difficult process as weight gain has recently been reported all over the world. In many countries, population weight gain is seen as part of the global obesity epidemic [2–8]. Data from 591 local and 369 national research studies were used by the author [9]. Another study based on 450 national studies determined the trends in weight gain from 1990 to 2020 [10]. The data mentioned in both research studies, as well as in many others, have showed overall weight gain in recent decades [11–13]. Regional and national studies in European countries (Figure 1) show that the situation is very similar all over Europe [14–17]. In 2002, the 95th, 98th and 99th percentiles for the body weight of men in the US were 114.6 kg, 131.61 kg and 141.17 kg [18].

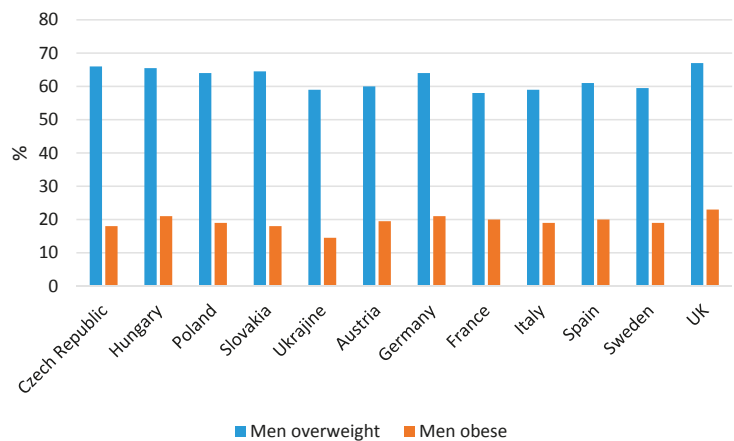


Figure 1. Overweight and obese men in European countries in 2016 [19].

Similar increase in average weight of users has been observed in the Slovak population as well. In 2017, the weight of more than 5% Slovak men was 110 kg (Figure 2). Moreover, the weight of 11% of these men was more than 130 kg. Based on BMI data in Slovakia, in 2017, 400,000 men in Slovakia suffered from obesity and 90,000 men suffered from severe obesity [19–23].

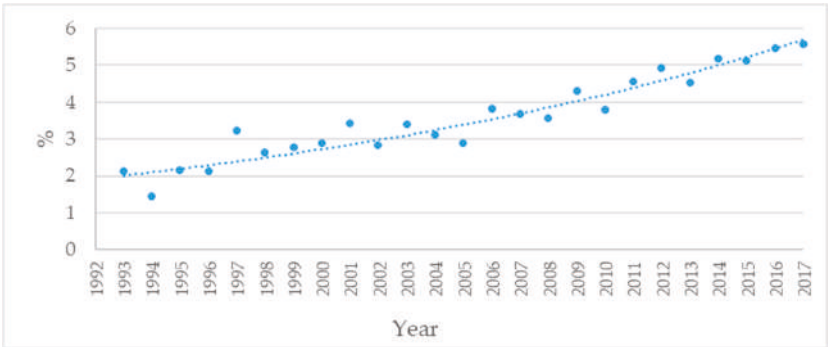


Figure 2. Percentage of Slovak men with weight more than 110 kg.

Various industrial sectors, such as automation, aviation, furniture manufacturing, footwear, and clothing industries have been affected by the current trend in human dimensions, especially steady weight gain and an increase in human height over the last few years [24–26]. In the case of furniture, these trends have been applied in some countries in the world recently, e.g., in the US, the standard BIFMA X6.1 (2012), as a new safety and performance standard for educational seating was accepted by the National Standards Institute (ANSI). Three sizes of school chairs were defined in the standard: A (seat height of less than 352 mm, user weight of 35 kg—it corresponds with the 95th percentile for boys aged 6), B (352 mm to 425 mm, 75 kg—it corresponds with the 95th percentile for girls aged 12), and C (more than 425 mm, 115 kg—it corresponds with 95% for adult male population) [27,28]. The standard resulted from long-term research that aimed at the importance of designing appropriate classroom furniture for schoolchildren [29–33]. Furniture for users with weight from 253 lb (115 kg) up to 400 lb (181 kg), which corresponds with the 99.5th percentile for men in the US, is specified in another accepted standard BIFMA X5.11 (2015) [34]. Similar standards were also accepted in Australia, e.g., the standard AFRDI 142 (2012) focused on four categories of users of “heavy duty” office

chairs: 135 kg for a single shift (8 h), 135 kg for multiple shifts, 160 kg for single/multiple shifts [35]. Another Australian standard AFRDI 151 (2014) deals with chairs for home, designed for users with weight more than 100 kg (four options—135 kg, 160 kg, 185 kg and chairs for bariatric patients with the weight more than 300 kg) [36]. In Europe, there is the standard BS 5459-2 focused on static and dynamic load of office pedestal chairs for persons with weight up to 225 kg [37]. This standard was designed by the company Satra, furniture testing facility in the UK (ISO 17025:2017) [38,39].

There are not many research studies dealing with furniture dimensions and construction in connection with overweight population or persons with disabilities [40]. References [41–44] suggest using anthropometric measurements in the process of designing furniture. The research of the authors [45,46] is focused on static analysis and testing the chairs in connection with the weight of users. In Slovakia, the effect of body weight on the size of chair joints was analysed in the study [46]. At the same time, the effect of a secular trend on functional dimensions of furniture was studied [47]. Czech authors [48] dealt with the use of anthropometric data in connection with seating and bed furniture as well. The authors [49] discussed the use of wider beds by healthcare providers in the case of patients with weight of more than 159 kg. The use of specific bed size for users with weight more than 147 kg or BMI score greater than 55 is suggested in another study [50]. Oversized beds for patients with BMI greater than 45 are recommended in the study [51].

Native wood and wood composites, besides plastics, and metals, are the most used materials in the manufacturing process of seating furniture. Fixed and flexible seating arrangement can be recognised in terms of constructing and joining structural elements of seating furniture. Stiffness required, especially in the case of dining chairs, is a typical feature of fixed seating arrangement made out of solid timber [52]. Flexible seating arrangement is especially used in manufacturing chairs designed for relaxation or as office chairs [53]. Wood is modified or wood-based composite materials are made of it in order to increase wood flexibility (as well as wood strength). Laminated furniture panels—lamellae and plywood—are widely used in furniture manufacturing. Properties of lamellae and plywood used in furniture projects depend on many various factors, such as moisture content of veneers, temperature, pressure and pressing time [54–58]. Adhesive properties, its viscosity, thickness of adhesive layer, quality of adhesive application, mechanical properties of veneers, treatment quality or removal of small elements from the surface (saw dust) are other factors affecting the bending strength [59–63]. Due to high bending strength of lamellae during dynamic loading, laminated wood is preferred in furniture manufacturing, especially chairs and beds [64].

At present, there are two directions in the research into chair anatomy. The first direction is focused on experimental testing of furniture construction. Experimental measurements and calculations are focused mainly on the weakest point—the joint—during static and dynamic loading and on the effect of tenon size on the ratio of dynamic to static loading rate [65–72]. The second direction deals with furniture design and construction using numerical and analytical methods. The finite element method (FEM) used to estimate or determine the load capacity of individual joint dimensions is the most often used method [73–78].

FEM allows manufacturers to optimise the shape and size of chairs. The developed models establish procedures to perform virtual testing on laminated bamboo chair to reduce product design and testing time [79]. This virtual testing results in design improvement and development of the laminated bamboo chair. The research study [80] is focused on classification of chairs according to their performance. Three hundred and fifteen chairs were tested and following the test results, acceptable light, medium and heavy design loads were determined for wood chair performance. Moreover, these values are in compliance with the allowable design loads.

Current European Standards associated with seating furniture (EN 1728:2012, EN 12520:2015, EN 1022:2018) are based on users with body weights of up to 110 kg [81–83]. Based on results of weight gain all around the world, the aim of the research is to determine the effect of the human weight on the load-carrying capacity and the dimensions of flexible chair consisting of lamellae. Mentioned data are required to a large extent by chair manufacturers.

The aim of this paper was to analyse the effect of laminated furniture panels with various thicknesses on the function of chair frame construction. Suggested minimum lamella thickness meeting the requirements of chairs for users with weight up to 110 kg and 150 kg resulted from the conducted research. For the ultimate load-carrying capacity and ability to use lamellae in flexible chairs, three thicknesses of lamellae were studied. Other thicknesses of lamellae, required to ensure overweight users feel safe, were tested. The methodology for evaluating the ultimate limit state of flexible chairs used based on ergonomics and chair safety can be considered for further research; normal and shear strength must be evaluated as well.

2. Materials and Methods

Three types of lamellae with various numbers of layers and total thickness were examined in the research on mechanical properties. Individual types of lamellae consisted of 9, 11 or 13 veneer layers created the final thickness of lamellae of 11.0 mm (type A), 13.5 mm (type B) or 16.0 mm (type C).

The lamellae were made of veneers of European beech wood (*Fagus sylvatica* L.) without defects by rotary peeling process using a 4-foot lathe (Královopolská strojírna, Brno, Czech Republic) at the Technical University in Zvolen, Slovakia from plasticized round wood. Beech wood is the most used wood species in furniture manufacturing in Slovakia. Its mechanical properties make it ideal for veneer production. The average thickness of veneers after drying to the moisture content of $6 \pm 1\%$ was 1.23 mm. Direction of wood grain in all veneers in lamella set was the same. PVAC dispersion Rakoll E WB 0301 (H. B. Fuller, Minnesota, USA) was used for gluing. The viscosity of the adhesive mixture was 5.500 mPa·s and pH value was 3.5 at the time of gluing. Adhesive was applied to the second veneer on both sides using a glue spreader with two rollers and an adhesive layer formed was $220 \text{ g}\cdot\text{m}^{-2}$.

Veneer set pressing was carried out in a hydraulic press using a press mold to form the final lamella shape. Forasmuch as the molds were under stress, the pressure during pressing process was $0.8 \text{ N}\cdot\text{mm}^{-2}$, at a temperature of 20°C for 30 min. The total dimension of pressed semi-finished products was as follows: length of 600 mm and width of 280 mm. The angle between the two adjacent lamella sides was 103° with radius of curvature of 80 mm. After stabilizing (120 h in standard climatic conditions), the semi-finished product was cut into final lamellae with width of 50 mm. Subsequently, individual lamellae were smoothed with 80-, 120- and 150-grit sandpaper to improve final surface quality.

Afterwards, test specimens were formed from lamellae in order to determine mechanical properties. Thirty test specimens of each type (A, B and C) with dimension of $250 \times 50 \text{ mm}$ were formed from the straight part of the lamellae. From the mold lamella part, 30 mold test specimens for each type (A, B and C) were formed. Subsequently, test specimens were air-conditioned at a temperature of $20 \pm 2^\circ\text{C}$ and air humidity of $65 \pm 5\%$. The moisture content (EMC) of specimens after air-conditioning was $12 \pm 1\%$.

Flat common specimens were tested using the standard methodology of the three-point bend test according to the standard EN 310: 1993. Mold unconventional specimens were tested by modified methodology created for the needs of this research. Mechanical testing of mold specimens was carried out using the modified three-point bend test. The load was spread evenly and the specimen was broken after $60 \pm 30 \text{ s}$.

Wood is a material whose properties possess orthogonal anisotropy, i.e., its physical and mechanical properties differ in three principal planes [84]. Three symmetry planes are differentiated in wood: cross-section perpendicular to the grain direction, longitudinal-radial and longitudinal-tangential, which are parallel with the wood grain direction and at the same time are mutually perpendicular. Due to its structural organization, lamella can be considered to be an anisotropy material in the plane perpendicular to the grain direction. The mechanical properties of lamella in both planes perpendicular to the grain direction are almost identical. Therefore, wood-based lamellae can be defined as transverse-axial anisotropic material. In the presented research, lamellae were formed as an orthogonal anisotropic material. Anisotropy must be taken into account in the modeling with the

finite element method. The physical and mechanical properties of lamellae used in the modelling are summarized in Table 1.

Table 1. Material constants for laminated beech lamellae, y direction is along the grain [85].

Young's Modulus (MPa)			Poisson's Ratio (-)			Shear Modulus (MPa)		
E_x	E_y	E_z	μ_{xy}	μ_{yz}	μ_{xz}	G_{xy}	G_{yz}	G_{xz}
1130.0	16670.0	630.0	0.044	0.33	0.027	1200.0	190.0	930.0

In the research on seating construction, a chair consisting of two frames was created. Base chair frame consisted of two U-shaped profiles were joined with transverse rails. The frame of seat and back was flexible and joined with transverse elements. Glued joints were used for chair construction because in comparison to other mechanical joining components, their stiffness was higher and they transferred the load better. Anthropometric measurements of users were taken into account for dimensions, construction and shape of the chair. Basic dimensions of designed chair are mentioned in Figure 3. Lamella dimensions and shape used in the project corresponded with those made and tested experimentally. While creating a chair model, three types of tested lamellae were used one after another (type A, B and C).

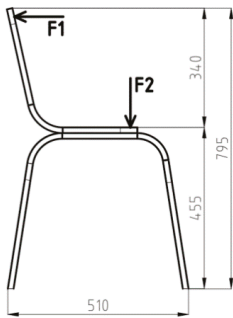


Figure 3. Static loading of the chair according to the standard EN 1728:2012 + dimensions of the designed chair.

The methodology for testing the chairs, especially loading, was based on the standard EN 1728:2012. The users' weight of 110 kg was regarded as maximum weight in the standard, while horizontal force acting on the back was $F_1 = 450$ N and the vertical force acting on the seat was $F_2 = 1300$ N. In the case of users with weight more than 110 kg, acting forces were not defined. However, statistics dealing with the weight of adult population showed the fact that designing the furniture for users with weight of up to 110 kg did not meet the actual requirements. Therefore, the forces resulting from the load caused by the overweight users had to be defined. 150 kg was the maximum user's weight set and the forces were determined using multiple linear regression. Acting forces of $F_1 = 613$ N and $F_2 = 1775$ N and user's weight of 150 kg were used in the process of creating a chair model. Direction and the point at which the force was applied are defined in Figure 3.

The loading analysis of the tested chair was conducted using the program ANSYS. In the software environment, a 3D volume model taking into consideration the orthotropic properties of wood-based lamellae was created. A coordinate system used was as follows: Y-axis was in the grain direction, X-axis was perpendicular to the grain in the radial direction and Z-axis was perpendicular to the grain in tangential direction. When mold lamellae were created—base, seat and chair back—the properties of lamellae were changed in relation to the lamella shape. Chair base lamella was created from three parts. Properties in individual planes were changed in relation to grain orientation. In the mold parts of lamella, the values of loading perpendicular to the grain were defined. Material constants are

defined in Table 1. Every element had to be assigned to a particular material. 3D element Solid 95 with 20 nodes was an element type. Boundary conditions were according to the standard EN 1728:2012. Supports of the back legs of a chair were regarded as fixed (fixed supports) in order to ensure that the loading was evenly transferred to the construction. Displacement supports were used in the front legs of the chair, movement in the y -axis direction was available. All joints in chair construction were considered fixed (bonded).

In terms of dimensioning the structural elements, limit state design requires the construction to meet two principal criteria: the ultimate limit state (ULS) used to evaluate the strength of construction, i.e., design strength and the serviceability limit state (SLS) used to evaluate the construction deformation.

The serviceability limit state, i.e., maximum deformation of flexible chair frame is defined neither in scientific journals nor in standards. It can result from an ergonomic chair design, suggested dimensions and seat-to-back angle. The angle recommended for designing a relaxed chair ranges from 103° to 110° . When 110° was the maximum value of an angle that could not be exceeded during loading, then the maximum displacement of a chair back was 40 mm backwards (Figure 4). This value of displacement was considered the maximum value for evaluating the serviceability limit state.

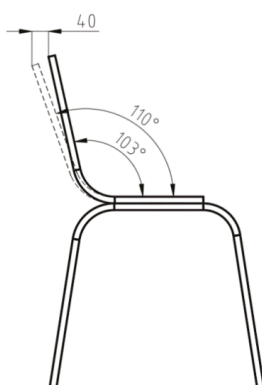


Figure 4. Deformation of the flexible chair.

When determining the serviceability limit state for flexible chairs, maximum limit displacement of the chair back in the highest point could be $u_{max} = 40$ mm. It resulted from the suggested seat-to-back angle of 110° (Figure 4). Reliability of the designed displacement u_d (determined by the FEM calculation) is:

$$u_d \leq u_{max} \quad (1)$$

However, in terms of safety, a chair with mentioned limit displacement of back must be safe and stable, i.e., backward overturning must not occur (chair must not tip over). Calculation of stability is mentioned in the standard EN 1022:2018. Loading is shown in Figure 5. Considering the flexibility, the studied lamella chair was a chair with variable geometry. According to the mentioned standard, the chair was considered stable when it does not tip after applying a load of $m = 110$ kg. When the seat-to-back angle was 110° , the centre of gravity of the load could not be positioned behind the tipping point of a chair, i.e., the point when the back leg is in contact with the floor. The position of the centre of gravity of the load can be defined using the graphical method (Figure 5).

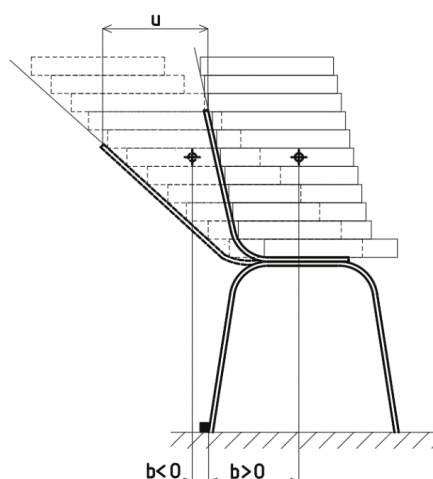


Figure 5. Defining the maximum possible deformation of the flexible chair.

The serviceability limit state boundary conditions resulting from the lamella stiffness determined experimentally was defined specifically in the chair construction. Following the results of the FEM analysis, normal and shear stresses were determined. When structural elements were dimensioned, normal and shear stresses were considered to be a design stress. In the process of dimensioning the chair components according to the serviceability limit state, requirements for reliable molding had to be met:

$$\sigma_{0,d} \leq f_{b,0,d} \quad (2)$$

where: $\sigma_{0,d}$ —design stress in the beech lamella mold (MPa),

$f_{b,0,d}$ —design strength in the beech lamella mold (MPa).

The value of characteristic strength had to be determined in order to calculate the design strength of lamella. Mean value of the bending strength ($\bar{\sigma}$) of tested lamellae achieved experimentally at a temperature of $t = 20\text{ }^{\circ}\text{C}$ and $\varphi = 65\%$ was an essential condition to determine the characteristic strength. Characteristic bending strength is a value corresponding with α quantile of assumed statistical division of evaluated strength. When $\alpha = 5\%$, the formula is:

$$f_{b,0,k} = \bar{\sigma} \cdot (1 - t_{95} \cdot \vartheta_x) \quad (3)$$

where: $f_{b,0,k}$ —characteristic bending strength of glued lamella (MPa),

$\bar{\sigma}$ —mean value of bending strength (MPa),

t_{95} —quantile of Student's t-distribution (one-side test), when $t_{95} = 1.64$,

ϑ_x —coefficient of variation (absolute value) (MPa).

When the characteristic bending strength is known, design strength $f_{b,0,d}$ is determined using the formula:

$$f_{b,0,d} = k_{mod} \cdot \frac{f_{b,0,k}}{\gamma_M} \quad (4)$$

where: $f_{b,0,k}$ —characteristic strength of beech lamella in mold (MPa),

γ_M —partial safety factor (-), for wood-based materials $\gamma_M = 1.3$,

k_{mod} —modification coefficient (-) (takes into account the effect of loading time and moisture content on the characteristic strength of material) for the action/load with the shortest design situation $k_{mod} = 1.10$.

3. Results and Discussion

Values of bending strength were determined experimentally using the specimens made of lamellae described in methodology. Bending strength was defined individually for flat and mold parts of lamellae. Mean values of bending strength, characteristic values, as well as design values for flat and mold lamella parts determined experimentally are summarised in the following tables (Tables 2 and 3). The values in Table 3 highlighted in bold ($f_{b,0,d}$) were used for evaluation of the ultimate limit state.

Table 2. Calculated values of flat lamella.

Type of Lamella	Mean Value σ (MPa)	Coefficient of Variation ϑ (%)	Characteristic Bending Strength $f_{b,0,k}$ (MPa)	Design Bending Strength $f_{b,0,d}$ (MPa)
A	111.85	4.96	102.76	86.86
B	104.64	6.57	93.37	79.01
C	93.80	6.11	84.41	71.42

Table 3. Calculated values of mold lamella.

Type of Lamella	Mean Value σ (MPa)	Coefficient of Variation ϑ (%)	Characteristic Bending Strength $f_{b,0,k}$ (MPa)	Design Bending Strength $f_{b,0,d}$ (MPa)
A	123.85	4.55	114.61	96.98
B	98.13	3.59	92.35	78.15
C	89.48	5.97	80.70	68.28

3.1. Ultimate Limit State Assessment

With dependence on the type of chair construction, the joint between the side rail and back leg or the seat-back joint is the most stressed joint [86–88]. This fact was confirmed in the process of lamella chair construction with the stress concentrated especially in the mold of seat frame. In terms of anisotropy, lamella mold is stressed in a direction perpendicular to the grain. Due to the direction of chair loading and according to the theory of simple bending, the inner mold part is affected by the compression parallel to the grain direction; on the other hand, outer mold part is affected by tension parallel to the grain direction. Bending strength of wood perpendicular to the grain direction is greater than the compression strength parallel to the grain direction and lower than the tensile strength parallel to the grain direction. Therefore, when evaluating the ultimate limit state, design bending strength of lamella $f_{b,0,d}$ (gathered experimentally) is compared to maximum normal stress (in tension $\sigma_{t,0,d}$ or on compression $\sigma_{c,0,d}$) gathered using FEM. Design stress determined by FEM cannot exceed the value of design bending strength of lamella resulting from specimen testing in order to meet the conditions associated with the ultimate limit state. Due to the fact that the most significant effect of stresses is in lamella mold, values determined in mold lamellae were used for comparison. Maximum values of normal stress achieved using the FEM for chairs made of lamellae (type A, B and C) and for loading of 110 kg and 150 kg are mentioned in Table 4. FEM visual outputs of stresses are shown in Figure 6. Values highlighted in red colour are not suitable in terms of ultimate limit state.

Table 4. Maximum values of normal stress for the pitch seat-to-back angle of 103°.

Type of Lamella	Loading of 110 kg		Loading of 150 kg	
	Design Stress FEM (MPa)		Design Stress FEM (MPa)	
	In Tension $\sigma_{t,0,d}$	In Compression $\sigma_{c,0,d}$	In Tension $\sigma_{t,0,d}$	In Compression $\sigma_{c,0,d}$
A	85.90	122.55	117.06	167.38
B	69.04	104.52	82.55	142.77
C	47.18	65.14	64.25	88.98

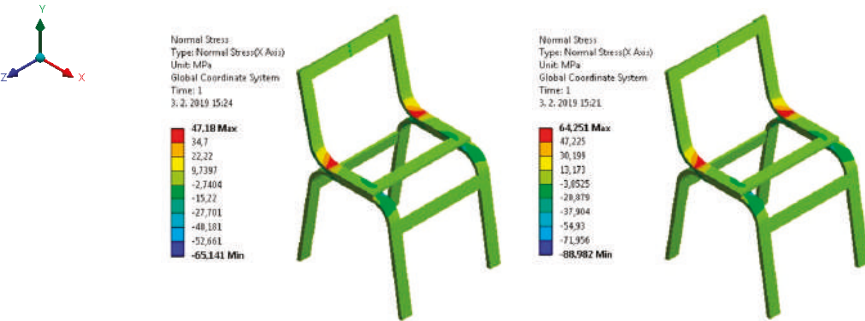


Figure 6. FEM visual outputs and stress concentration in tension and compression parts of lumbar curve of chair. Left for 110 kg tension (max. 47.18 MPa) and compression (max. 65.14 MPa) design stress and right for 150 kg tension (max. 64.25 MPa) and compression (max. 88.98 MPa).

Following the analysis of data gathered by comparing design values of bending strength determined experimentally and the values of design bending strength resulting from the use of FEM, the fact that ultimate limit state conditions were met can be stated. The values in Table 4 show that lamella with thickness of 11 mm (type A) met the requirements for use for a user with weight of 110 kg, only in the case of tensile stress. The value of compression stress was exceeded by 25.57 MPa. When the customer’s weight was 150 kg, design tensile stress was exceeded by 20.08 MPa and design compression stress by 70.40 MPa. Following the results, the fact that this type of lamella cannot be used in chair construction for overweight users can be stated.

Lamella with thickness of 13.5 mm (type B) met the requirements of the ultimate limit state when the user’s weight was 110 kg. In the case of a user with weight of 150 kg, design values of tensile stress were exceeded by 4.40 MPa and design compression stress by 64.62 MPa. Therefore, the lamella cannot be used when the chair is loaded with 150 kg.

The thickness of the last tested lamella was 16 mm (type C). It met the ultimate limit state conditions when the weight of a user is 110 kg. However, in the case of weight of 150 kg, it only met conditions in terms of tensile stress. Design value of compression stress was exceeded by 20.70 MPa. It means that lamella C cannot be used for chair construction for a user with weight of 150 kg as well.

3.2. Serviceability Limit State Assessment

Maximum values of the displacement of the upper edge of the seat u (mm) with loading of 110 kg and 150 kg and corresponding values of the distance of the centre of gravity of the load from the tipping point b (mm) in the direction of x -axis are mentioned in Table 5. FEM visual outputs to analyze the displacement of the back are shown in Figure 7. The values of displacement highlighted in red color are not satisfactory in terms of the serviceability limit state.

Table 5. Maximum values of the backward displacement of the back u (mm) and values of the distance of the centre of gravity of the load from the tipping b (mm) in the direction of x-axis.

Type of Lamella.	Loading of 110 kg		Loading of 150 kg	
	u (mm)	b (mm)	u (mm)	b (mm)
A	289.15	−63.5	343.15	−140.1
B	189.13	+33.7	256.16	−54.6
C	96.72	+157.4	128.34	+74.2

Note: In case the back is not loaded, the distance between the centre of gravity of the load and the back leg is $b = +237.2$ mm in the direction of x-axis.

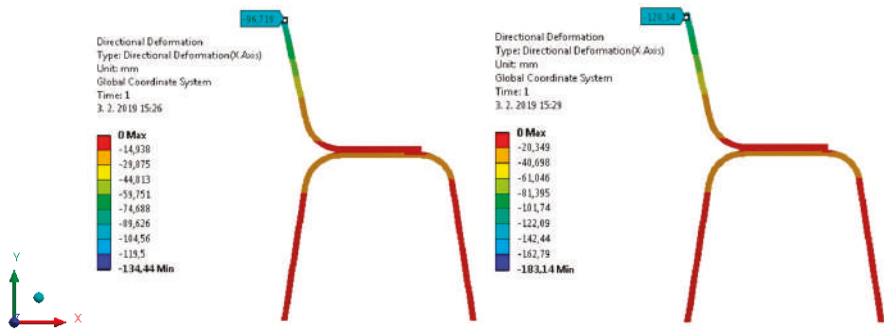


Figure 7. FEM visual outputs of deformation and displacement of the back while the load is applied. Left figure for 110 kg and right figure for 150 kg.

Analyzing the data summarized in Table 5, the serviceability limit state conditions can be evaluated. According to the requirements, seat-to-back angle must not exceed 110° (meeting the conditions results from the displacement of the upper edge of the seat). At the same time, the position of the centre of gravity must not be behind the tipping point and b value must not be negative in the direction of the x-axis. Tipping point is defined in the position of the back edge of the back leg.

Following the values determined by FEM for the lamella-type A, it is clear that the lamella did not meet defined conditions in the case of the loading of neither 110 kg nor 150 kg. In both loadings, allowable value of the displacement of the upper edge of the chair back was exceeded, and the value describing the position of the centre of gravity was negative in the direction of x-axis. Support provided by this lamella in the chair back was not adequate. Therefore, there was a danger of tipping over.

The lamella-type B did not meet the requirements for allowable back deformation for user weight of 110 kg and 150 kg. In terms of the position of the centre of gravity, the requirement is met only in case of loading of 110 kg. When user weight is 150 kg, there is a danger of tipping over because the centre of gravity was positioned behind the back leg of the chair.

The lamella-type C met the requirements for the position of the centre of gravity in the case of both weights of users. In spite of these findings, its use was not accepted due to the deformation of the chair back. Its value exceeded the allowable value for user weight of 110 kg or 150 kg.

The mentioned findings associated with meeting the requirements of the ultimate limit state as well as the serviceability limit state and the use of lamellae implied that no lamella type can be used in any tested cases of chair construction. Albeit the lamella-type C met the requirement for the ultimate limit state for the user with weight of 110 kg, the requirements for the serviceability limit state were not met.

3.3. Lamella Construction Meeting the Requirements of Ultimate States

Following the mentioned findings, the fact that lamella used in given chair construction should consist of a higher number of layers, thus, with greater thickness can be stated. Therefore, the group of

specimens of lamella (type D) with 17 layers with total thickness of 21 mm was formed. Following the testing, design value of bending strength $\bar{\sigma} = 35.83$ MPa with the coefficient of variation of $\vartheta = 5.3\%$ was determined. Consequently, FEM analysis was carried out to determine the values of design stresses and deformation of the chair back. Calculated values are summarized in Table 6. FEM visual outputs of the stresses and displacement of the chair back are shown in Figure 8.

Table 6. Values of design compression and tensile stresses and values of the backward displacement of the chair back u (mm) in the case of the lamella type D when loading is 150 kg.

Type of Lamella	Design Stress-FEM (MPa)		Displacement of the Chair Back
	in Tension	in Compression	u (mm)
D	28.16	26.78	37.41

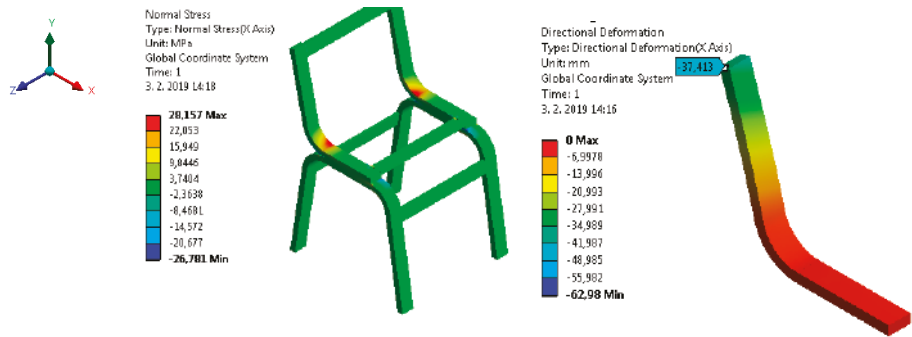


Figure 8. FEM visual outputs of stresses and displacement of the chair back with thickness of 21 mm when loading is 150 kg. Left: Values of design compression (23,781 MPa) and tensile stresses (28,157 MPa), right: value of the backward displacement of the chair back (37,413 mm).

Comparing the values of design bending strength and design values of stresses and values of the displacement of the upper edge of chair back achieved by the FEM analysis, it is clear that the lamella-type D with thickness of 21 mm would meet the requirements for both ultimate states in the case of loading of 150 kg. Due to the fact that in the research only a small sample size of this lamella type was made, testing lamella type D will offer an excellent opportunity for further research focused on dynamic loading.

Comparing the results to other studies dealing with chair modeling using FEM is quite difficult because of the evaluation stress according to von Mises mentioned by most authors. Wood is a material whose properties possess orthogonal anisotropy with nonlinear performance in elastic and plastic deformation. According to our opinion, two mentioned facts are key factors not allowing researchers to evaluate the stresses in wood-based material according to von Mises. The von Mises stress criterion is weighing the different oriented stresses to one “mixed” stress, which is not suitable to be compared to a scalar failure value for wood [89].

4. Conclusions

Various areas of economy, including furniture design and construction, have been affected by weight gain trends across populations in the last years. In Slovakia, the average weight of the population has increased by almost 10 kg over the last 25 years. A similar trend is observed globally. Almost 6% of the Slovak population is men with weight more than 110 kg. Therefore, the current standards must be re-evaluated. Valid legislation dealing with furniture design takes into account users’ weight of 110 kg. However, according to anthropometric studies, 150 kg is the weight of users that should be taken into account in the future.

- The research presented was focused on the assessment of two ultimate states of flexible chair construction. Minimum thickness requirements for lamellae needed for chairs for users with weight up to 110 kg and 150 kg resulted from the research.
- Following the mechanical properties of laminated veneer lamellae and the assessment of ultimate limit state and serviceability limit state, as well as the use of lamella in flexible chairs, four thicknesses of lamellae were examined.
- Requirements for the strength of structural elements were evaluated by the ultimate limit state and allowable deformation of chair construction and the position of the centre of gravity during the loading were evaluated by the serviceability limit state. Following the results of the research, the fact that three types of tested lamellae (thickness 11 mm, 13.5 mm and 16 mm) did not meet the requirements of the both ultimate states. Lamella with thickness of 21 mm met the requirements for both ultimate states in the case of loading of 110 kg and 150 kg.
- The methodology to evaluate the serviceability limit state of flexible chairs based on ergonomics and chair safety can be considered as another contribution of the research.

Weight gain is a global problem affecting the industrial goods sector. In the case of research, the cooperation of professionals in anthropology, ergonomics, construction, design and health is needed, in order to modify the size and function of furniture. Designing wooden furniture should be connected with a sustainable strategy of economy aimed at efficient use of local renewable resources. Only a complex approach can contribute to meeting the goals of sustainability of the furniture industry leading to sustainability of standards and timeliness.

Author Contributions: Conceptualization, N.L., M.H., P.J. and R.I.; Data curation, N.L., R.R. and M.H.; Visualization, R.R., L.K., R.I.; Writing-original draft, N.L., R.R., L.K. and R.I.

Acknowledgments: This research was supported by the Slovak Research and Development Agency under Contract No. APVV-16-0297, Contract No. APVV-14-0506, Contract No. APVV-17-0583, VEGA 1/0717/19, VEGA 1/0556/19 and KEGA 012TU Z-4/2017.

Conflicts of Interest: The authors declare no conflict of interest.

References

1. Joščák, P.; Dudas, J.; Gáborík, J.; Gaff, M.; Langová, N.; Navrátil, V.; Slabejová, G. *Wood and Wood-Based Furniture Constructions*; Technická univerzita vo Zvolene: Zvolen, Slovakia, 2014.
2. Wang, Y.; Beydoun, M.A. The obesity epidemic in the United States—Gender, age, socioeconomic, racial/ethnic, and geographic characteristics: A systematic review and meta-regression analysis. *Epidemiol. Rev.* **2007**, *29*, 6–28. [[CrossRef](#)] [[PubMed](#)]
3. Stevens, G.A.; Singh, G.M.; Lu, Y.; Danaei, G.; Lin, J.K.; Finucane, M.M.; Bahalim, A.N.; McIntire, R.K.; Gutierrez, H.R.; Cowman, M.; et al. National, regional, and global trends in adult overweight and obesity prevalences. *Popul. Health Metr.* **2012**, *10*, 22. [[CrossRef](#)] [[PubMed](#)]
4. Tremmel, M.; Gerdtham, U.G.; Nilsson, P.M.; Saha, S. Economic Burden of Obesity: A Systematic Literature Review. *Int. J. Environ. Res. Public Health* **2017**, *14*, 435. [[CrossRef](#)] [[PubMed](#)]
5. González-Rodríguez, L.G.; Perea Sánchez, J.M.; Aranceta-Bartrina, J.; Gil, Á.; González-Gross, M.; Serra-Majem, L.; Varela-Moreiras, G.; Ortega, R.M. Intake and Dietary Food Sources of Fibre in Spain: Differences with Regard to the Prevalence of Excess Body Weight and Abdominal Obesity in Adults of the ANIBES Study. *Nutrients* **2017**, *9*, 326. [[CrossRef](#)] [[PubMed](#)]
6. Burke, N.L.; Shomaker, L.B.; Brady, S.; Reynolds, J.C.; Young, J.F.; Wilfley, D.E.; Sbrocco, T.; Stephens, M.; Olsen, C.H.; Yanovski, J.A.; et al. Impact of Age and Race on Outcomes of a Program to Prevent Excess Weight Gain and Disordered Eating in Adolescent Girls. *Nutrients* **2017**, *9*, 947. [[CrossRef](#)] [[PubMed](#)]
7. Chan, R.S.; Woo, J. Prevention of Overweight and Obesity: How Effective is the Current Public Health Approach. *Int. J. Environ. Res. Public Health* **2010**, *7*, 765–783. [[CrossRef](#)]
8. Peltzer, K.; Pengpid, S.; Samuels, T.A.; Özcan, N.K.; Mantilla, C.; Rahamefy, O.H.; Wong, M.L.; Gasparishvili, A. Prevalence of Overweight/Obesity and Its Associated Factors among University Students from 22 Countries. *Int. J. Environ. Res. Public Health* **2014**, *11*, 7425–7441. [[CrossRef](#)]

9. Finucane, M.M.; Stevens, G.A.; Cowan, M.J.; Danaei, G.; Lin, J.K.; Paciorek, C.J.; Singh, G.M.; Gutierrez, H.R.; Lu, Y.; Bahalim, A.N. Global burden of metabolic risk factors of chronic diseases collaborating group body mass index. *Lancet* **2011**, *377*, 557–567. [\[CrossRef\]](#)
10. De Onis, M.; Blössner, M.; Borghi, E. Global prevalence and trends of overweight and obesity among preschool children. *Am. J. Clin. Nutr.* **2010**, *92*, 1257–1264. [\[CrossRef\]](#)
11. Rockholm, B.; Baker, J.L.; Sorensen, T.I.A. The levelling off of the obesity epidemic since the year 1999- A review of evidence and perspectives. *Obes. Rev.* **2010**, *11*, 835–846. [\[CrossRef\]](#)
12. Odunitan-Wayas, F.; Okop, K.; Dover, R.; Alaba, O.; Micklesfield, L.; Puaone, T.; Uys, M.; Tsolekile, L.; Levitt, N.; Battersby, J.; et al. Food Purchasing Characteristics and Perceptions of Neighborhood Food Environment of South Africans Living in Low-, Middle- and High-Socioeconomic Neighborhoods. *Sustainability* **2018**, *10*, 4801. [\[CrossRef\]](#)
13. Manzano, S.; Doblaré, M.; Hamdy Doweidar, M. Altered Mechano-Electrochemical Behavior of Articular Cartilage in Populations with Obesity. *Appl. Sci.* **2016**, *6*, 186. [\[CrossRef\]](#)
14. Ng, M.; Fleming, T.; Robinson, M.; Tomson, B.; Graetz, N.; Margono, C.; Mullany, E.C.; Biryukov, S.; Abbafati, C.; Abera, S.F.; et al. Global, regional, and national prevalence of overweight and obesity in children and adults during 1980–2013: A systematic analysis for the Global Burden of Disease Study 2013. *Lancet* **2014**, *384*, 766–781. [\[CrossRef\]](#)
15. Di Cesare, M.; Bentham, J.; Stevens, G.A.; Zhou, B.; Danaei, G.; Lu, Y.; Bixby, H.; Cowan, M.J.; Riley, L.M.R.; Hajifathalian, K.; et al. Trends in adult body-mass index in 200 countries from 1975 to 2014: A pooled analysis of 1698 population-based measurement studies with 19.2 million participants. *Lancet* **2016**, *387*, 1377–1396.
16. Hitka, M.; Hajduková, A. Antropometrická optimalizácia rozmerov lôžkového nábytku. *Acta Facultatis Xylogiae Zvolen* **2013**, *55*, 101–109.
17. Čuta, M.; Kukla, L.; Novák, L. Modelling the development of body height (length) in children using parental height data. *Československá Pediatrie* **2010**, *65*, 159–166.
18. Harrison, C.R.; Robinette, K.M. CAESAR > Summarz Statistics for the Adult Population (Ages 18–65) of the United States of America; United States Air Force Research Laboratorz: Wright-Patterson AFB, OH, USA, 2002.
19. Réh, R.; Krišťák, L.; Hitka, M.; Langová, N.; Joščák, P.; Čambál, M. Analysis to Improve the Strength of Beds Due to the Excess Weight of Users in Slovakia. *Sustainability* **2019**, *11*, 624. [\[CrossRef\]](#)
20. Ministry of Health of the Slovak Republic. Report on Health Status in Slovakia. Health 2016. Available online: <http://health.gov.sk> (accessed on 31 September 2018).
21. Public Health Authority of the Slovak Republic. Annual Report on the Activities of the Public Health Office for 2017. Available online: http://uvzsrs.sk/docs/vs/vyrocnna_sprava_2017.pdf (accessed on 31 September 2018).
22. Statistical Office of the Slovak Republic. View of Health Status of the Slovak Population and Its Determinants (Results of EHIS 2016). Available online: <http://slovak.statistics.sk> (accessed on 31 September 2018).
23. World Health Organization Regional Office for Europe. The Health Systems in Transition (HiT). Available online: <http://euro.who.int/en/countries/slovakia> (accessed on 31 September 2018).
24. Porta, J.; Saco-Ledo, G.; Cabanas, M.D. The ergonomics of airplane seats: The problem with economy class. *Int. J. Ind. Ergon.* **2019**, *69*, 90–95. [\[CrossRef\]](#)
25. Quigley, C.; Southall, D.; Freer, M.; Moody, A.; Porter, M. Anthropometric Study to Update Minimum Aircraft Seating Standards. Available online: <https://dspace.lboro.ac.uk/2134/701> (accessed on 18 January 2019).
26. Roggla, G.; Moser, B.; Roggla, M. Seat space on airlines. *Lancet* **1999**, *353*, 1532. [\[CrossRef\]](#)
27. BIFMA X6.1. Educational Seating. American National Standard for Office Furnishings (Revised in 2018); BIFMA: Grand Rapids, MI, USA, 2018.
28. Bellinger, T.A.; Benden, M.E. New ANSI/BIFMA standard for testing of educational seating. *Ergon. Des. Q. Hum. Factors Appl.* **2015**, *23*, 23–27. [\[CrossRef\]](#)
29. Parcells, C.; Stommel, M.; Hubbard, R.P. Mismatch of classroom furniture and student body dimensions: Empirical findings and health implications. *J. Adolesc. Health* **1999**, *24*, 265–273. [\[CrossRef\]](#)
30. Panagiotopoulou, G.; Christoulas, K.; Papanicolaou, A.; Mandroukas, K. Classroom furniture dimensions and anthropometric measures in primary school. *Appl. Ergon.* **2004**, *35*, 121–128. [\[CrossRef\]](#) [\[PubMed\]](#)
31. Mohamed-Thariq, M.G.; Munasinghe, H.P.; Abeysekara, J.D. Designing chairs with mounted desktop for university students Ergonomics and comfort. *Int. J. Ind. Ergon.* **2010**, *40*, 8–18. [\[CrossRef\]](#)
32. Oyewole, S.A.; Haight, J.M.; Freivalds, A. The ergonomic design of classroom furniture/computer work station for first graders in the elementary school. *Int. J. Ind. Ergon.* **2010**, *40*, 437–447. [\[CrossRef\]](#)

33. Agha, S.R.; Alnahhal, M.J. Neural network and multiple linear regression to predict school children dimensions for ergonomic school furniture design. *Appl. Ergon.* **2012**, *43*, 979–984. [CrossRef] [PubMed]
34. BIFMA X5.11. *Large Occupant Office Chair Standard*. American National Standard for Office Furnishings; BIFMA: Grand Rapids, MI, USA, 2015.
35. AFRDI 142. *Certification for Heavy Duty Office Chairs*; Australian Furnishings Research and Development Institute: Launceston, Australia, 2012.
36. AFRDI 151. *Rated Load Standard for Fixed Height Chairs*; Australian Furnishings Research and Development Institute: Launceston, Australia, 2014.
37. BS 5459-2:2000 and A2:2008. *Specification for Performance Requirements and Tests for Office Furniture*; British Standards Institutions: London, UK, 2000.
38. ISO 17025. *General Requirements for the Competence of Testing and Calibration Laboratories*; International Organization for Standardization: Geneva, Switzerland, 2017.
39. SATRA. Satra Technology—International Product Research, Testing and Supply Chain Quality. Available online: <http://satra.com> (accessed on 31 September 2018).
40. Bonenberg, A.; Branowski, B.; Kurcyewski, P.; Lewandowska, A.; Sydor, M.; Torzynski, D.; Zablocki, M. Designing for human use: Examples of kitchen interiors for person with disability and elderly people. *Hum. Factors Ergon. Manuf.* **2019**, *29*, 177–186. [CrossRef]
41. Mehrparvar, A.H.; Mirmohammadi, S.J.; Hafezi, R.; Mostaghaci, M.; Davari, M.H. Static anthropometric dimensions in a population of Iranian high school students: Considering ethnic differences. *Hum. Factors J. Hum. Factors Ergon. Soc.* **2015**, *57*, 447–460. [CrossRef]
42. Qutubuddin, S.M.; Hebbal, S.S.; Kumar, C.S. Anthropometric consideration for designing students desks in engineering colleges. *Int. J. Curr. Eng. Technol.* **2013**, *3*, 1179–1185.
43. Shin, D.; Kim, J.Y.; Hallbeck, M.S.; Haight, J.M.; Jung, M.C. Ergonomic hand tool and desk and chair development process. *Int. J. Occup. Saf. Ergon.* **2008**, *14*, 247–252. [CrossRef]
44. Masson, A.E.; Hignett, S.; Gyi, D.E. Anthropometric Study to Understand Body Size and Shape for Plus Size People at Work. *Procedia Manuf.* **2015**, *3*, 5647–5654. [CrossRef]
45. Smardzewski, J. *Furniture Design*; Springer International Publishing: Cham, Switzerland, 2015.
46. Hitka, M.; Joščák, P.; Langová, N.; Krišťák, L.; Blašková, S. Load-Carrying Capacity and the Size of Chair Joints Determined for Users with a Higher Body Weight. *Bioresources* **2018**, *13*, 6428–6443.
47. Hitka, M.; Sedmák, R.; Joščák, P.; Ližbetinová, L. Positive Secular Trend in Slovak Population Urges on Updates of Functional Dimensions of Furniture. *Sustainability* **2018**, *10*, 3474. [CrossRef]
48. Dvoulétá, K.; Káňová, D. Utilization of anthropometry in the sphere of sitting and bed furniture. *Acta Univ. Agric. Silv. Mendel. Brun.* **2014**, *62*, 81–90. [CrossRef]
49. Muir, M.; Archer-Heese, G. Essentials of a bariatric patient handling program. *OJIN Online J. Issues Nurs.* **2009**, *14*, 5.
50. Gourash, W.; Rogula, T.; Schauer, P.R. *Essential Bariatric Equipment: Making Your Facility More Accommodating to Bariatric Surgical Patients*; Springer: New York, NY, USA, 2007.
51. Wiggermann, N.; Smith, K.; Kumpar, D. What bed size does a patient need? The relationship between body mass index and space required to turn in bed. *Nurs. Res.* **2017**, *66*, 483–489. [CrossRef] [PubMed]
52. Ko, Y.C.; Lo, C.H.; Chen, C.C. Influence of Personality Traits on Consumer Preferences: The Case of Office Chair Selection by Attractiveness. *Sustainability* **2018**, *10*, 4183. [CrossRef]
53. Nüesch, C.; Kreppke, J.N.; Mündermann, A.; Donath, L. Effects of a Dynamic Chair on Chair Seat Motion and Trunk Muscle Activity during Office Tasks and Task Transitions. *Int. J. Environ. Res. Public Health* **2018**, *15*, 2723. [CrossRef]
54. Borůvka, V.; Dudík, R.; Zeidler, A.; Holeček, T. Influence of Site Conditions and Quality of Birch Wood on Its Properties and Utilization after Heat Treatment. Part I—Elastic and Strength Properties, Relationship to Water and Dimensional Stability. *Forests* **2019**, *10*, 189. [CrossRef]
55. Wei, P.; Rao, X.; Yang, J.; Guo, Y.; Chen, H.; Zhang, Y.; Chen, S.; Deng, X.; Wang, Z. Hot pressing of wood-based composites: A review. *For. Prod. J.* **2016**, *66*, 419–427. [CrossRef]
56. Derikvand, M.; Kotlarewski, N.; Lee, M.; Jiao, H.; Nolan, G. Characterisation of Physical and Mechanical Properties of Unthinned and Unpruned Plantation-Grown Eucalyptus nitens H. Deane & Maiden Lumber. *Forests* **2019**, *10*, 194.

57. Šubic, B.; Fajdiga, G.; Lopatič, J. Bending Stiffness, Load-Bearing Capacity and Flexural Rigidity of Slender Hybrid Wood-Based Beams. *Forests* **2018**, *9*, 703. [[CrossRef](#)]
58. Réh, R.; Igaz, R.; Krišťaľ, L.; Ružiak, I.; Gajtanska, M.; Božíková, M.; Kučerka, M. Functionality of beech bark in adhesive mixtures used in plywood and its effect on the stability associated with material systems. *Materials* **2019**, *12*, 1298. [[CrossRef](#)] [[PubMed](#)]
59. Morales, G.A. Potential of Gmelina arborea for solid wood products. *New For.* **2004**, *28*, 331–337. [[CrossRef](#)]
60. Sikora, A.; Svoboda, T.; Záborský, V.; Gaffová, Z. Effect of selected factors on the bending deflection at the limit of proportionality and at the modulus of rupture in laminated veneer lumber. *Forests* **2019**, *10*, 401. [[CrossRef](#)]
61. Zhang, X.; Zhu, Y.; Yu, Y.; Song, J. Improve Performance of Soy Flour-Based Adhesive with a Lignin-Based Resin. *Polymers* **2017**, *9*, 261. [[CrossRef](#)] [[PubMed](#)]
62. Gejdoš, M.; Tončíková, Z.; Němec, M.; Chovan, M.; Gergel', T. Balcony cultivator: New biomimicry design approach in the sustainable device. *Futures* **2018**, *98*, 32–40. [[CrossRef](#)]
63. Bekhta, P.; Hiziroglu, S.; Potapova, O.; Sedliačik, J. Shear Strength of Exterior Plywood Panels Pressed at Low Temperature. *Materials* **2009**, *2*, 876–882. [[CrossRef](#)]
64. Erdil, Y.Z.; Zhang, J.; Eckelman, C.A. Withdrawal and bending strength of dowel-nuts in plywood and oriented strandboard. *For. Prod. J.* **2003**, *53*, 54–57.
65. Prekrat, S.; Smardzewski, J. Effect of gluline shape on strength of mortise and tenon joint. *Drv. Ind.* **2010**, *61*, 223–228.
66. Kilic, H.; Kasal, A.; Kuskun, T.; Acar, M.; Erdil, Y.Z. Effect of Tenon Size on Static Front to Back Loading Performance of Wooden Chairs in Comparison with Acceptable Design Loads. *Bioresources* **2018**, *13*, 256–271.
67. Kuskun, T.; Kasal, A.; Haviarova, E.; Kilic, H.; Uysal, M.; Erdil, Y.Z. Relationship between static and cyclic front to back load capacity of wooden chairs, and evaluation of the strength values according to acceptable design values. *Wood Fiber Sci.* **2018**, *50*, 1–9. [[CrossRef](#)]
68. Oktae, J.; Ebrahimi, G.; Layeghi, M.; Ghofrani, M.; Eckelman, C.A. Bending moment capacity of simple and haunched mortise and tenon furniture joints under tension and compression loads. *Turk. J. Agric. For.* **2014**, *38*, 291–297. [[CrossRef](#)]
69. Likos, E.; Haviarova, E.; Eckelman, C.A.; Erdil, Y.Z.; Ozciftci, A. Technical note: Static versus cyclic load capacity of side chairs constructed with mortise and tenon joints. *Wood Fiber Sci.* **2013**, *45*, 223–227.
70. Gaff, M.; Gašparik, M.; Boruvka, V.; Haviarová, E. Stress simulation in layered wood-based materials under mechanical loading. *Mater. Des.* **2015**, *87*, 1065–1071. [[CrossRef](#)]
71. Grič, M.; Joščák, P.; Tarvainen, I.; Ryonankoski, H.; Lagaňa, R.; Langová, N.; Andor, T. Mechanical properties of furniture self-locking frame joints. *Bioresources* **2017**, *12*, 5525–5538. [[CrossRef](#)]
72. Branowski, B.; Zablocki, M.; Sydor, M. Experimental analysis of new furniture joints. *Bioresources* **2018**, *13*, 370–382. [[CrossRef](#)]
73. Hajdarevič, S.; Busuladžić, I. Stiffness Analysis of Wood Chair Frame. *Procedia Eng.* **2015**, *100*, 746–755. [[CrossRef](#)]
74. Staneva, N.; Genchev, Y.; Hristodorova, D. Approach to designing an upholstered furniture frame by the finite element method. *Acta Fac. Xylologiae* **2018**, *60*, 61–70.
75. Hu, W.G.; Guan, H.Y. Research on withdrawal strength of mortise and tenon joint by numerical and analytic methods. *Wood Res.* **2017**, *62*, 575–586.
76. Derikvand, M.; Ebrahimi, G. Finite element analysis of stress and strain distributions in mortise and loose tenon furniture joints. *J. For. Res.* **2014**, *25*, 677–681. [[CrossRef](#)]
77. Hu, W.G. Study of finite element analysis of node in solid wood structure furniture based on ANSYS. *Furnit. Inter. Des.* **2015**, *46*, 65–67.
78. Kasal, A.; Eckelman, C.A.; Haviarova, E.; Yalcin, I. Bending moment capacities of L-shaped mortise and tenon joints under compression and tension loadings. *Bioresources* **2016**, *1*, 6836–6853. [[CrossRef](#)]
79. Diler, H.; Efe, H.; Erdil, Y.Z.; Kuskun, T.; Kasal, A. Determination of allowable design loads for wood chairs. In Proceedings of the XXVIII International Conference Research for Furniture Industry, Poznan, Poland, 21–22 September 2017.
80. Laemlaksakul, V. Innovative Design of Laminated Bamboo Furniture Using Finite Element Method. *Int. J. Math. Comput. Simul.* **2008**, *3*, 274–284.
81. EN 1728. Furniture. Seating. Test Methods for the Determination of Strength and Durability; BSI: London, UK, 2012.
82. EN 12520. Furniture—Strength, Durability and Safety—Requirements for Domestic Seating; BSI: London, UK, 2015.

83. EN 1022. *Domestic Furniture. Seating. Determination of Stability*; BSI: London, UK, 2018.
84. Sydor, M.; Wieloch, G. Construction properties of wood taken into consideration in engeneering practice. *Drewno* **2009**, *52*, 63–73.
85. Požgaj, A.; Chovanec, D.; Kurjatko, S.; Babiak, M. *Štruktúra a Vlastnosti Dreva*; Príroda a.s.: Bratislava, Slovakia, 1993.
86. Sedlecký, M.; Kvietková, M.S.; Kminiak, R. Medium-density fiberboard (MDF) and Edge-glued Panels (EGP) after edge milling—Surface roughness after machining with different parameters. *Bioresources* **2018**, *13*, 2005–2021. [[CrossRef](#)]
87. Němec, M.; Kminiak, R.; Danihelová, A.; Gergel, T.; Ondrejka, V. Vibrations and workpiece surface quality at changing feed speed of CNC machine. *Akustika* **2017**, *28*, 117–124.
88. Ke, Q.; Zhang, F.; Zhang, Y. Optimisation design of pine backrest chair based on Taguchi method. *Int. Wood Prod. J.* **2017**, *8*, 18–25. [[CrossRef](#)]
89. Szalai, J. Festigkeitstheorien von anisotropen Stoffen mit sprodem bruchverhalten. *Acta Silv. Lign. Hung.* **2008**, *4*, 61–79.



© 2019 by the authors. Licensee MDPI, Basel, Switzerland. This article is an open access article distributed under the terms and conditions of the Creative Commons Attribution (CC BY) license (<http://creativecommons.org/licenses/by/4.0/>).

Article

Preferences for Urban Building Materials: Does Building Culture Background Matter? [†]

Olav Høibo ^{1,*}, Eric Hansen ², Erlend Nybakk ³ and Marius Nygaard ⁴

¹ Faculty of Environmental Sciences and Natural Resource Management, Norwegian University of Life Sciences (NMBU), P.O. Box 5003, NO-1432 Ås, Norway

² Department of Wood Science & Engineering, Oregon State University, 119 Richardson Hall, Corvallis, OR 97331, USA; eric.hansen@oregonstate.edu

³ Department of Marketing, Economics and Innovation, Kristiania University College, P.O. 1190 Sentrum, 0107 Oslo, Norway; Erlend.Nybakk@kristiania.no

⁴ Department of Architecture, Oslo School of Architecture and Design, P.O. Box 1633, Vika, 0119 Oslo, Norway; Marius.Nygaard@aho.no

* Correspondence: olav.hoibo@nmbu.no; Tel.: +47-67-231-743

[†] Some of the result in this article was presented by Olav Høibo ^{1,*}, Eric Hansen ², Erlend Nybakk ³ and Marius Nygaard ⁴ in a poster at SWST 2015 International Convention, Jackson Lake Lodge, Grand Teton National Park, Wyoming, USA; 2015-06-07–2015-06-12.

Received: 24 July 2018; Accepted: 14 August 2018; Published: 17 August 2018

Abstract: A fast-growing global population, increasing urbanization, and an increasing flow of people with different building cultural backgrounds bring material use in the housing sector into focus. The aim of this study is to identify material preferences in the building environment in cities and to determine if the building cultural background impacts those preferences. The data in this study consisted of responses from two groups of dwellers in Norway, including immigrants from countries where wood is an uncommon building material and native Norwegians from a building culture where wood is common. We found that the most preferred materials were often the same as the most common materials currently used in city buildings. Only small differences were found between the two groups of dwellers that were studied. Most differences were related to concerns about material choice in general and where individuals wanted to live. Respondents who preferred city living preferred commonly used city materials, such as concrete and steel. For cladding materials, stone/bricks were the most preferred. However, stained or painted wood was one of the most preferred, even though it is not commonly used in city buildings.

Keywords: marketing; material preference; urban housing; immigrants; building culture background; building material

1. Introduction

A fast-growing global population [1] and a focus on sustainable development and climate change bring the housing sector and materials used for housing into focus. United Nations estimates place the global population at approximately 9.6 billion by 2050 [2]. Currently, the global demand for new housing is approximately five million units per year [3]. Given the state of housing stock and the mentioned growth in the population, a significant increase of housing units is needed by 2050. A growing proportion of the global population will reside in urban areas, where housing density is a factor in sustainable development [4].

In addition to the fast-growing global population and increasing urbanization, immigrant flow is accelerating due to differences in income, social networks, and various state policies, thus leading to an overall growing number of immigrant cities [5]. In Western Europe, an unprecedented number of

newcomers have arrived during the last two decades. When considering cities with more than 100,000 immigrants, North American and Western European cities are key immigrant destinations [6].

Impending climate change means that the carbon footprint has gained importance as a key metric in the assessment of the environmental impacts of buildings. Embodied energy and emissions of materials are vital parts of this picture. In the future, embodied energy and choice of material will be even more important since energy consumption from operational use will decrease and building material consumption will increase [7]. Therefore, timber-framed buildings, which are found to have lower global warming potential than concrete and steel structures [8,9], might play an important role with regard to the reduction of environmental consequences of city buildings. However, wood is not a common modern city building material, and might therefore be a material less preferred by consumers. Further, residents from countries where wood is hardly used in any buildings might have lower preferences for wood than people coming from countries where wood is more common.

In Norway, developments close to city centers are mainly buildings of four to eight stories. These building types are easily constructed with wood-based products [10]. New building codes and more sprinkler systems further facilitate timber use.

There is a growing body of consumer preference studies on building materials [11,12]. However, little research has been done on material preferences in the context of the urban built environment and changes in demographics resulting from immigration and movement.

As city officials, urban planners, architects, and construction companies plan for future housing, it is imperative that they understand the housing [1] and material preferences of city dwellers, especially in light of the changing demographics of regions resulting from immigration and movement to urban locales. Additionally, in Norway, the population is urbanizing. In a recent forecast, it was suggested that the Oslo region will receive up to 310,000 new inhabitants by 2020, thus adding to its current population, and an additional 600,000 in the period from 2020 to 2040. Housing these new arrivals will significantly impact the Oslo region [13]. The newcomers will partly come from Norway, where wooden houses are common, but newcomers will also come from countries where wood is hardly used. Accordingly, this study seeks to identify the differences between consumers with different building material backgrounds with regard to their preferences for materials in structural, interior, and exterior urban housing applications.

In the remainder of this article, we first provide a background regarding material preferences and the context of housing related to an urbanizing population that includes a significant proportion of immigrants. Next, we provide a background leading to research questions regarding the material preference differences between residents that have immigrated to Norway from countries where wood is hardly used in any buildings and native Norwegians. We use this as an example that may be considered in other global settings as cities plan their future housing expansion. We then discuss the methods used in the study, provide a description of the results, discuss those results, and provide specific policy and business implications.

Background

The materials used in buildings are a function of the availability and suitability of materials, as well as various cultural norms and traditions. For instance, in regions with termites, wood is less frequently used, and brick and stone buildings are more common. In some cultures or countries, wood-based housing is seen as inferior [12] and can even be considered a material associated with low social status, while in other countries, the traditions for using wood are strong. In Norway, a long tradition of using wood is illustrated with more than 800-year-old wooden buildings, and today, approximately 78% of the dwellings in Norway are one- and two-story wood structures [14].

Earlier studies have found relationships between tradition and material preferences [15] and between personal tradition and residential choice from a life style perspective [16], and have also revealed that choices are related to familiarity [1]. Extensive research has investigated the relationship between preferences and social expectations and the idea that the exterior of a house conveys meaning

about the owner to others [17,18]. Individuals may also use the house exterior to define their identity [19]. Hauge and Kolstad [20] suggest that there may be differences between genders or among ethnicities and cultural backgrounds with regard to what the interior and exterior of a house says about the owner. Accordingly, we might expect that people coming from different regions with different material traditions have different preferences. On the other hand, since preferences are also most likely related to where the material is used and modern building traditions in cities around the world tend to be similar, less differences between people from different parts of the world with regard to what they expect and prefer regarding materials used in multistory city housing may be expected.

In addition to studying differences between people with backgrounds from regions with different building material traditions, our study also includes analyses of the stated preferences for how and where to live. Since the exterior of a house might convey meaning about the owner to others [17,18] and people might use the house to define their identity [19], individuals who prefer city living might, to a greater extent, identify themselves with and be more positive regarding the buildings made of materials that are common in cities compared to buildings made of materials that are more common outside cities.

2. Materials and Methods

The work described below is partly based on the same survey as that used by Høibø et al. [21]. Here, we emphasize how material preferences are related to the respondent's origin and where and how they want to live, while Høibø et al. [21] focused on material preferences related to attitudes regarding durability and solidity, how environmentally friendly the material is, knowledge about wood, and experience with remodeling.

We collected responses through an online survey from individuals in immigrant families coming from countries where wood is not commonly used in houses (hereafter referred to as immigrants) and native Norwegians. Native Norwegians in this study are defined as those born in Norway with both parents from Norway. Immigrants are those with both parents born outside Norway (the individual respondent could be born inside or outside Norway).

2.1. Sampling

A total of 1751 persons were asked to participate in the study. However, the collection of data stopped when six hundred and sixty two people had completed the questionnaire. The respondents were part of the TNS Gallup As (today Kantar TNS AS) recruited probability panel, certified according to ISO 9001, ISO 20252, and ISO 26362:2009. The recruitment of the Gallup panel is mainly done through telephone listings and their sampling matrix design weights for biases based on how easy different groups of people are to reach. Panel members do not know the nature of the study before they access the electronic questionnaire. Demographic data about the respondents from the TNS Gallup AS database were added to our data set.

TNS Gallup AS did not have a large enough panel of immigrants specific to Oslo and several surrounding communities (Oslo region). Therefore, an additional set of respondents outside the Oslo region was targeted, in addition to the survey that Høibø et al. [21] used. Of the 662 responses received, 532 responses fit our definition of native Norwegians and immigrants, thus resulting in 437 native Norwegian responses and 95 immigrant responses. Of the 95 immigrant respondents, 67 were born in countries other than Norway. Thirty-nine immigrant respondents reside outside the Oslo region. Since there were two groups of immigrants, one residing in the same counties as the native Norwegian respondents, and a group residing in other counties, the total material is not completely random. Adjustments with a dummy variable were therefore made in some analyses. If there was no significant effect of this grouping, all respondents were considered to represent the same region. Most of the immigrants (71) had a background from Asia, Africa, or South America, while the rest came from Poland, which represents a large immigrant group in Norway.

Figure 1 shows distributions of the types of houses, in terms of structural material, that the immigrants and the native Norwegians had mainly lived in until they were 16 years old. The respondents that did not know how they lived in this period are not included in the figure. Table 1 provides additional information about the respondents.

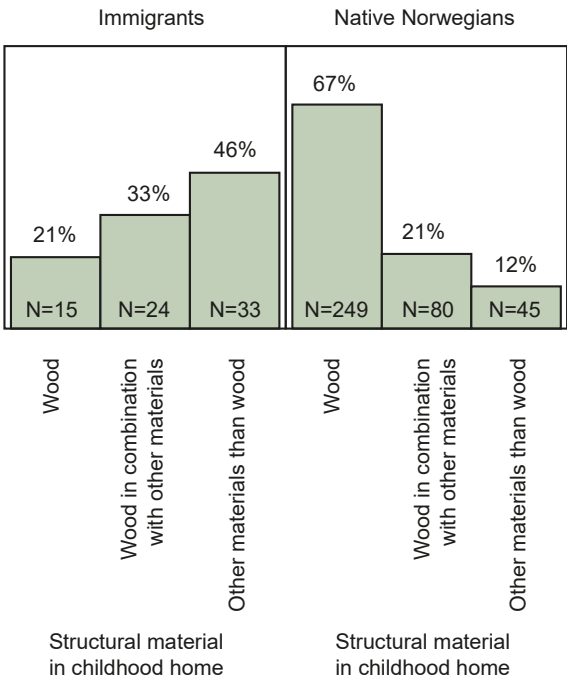


Figure 1. Distributions in N (number) and % of what kind of houses with respect to the structural material that the immigrants and the native Norwegians respectively had lived in the most until they were 16 years old.

Table 1. Statistics for the respondents.

Description of the Respondents	N (Number)
Region of origin immigrants/native Norwegians	95/437
Age (mean = 45.4, Standard deviation = 16.6)	
Gender female/male	277/255
Currently living in city	343
Currently living in large town	87
Currently living in small town	87
Currently living rural	13
Currently living in apartment, 3-story building or more	271
Currently living in row house	125
Currently living in detached house	104
Currently living in other type of housing	30

2.2. Description of Variables and Questions

Even though it may have been more difficult for respondents, we did not want them to react to visual images, but rather to provide their more basic material preferences. To help mitigate the issue of lack of knowledge, we provided an “I don’t know” category for many questions. The questionnaire

was tested on a small sample of respondents. The feedback was positive, and we made no major changes to the questionnaire.

All variables used in the statistical tests and models are shown in Table 2. For importance, knowledge, and preferences, a nine-point scale was used. For example, the scale ranged from “not important” to “very important” or from “do not like” to “like very much” [21]. Because we collected data via a questionnaire, all measures of preferences were stated preferences, as is commonly recommended [1].

Table 2. Variable definitions and abbreviation list.

Variables	Abbreviation	N Levels
Type of material for structural use	MStr	3 types 9 point scale
Type of material used on indoor walls and ceilings	MInd	5 types 9 point scale
Type of material for outdoor cladding	MCl	4 types 9 point scale
Preference for living in city, population more than 100,000	PrCity	9 point scale
Preference for living in rural areas	PrRur	9 point scale
Respondents' region of origin: immigrants and native Norwegians	ResOr	2 levels
Importance of the structural materials used	ImpStru	9 point scale
Importance of the materials used for indoor walls and ceilings	ImpInd	9 point scale
Importance of the materials used for outdoor cladding	ImpCl	9 point scale
Effect of different sampling between immigrants and inside and outside the Oslo region	EfSamp	2 levels

Three main questions about material preferences were included in the questionnaire [21]. One question was about the materials used in the structural part of the building. Answers were given individually for concrete, steel, and wood [21]. The next question was about the materials used for cladding. Answers were given individually for untreated wood cladding, painted or stained wood cladding, metal sheeting, and stone/bricks [21]. The last question was about the materials used for inside walls and ceilings. Untreated wood; lacquered, stained, or painted wood; paint or wallpaper on gypsum boards; paint or wallpaper on wood-based boards; and paint or wallpaper on concrete were the options [21]. Individual questions about the importance of the material used for structural purposes, outdoor cladding, and indoor walls and ceilings were also included [21].

Other questions included the following:

In what setting would the respondent prefer to live?

In a city (population more than 100,000).

In a large town (population between 10,000 and 100,000).

In a small town (population less than 10,000), or

In a rural area.

In what type of housing would they prefer to live?

In a detached house.

In a row house, or

In an apartment in an apartment block with three stories or more.

Importance of closeness to stores, schools and other services.

Importance of closeness to family, friends, and acquaintances.

Importance of low price.

Relationship to and knowledge about buildings and the construction industry.

2.3. Analysis

The statistical software JMP version 10.0 from the SAS Institute Inc. (Cary, NC, USA) [22] was used in the data analyses. Where appropriate, contrasts were tested with F-tests. However, some of the data exhibited heteroscedasticity and nonnormality, and so we chose to use a logistic regression and chi square tests in most analyses. For the comparison of groups, we used chi square tests and, when necessary, we merged cells to maintain greater than 80% of cells with five or more responses. The responses of “do not know” were not included in the analyses. The logistic regression calculated the probabilities for each level of the response and gave nine probabilities, depending on the values of the independent variables. To do this, eight fitting lines were calculated (when a nine-point scale was used) (see figure caption Figure 3).

A small effect of the difference in sampling between immigrants inside and outside the Oslo region was found for the analyses on indoor wall and ceiling material preferences and where they want to live, thus requiring a correction via a dummy variable. If nothing else was said, variables were rejected if the probability of type I error was smaller than 0.05.

3. Results

3.1. Material Preferences

Native Norwegians had somewhat higher mean preferences for concrete and steel structural materials than immigrants (Figure 2a). However, the differences were small. For wood as a structural material, it was the opposite, but the difference was minor (Figure 2a). The differences in preferences between wood and concrete and between wood and steel, respectively, were not significantly different between immigrants and native Norwegians.

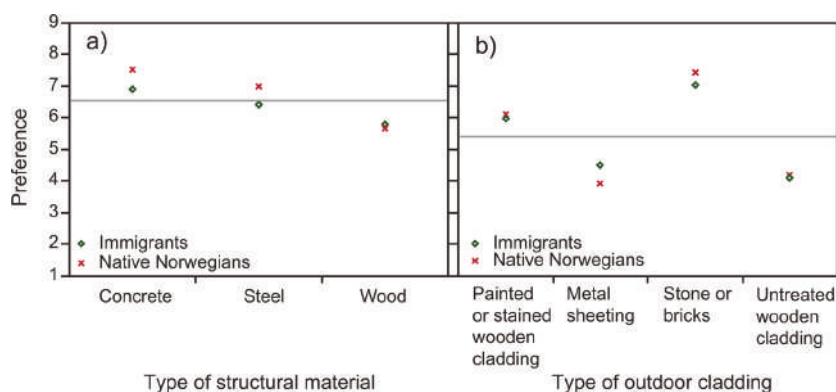


Figure 2. Mean preferences for different structural materials (a) and cladding materials (b).

For outdoor cladding, the only significant difference between immigrants and native Norwegians was the native Norwegians' somewhat higher preference for stone/brick cladding ($p = 0.038$, chi-square test). However, when testing the difference with an F-test, the p -value was only 0.088. Immigrants had a somewhat higher preference for metal sheeting, but this difference was not statistically significant (Figure 2b). For painted or stained wooden cladding and untreated wooden cladding, native Norwegians and immigrants had almost the same preferences (Figure 2b). Overall, there were significant differences in the preferences for the different cladding materials ($p < 0.0001$, chi-square test).

No significant differences were found between native Norwegians and immigrants for the five indoor materials. Overall, there were significant differences in indoor material preferences ($p < 0.0001$, chi-square test).

3.2. Location and House Type Preference

No significant differences were found between immigrants in the Oslo region and native Norwegians with respect to detached and row houses. However, across all respondents, a significant difference in the preferences between types of house was found ($p < 0.0001$, chi-square test). Detached houses were the most preferred, while row houses and apartments in multistory buildings had almost the same preference for respondents from the Oslo region. For immigrants outside the Oslo region, apartments in multistory buildings were less preferred than other types of housing.

Closeness to stores, schools, and other services was significantly more important for immigrants from the Oslo region than for non-Oslo region immigrants and native Norwegians ($p = 0.023$, chi-square test). Closeness to family was also significantly more important for immigrants from the Oslo region than for native Norwegians ($p = 0.029$, chi-square test). For immigrants outside the Oslo region, the importance for living close to family was less important than it was for immigrants in the Oslo region. The effect of the dummy variable was almost significant at the 5% level. When excluding this effect, no significant effect of respondents' region of origin was found. No significant difference between immigrants and native Norwegians was found for the importance of closeness to friends and acquaintances.

Finally, low price was significantly more important for immigrants, regardless of where they currently reside, than for native Norwegians ($p < 0.0001$, chi-square test).

3.3. Multiple Models

Model 1 (Table 3) includes the variables that were found to be important for structural material preferences. Concrete was the most preferred material (largest probability for 9 and 8 preferences, left column plots, Figure 3).

Table 3. Statistics for the multiple logistic regressions.

	Model 1 Structural Materials	Model 2 Outdoor Cladding	Model 3 Indoor Walls & Ceilings
Summary statistics for the different models			
Entropy R^2 (Coef. of determin.)/Gen R^2 (Coef. of determin.)	0.049/0.18	0.079/0.29	0.024/0.098
N	1165	1725	2325
<i>p</i> -values for the independent variables in the different regressions			
MStr	<0.0001		
ResOr	0.73	0.35	0.31
PrCity	<0.0001	0.0011	0.0025
MStr \times PrCity	0.021		
ImpStru	<0.0001		
ResOr \times ImpStru	0.0006		
PrRur	0.0001	0.0010	
PrCity \times PrRur	0.0002		
MInd			<0.0001
MInd \times PrCity			0.0033
Implnd			<0.0001
ResOr \times Implnd			0.0036
MInd \times Implnd			0.0002
MCl		<0.0001	
MCl \times PrCity		0.0841	
ImpCla		<0.0001	
ResOr \times ImpCla		0.0038	
MCl \times ImpCla		0.014	
EfSamp			0.048

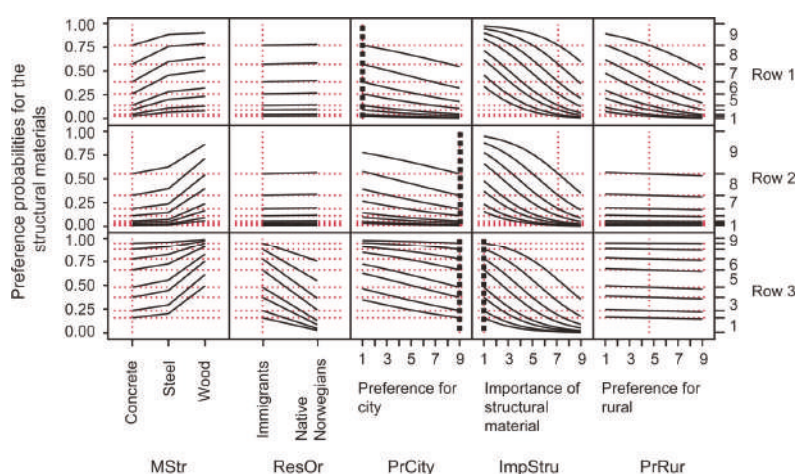


Figure 3. Profile plots showing the preferences for different structural materials, depending on the values of various independent variables in Model 1. The profile plots show the preferences for different structural materials, depending on the values of various independent variables in Model 1 (Table 3). Three rows of plots are included to show how the preferences for the different structural materials change with changes in the independent variable values. The thick vertical dashed lines indicate where the researcher set the value of the independent variables. The distances between the horizontal lines in the first column of plots show the probability for the different preference values. The probability for preference 9 is the distance between the upper most line and 1.00. The distance between lines 7 and 8 shows the probability for preference value 8. The probability for the lowest preference value is between 0.00 and the lowest line. For example, in row 2, column 1, approximately 40% of the respondents rated their preference for concrete as the highest value of 9, given by the independent variables setting values, as shown by the vertical dashed lines. Although some of the data in Figure 2 is categorical, the lines between categories are provided only for the ease of the visual interpretation of changes in level from one category to the next. This figure text is partly the same as the figure text in Figure 1 in the article of Høibø et al. [21].

Model 1 includes a significant interaction effect between the type of structural material and preference for living in a city. A higher preference for living in a city corresponds with an increasing preference for steel and concrete (changes are larger for steel than concrete) rather than wood (Figure 3, row 1 and row 2). Preference for living in a city was the only variable with a significant interaction effect on the 5% level with the type of structural material.

The other interaction effects are mainly related to the level of structural material preferences. Nevertheless, for respondents saying that the structural material type in general is of little importance, the probability for the highest preference decreases the most for concrete, somewhat less for steel, and the least for wood, compared to that of the respondents who reported that structural material was important for them (Figure 3, row 2 and row 3). However, the probability for the lowest preference increases the most for wood with the respondents saying that the structural material type in general is of little importance, compared to that of the respondents who stated that structural material was important (Figure 3, row 2 and row 3). Model 1 also includes a significant interaction effect between the respondent's region of origin and the importance of the structural material. For the respondents saying that the type of structural material was of little importance, the immigrants responded with lower preferences than the native Norwegians (Figure 3, row 3). A significant interaction effect between preferences for living in cities and preferences for living in rural areas was also included. This effect only affected the levels of preferences across the different structural materials.

An interaction effect between the type of structural material and the respondent's region of origin was also tested, but it was not significant. This result means that the differences in preferences between the different structural materials were not significantly different between immigrants and native Norwegians.

Model 2 (Table 3) includes variables that were important for the preferences for the different materials used for outdoor cladding. Stone/bricks were the most preferred cladding material, followed by painted or stained wood. Metal sheeting and untreated wood were the least preferred (Figure 4, row 1, column 1). Model 2 includes an interaction effect between the type of material for outdoor cladding and preference for living in a city, even though it was only significant at the 8.4% level. The interaction effect resulted in higher preferences for stone/bricks than for the other materials when preferences for living in a city were high (Figure 4, row 1 and row 2). A significant interaction effect between the type of material for outdoor cladding and the importance of the material used for outdoor cladding was also included in Model 2. The interaction effect resulted in fewer differences in preferences between the different types of claddings when the importance of the material used for outdoor cladding was small (Figure 3, row 2 and row 3). Model 2 also includes a significant interaction effect between the respondent's region of origin and the importance of the materials used for outdoor cladding. For respondents saying that the material used for outdoor cladding was not important, the native Norwegians responded with higher material preferences in general than immigrants (Figure 4, row 3). Higher preferences for rural living adjusted the level of the fitted lines, thus resulting in a general increase in preferences across the different cladding materials (Figure 4, the last column of plots).

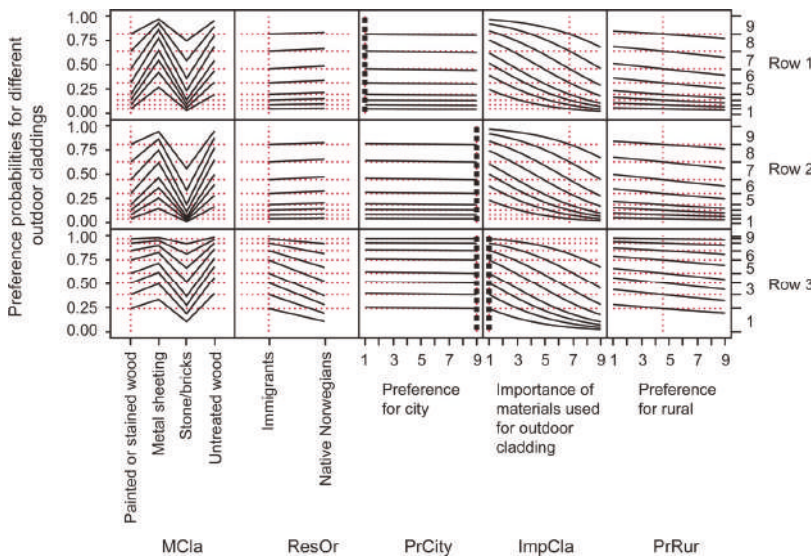


Figure 4. Profile plots showing the preferences for different outdoor cladding materials, which depend on the values of the different independent variables in Model 2. Three rows of plots are included in the figure to show how the preferences for the different outdoor cladding materials change with differing settings of the independent variables. This figure text is partly the same as that in Figure 4 in the article of Høibø et al. [21].

Model 3 includes the variables found to be important for the preferences for different materials used on indoor walls and ceilings (Table 3). Model 3 shows that lacquered, stained or painted wood,

and paint or wallpaper on different boards were the most preferred (Figure 4 first row). Paint or wallpaper on concrete together with untreated wood were the least preferred indoor materials for respondents that did not prefer to live in a city (Figure 5, row 1). When respondents preferred to live in a city, the preference for untreated wood was the lowest (Figure 5, row 2). Respondents who preferred to live in a city and also said that the material used on indoor walls and ceilings was of low importance, preferred paint or wallpaper on concrete the most (Figure 5, row 3). For these respondents, lacquered, stained, or painted wood together with untreated wood were the least preferred materials (higher probability for the lower preferences).

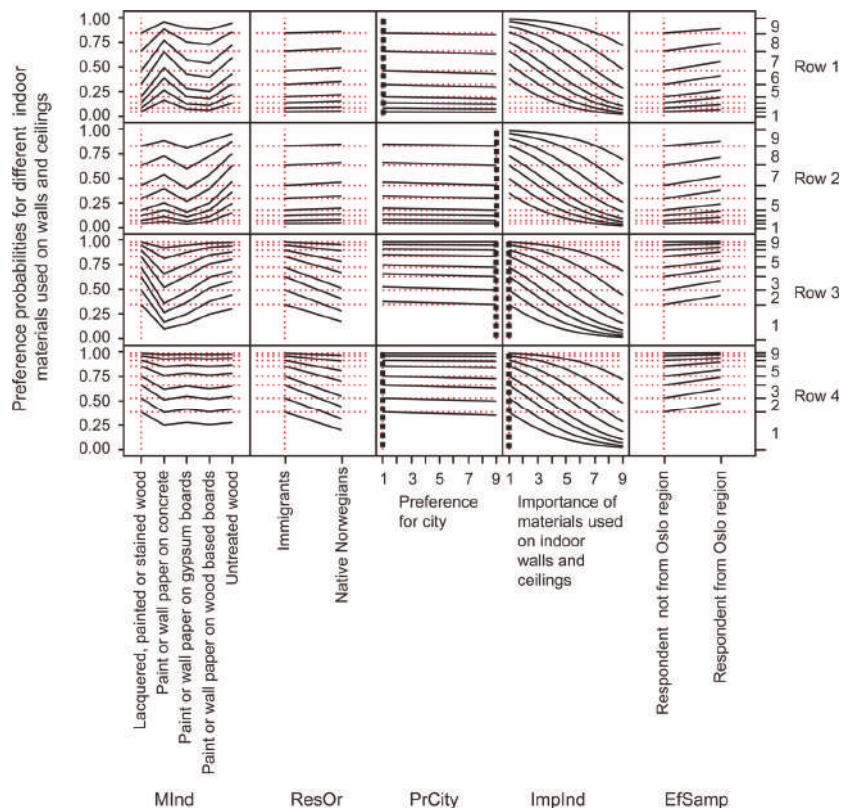


Figure 5. Profile plots showing the preferences for different indoor materials, which depend on the values of the different independent variables in Model 3. The four rows of plots are included in the figure to show how the preferences for the different indoor materials change with changes in independent variables. This figure text is partly the same as that in Figure 3 in the article of Høibø et al. [21].

Respondents with low preferences for living in large cities who also said that the material used on indoor walls and ceilings was of low importance had relatively equal scores for the different materials (Figure 5, row 4). When the materials used on indoor walls and ceilings was of low importance, the native Norwegians gave a higher score for all materials than the immigrants. Nevertheless, the relative difference between the different materials did not vary much between native Norwegians and immigrants.

4. Discussion

Craig et al. [15] found relationships between material traditions and material preferences, Vasanen [1] found that choices are related to familiarity, and Hauge and Kolstad [20] suggested that there might be differences between genders or among ethnicities and cultural backgrounds with respect to what the interior and exterior of a house says about the owner. Accordingly, we could expect to find differences between native Norwegians and immigrants regarding material preferences since the two groups have different building cultural backgrounds and different experiences with regard to building environments. However, only small differences were found between the two groups. Even with the extensive use of wood in one- and two-story houses in Norway, which represents approximately 78% of housing [14], the structural material preferences of Norwegians did not differ from those of immigrants. For both groups, concrete was the most preferred structural material, followed by steel. Wood was the least preferred. Since native Norwegians also had a significantly higher preference for stone/brick cladding than immigrants, and the immigrant group in this study have a building culture background from areas where wood is less frequently used and stone is more frequently used, the strong Norwegian wood tradition outside cities appears to play almost no positive role for wood used in a city context.

However, the overall high preferences for concrete and low preferences for wood fit well with the material tradition [15] in cities. Concrete is the dominant structural material in large buildings in Norway [23], while wood structures in multistory city buildings are uncommon. It therefore seems that preferences are mostly related to city building material traditions. However, according to the hypothesis of the material traditions in cities, we would not have expected painted or stained wooden cladding to fare that well in the evaluation. The visual presence of wood in landmark buildings and a general focus on wood as a natural and renewable resource may have influenced general attitudes. The diverse profiles and variety of colors associated with timber architecture may have had a positive impact on the acceptance of wooden cladding also in an urban setting.

Nevertheless, the most preferred cladding material was stone/bricks, which is also a common city cladding material. This finding is in accordance with those of McManus and Baxter [24], Craig et al. [15], and National Association of Home Builders (NAHB) [11], who found bricks to be the most preferred outdoor cladding material. The high preference for stone/bricks, particularly for native Norwegians, might be related to attitudes connected to the upmarket status, since stone and brick claddings are more expensive than the other cladding materials. It might also be related to the high focus in Norway on the maintenance and durability of claddings [21] and that stone bricks are regarded to be the most durable [15], which also fits with the finding of increasing differences in preferences among cladding materials for respondents that are more concerned about outdoor cladding (Figure 4, row 2 and row 3).

Our findings show that there are other factors that have a stronger influence on respondents' material preferences in city buildings than if they come from a country where wood is an uncommon building material, or from a country where wood is extensively used. We found some significant differences between the two groups of dwellers studied. However, most of the differences with regard to material preferences were related to different attitudes, such as preferences regarding where the respondents wanted to live. Since increased preferences for city living increased the preferences for materials that are common in cities, individuals who prefer city living to a greater extent identify themselves with buildings made of materials that are common in cities rather than buildings made of materials that are more common outside cities. This finding is in accordance with those of Nasar and Kang [17] and Sadalla and Sheets [18], who say that the exterior of a house might convey a meaning about the owner to others, and Desprès [19], who found that people might use the house to define identity. Higher preferences for city living combined with higher preferences for common city building structural materials (Figure 3, row 1 and row 2) therefore fits well with the expected relationship between tradition and material preferences in a city context, personal tradition, and residential choice from a life style perspective [16], and other choices related to familiarity [1]. This finding is also

in accordance with our findings on residential choice, where we found that immigrants and native Norwegians inside the Oslo region prefer apartments in multistory buildings more than immigrants outside the Oslo region, who preferred apartments in multistory buildings the least.

Within the category of respondents who prefer to live in a city and said that the material that is used indoors is not important, the highest preferred indoor material was paint or wall paper on concrete, while for the respondents who said that indoor materials was important, paint or wallpaper on concrete was one of the least preferred materials. Our study therefore shows that there were different preferences for using concrete as a structural material and concrete used as an indoor wall and ceiling material, but that this difference depended to a large extent both on the respondent's attitudes regarding the importance of indoor material use and preferences for living in a city (Figure 5, row 2 and row 3 and Figure 3). The experience of concrete as a "cold" absorber of body heat radiation might be the reason why respondents who both prefer city living and said that indoor materials are important state low preferences for indoor concrete surfaces. Mechanical resistance and noise related to the boring of holes and simple interior modifications may also play a role. Our findings show that for concrete structures, inner surfaces other than paint or wallpaper on concrete should be considered.

It is logical that the same materials see different preferences for structural use and indoor surface use because each fulfills different needs. For visual surfaces, both visual and tactile properties are important. Brandt and Shook [25] found that consumers' quality attributes for forest products are usually visual or tactile. Consumer preferences for wood are found to depend on harmony, activity, and social status [26]. Harmony is related to homogeneity [27], while a positive relationship between visual homogeneity and preferences is found for decking materials [28]. For structural materials, physical properties such as strength properties, fire safety, and sound insulation are more important.

The correspondence of preferences may be attributed to the common features of all urbanizing regions and may also relate to the fundamental role of buildings as the stable framework for social life. In Norway, the functional and technological standards of buildings are homogenous and highly regulated on governmental and municipal levels. Rental housing constitutes a very small part of the housing market. Varieties of individual and shared ownership dominate, also among immigrants. The typical, cooperative housing associations in Oslo require participation in decisions regarding maintenance and investments, which may be a strong integrating factor that may influence attitudes towards the design and materiality of buildings.

5. Conclusions

Our findings provide a few primary insights into consumer preferences for city-based housing in Norway. First, with respect to material preferences in city housing, there are only minor differences between Norwegian natives who represent countries where wood is extensively used in houses outside cities and immigrants coming from a country where wood is hardly used at all. Differences that do exist between respondents are more related to where an individual would prefer to live. Second, despite the longstanding tradition of wood use in single-family houses in Norway, other materials that have traditionally been used in city buildings are more preferred. The preferences seem, therefore, to be more related to material traditions and to the context in which the materials are used. Individuals who prefer city living seem to a greater extent to identify themselves with buildings made of materials that are common in cities rather than with buildings made of materials that are more common outside cities. Since the material tradition and the context seem to be important factors for consumers, consumer information is important when a material is introduced in a new context. Landmark wooden city buildings for housing are a useful tool for developers to introduce, teach, and make wood more familiar in a city context.

6. Limitations

As our goal was not the generalization of a population, but rather to compare two groups of Norwegians, we did not attempt to obtain a pure random sample. With respect to immigrant

participants, our sample size was smaller than ideal. This made the result less robust and hindered our ability to validate the models. Additionally, the variation within the immigrant group was large since they come from different continents and countries. This large variation may have decreased the probability of finding significant effects.

Author Contributions: O.H. contributed to the following parts: project administration, research design and data collection. He also conducted the statistical analyses and lead the writing. E.H. contributed to the following parts: project administration, research design, discussion around the statistical analyses and writing. E.N. contributed to the following parts: project administration, research design, discussion around the statistical analyses and writing. M.N. was the project leader and contributed to the following parts: project administration, research design, and writing.

Funding: The majority of funding for this project comes from The Research Council of Norway (project: Increased Use of Wood in Urban Areas, project number 225345).

Acknowledgments: The authors would like to thank the various parties responsible for making this research possible. We also thank Eva Fosby Livgard at TNS Gallup AS (today Kantar TNS AS) for giving us feedback on the research design. We also thank the Fulbright Foundation who partly funded a stay at Oregon State University for Olav Høibø, where most of this research was done.

Conflicts of Interest: The authors declare no conflict of interest. The founding sponsors had no role in the design of the study, in the collection, analyses, or interpretation of the data, in the writing of the manuscript, and in the decision to publish the results.

References

1. Vasanen, A. Beyond stated and revealed preferences: The relationship between residential preferences and housing choices in the urban region of Turku, Finland. *J. Hous. Built Environ.* **2012**, *27*, 301–315. [CrossRef]
2. UN Department of Economic and Social Affairs Population Division. Available online: http://www.un.org/en/development/desa/population/publications/pdf/trends/WPP2012_Wallchart.pdf (accessed on 19 October 2014).
3. UN Habitat. Available online: <http://mirror.unhabitat.org/content.asp?cid=5809&catid=206&typeid=6> (accessed on 19 October 2014).
4. Dunse, N.; Thanos, S.; Bramley, G. Planning policy, housing density and consumer preferences. *J. Prop. Res.* **2013**, *30*, 221–238. [CrossRef]
5. Price, M.; Benton-Short, L. Counting Immigrants in Cities across the Globe. Migration Policy Institute. Available online: <http://www.migrationpolicy.org/article/counting-immigrants-cities-across-globe> (accessed on 14 December 2007).
6. Price and Benton-Short. Available online: <http://www.migrationpolicy.org/article/counting-immigrants-cities-across-globe> (accessed on 13 November 2014).
7. Hernandez, P.; Kenny, P. Development of a methodology for life cycle building energy ratings. *Energy Policy* **2011**, *39*, 3779–3788. [CrossRef]
8. Robertson, A.B.; Lam, F.C.; Cole, R.J. A comparative cradle-to-gate life cycle assessment of mid-rise office building construction alternatives: Laminated timber or reinforced concrete. *Buildings* **2012**, *2*, 245–270. [CrossRef]
9. Ritter, M.A.; Skog, K.; Bergman, R. *Science Supporting the Economic and Environmental Benefits of Using Wood and Wood Products in Green Building Construction*; General Technical Report FPL–GTR–206; United States Department of Agriculture, Forest Service, Forest Products Laboratory: Washington, DC, USA, 2011; p. 9.
10. Mahapatra, K.; Gustavsson, L. Multi-storey timber buildings: Breaking industry path dependency. *Build. Res. Inf.* **2008**, *36*, 638–648. [CrossRef]
11. NAHB. Available online: <http://www.prnewswire.com/news-releases/new-nahb-study-shows-national-consumers-prefer-brick-197850191.html> (accessed on 28 November 2014).
12. Davies, I.; Walker, B.; Pendlebury, J. *Timber Cladding in Scotland*; ARCA Publications: Edinburgh, UK, 2002.
13. Tandberg, E.; Morstad, P. *Uttalelse Til Nasjonal Transportplan 2014–2023*; Byrådsavdeling for Miljø og Samferdse: Kirkegaten, Lillehammer, 2012; p. 7.
14. Statistics Norway. Available online: <http://www.ssb.no/boligstat> (accessed on 5 November 2014).

15. Craig, A.; Abbott, L.; Laing, R.; Edge, M. Assessing the Acceptability of Alternative Cladding Materials in Housing: Theoretical and Methodological Challenges. Available online: http://www.researchgate.net/publication/27250534_assessing_the_acceptability_of_alternative_cladding_materials_inhousing_theoretical_and_methodological_challenges (accessed on 16 December 2002).
16. Ærø, T. Residential choice from a lifestyle perspective. *Hous. Theory Soc.* **2006**, *23*, 109–130. [[CrossRef](#)]
17. Nasar, J.L.; Kang, J. House style preference and meanings across taste cultures. *Landsc. Urban Plan.* **1999**, *44*, 33–42. [[CrossRef](#)]
18. Sadalla, E.K.; Sheets, V.L. Symbolism in building materials. *Environ. Behav.* **1993**, *25*, 155–180. [[CrossRef](#)]
19. Desprès, C. The meaning of home: Literature review and directions for further research and theoretical development. *J. Archit. Plan. Res.* **1991**, *8*, 96–115.
20. Hauge, Å.L.; Kolstad, A. Dwelling as an expression of identity. A comparative study among residents in high-priced and low-priced neighbourhoods in Norway. *Hous. Theory Soc.* **2007**, *24*, 272–292. [[CrossRef](#)]
21. Høibø, O.; Hansen, E.; Nybakk, E. Building material preferences with a focus on wood in urban housing: Durability and environmental impacts. *Can. J. For. Res.* **2015**, *45*, 1617–1627. [[CrossRef](#)]
22. JMP, Version 10.0.0. Statistical Discovery, SAS Institute Inc.: Cary, NC, USA, 2012.
23. Store Norske Leksikon. Available online: <https://snl.no/h\T1\oyhus> (accessed on 25 November 2014).
24. McManus, B.R.; Baxter, D.O. Revealed preferences for building materials: A survey of low and moderate income households. *Hous. Soc.* **1981**, *8*, 45–51. [[CrossRef](#)]
25. Brandt, J.P.; Shook, S.R. Attribute elicitation: Implications in the research context 1. *Wood Fiber Sci.* **2007**, *37*, 127–146.
26. Broman, N.O. Means to Measure the Aesthetic Properties of Wood. Ph.D. Thesis, Luleå University of Technology, Luleå, Sweden, 2000.
27. Nyrud, A.Q.; Roos, A.; Rødbotten, M. Product attributes affecting consumer preference for residential deck materials. *Can. J. For. Res.* **2008**, *38*, 1385–1396. [[CrossRef](#)]
28. Høibø, O.; Nyrud, A.Q. Consumer perception of wood surfaces: The relationship between stated preferences and visual homogeneity. *J. Wood Sci.* **2010**, *56*, 276–283. [[CrossRef](#)]



© 2018 by the authors. Licensee MDPI, Basel, Switzerland. This article is an open access article distributed under the terms and conditions of the Creative Commons Attribution (CC BY) license (<http://creativecommons.org/licenses/by/4.0/>).

Investigation of Bamboo Grid Packing Properties Used in Cooling Tower

Li-Sheng Chen ^{1,2}, Ben-Hua Fei ^{1,2}, Xin-Xin Ma ^{1,2}, Ji-Ping Lu ³ and Chang-Hua Fang ^{1,2,*}

¹ Department of Biomaterials, International Center for Bamboo and Rattan, Beijing 100102, China; chenlisheng@icbr.ac.cn (L.-S.C.); feibenhua@icbr.ac.cn (B.-H.F.); maxx@icbr.ac.cn (X.-X.M.)

² SFA and Beijing Co-built Key Laboratory of Bamboo and Rattan Science & Technology, State Forestry Administration, Beijing 100102, China

³ Hengda Bamboo Filler Limited Company, Yixing 214200, China; hdlwz@163.com

* Correspondence: cfang@icbr.ac.cn; Tel.: +86-010-84789786

Received: 1 November 2018; Accepted: 5 December 2018; Published: 7 December 2018

Abstract: Due to its advantages of good heat-resistance, environmental-friendliness, and low cost, bamboo grid packing (BGP) has become a promising new type of cooling packing. It is being increasingly used in Chinese industrial cooling towers to replace cooling packings made of polyvinyl chloride, cement, and glass fiber reinforced plastic. However, mechanical properties and fungal resistance are a concern for all bamboo applications. In this study, the modulus of rupture (MOR), modulus of elasticity (MOE), density, crystallinity, and environment scanning electron microscope (ESEM) properties were compared between fresh BGPs and those that had been in service for nine years in the cooling towers. The results showed that the MOR, MOE, density, crystallinity, and the crystal size of the used BGPs decreased to some extent, but still met the requirements for normal use in a cooling tower. The ESEM observation showed that the used BGPs were not infected by fungi. The decrease in mechanical properties could be caused by the decrease of density, crystallinity, and the decomposition of the chemical components of bamboo, but not by fungal infection.

Keywords: bamboo grid packing; cooling packing; cooling tower; mechanical properties; fungi; bamboo

1. Introduction

Hyperbolic cooling towers are widely installed at power plants, steel mills, petroleum refineries, and petrochemical plants due to their high capacity for heat rejection and energy saving. Compared to package-type cooling towers, hyperbolic cooling towers are generally much larger in size and require much more cooling packing. Cooling packing is the core component of cooling towers, and is responsible for 60%–70% of the heat dissipation in the cooling tower [1–4]. The type of packing material has an important role, as it provides a large surface area for evaporative heat and mass transfer from hot water to the ambient air and increases the contact time between both the two [5]. Different materials such as polyvinyl chloride (PVC), cement, and glass fiber reinforced plastic have been used as cooling packing. Currently the most popular cooling packing is made of PVC, with a market share exceeding 70% in China [6]. However, the PVC packing industry is facing major challenges, such as diminishing availability of petrochemical resources, increases in their prices, and the residues of PVC in the environment beyond its functional life [7]. In China, there are many power plants, steel mills, petroleum refineries, and petrochemical plants, from which the discarded cooling packing could cause severe environmental pollution. Furthermore, PVC packing has a short service life and poor anti-fouling properties. Thus, researchers and entrepreneurs have been seeking environmentally-friendly and longer-serving alternatives to PVC.

Recently, packing material made of bamboo has been put to use in several hyperbolic cooling towers in China [8]. Bamboo, as one of the fastest-growing and most versatile plants, grows widely across tropical and temperate zones with wet climate. It is a raw material with great economic importance that has been used since ancient times. Accounting for around 1% of the world's total forest area [9], there is a total area of 31.5 million hectares of bamboo, 60% of which are concentrated in rapidly developing countries, such as China, India, and Brazil [10]. Bamboo is also an invasive plant in some parts of the world [11], the expansion of which tends to reduce the biological diversity in local environment, affect the physico-chemical properties and microbial composition of soil, weaken the ecosystem function, and change the forest landscape [12]. However, due to the combination of advantages of fast growth, short life cycle, high mechanical strength, and low energy consumption [13], bamboo also has an outstanding natural potential for use as packing material, which may help control the expansion of bamboo forests, reduce greenhouse gas, and provide carbon sequestration. Compared to PVC packing, bamboo grid packing (BGP) also has certain advantages in temperature adaptability, anti-fouling properties [6,8], as well as a good cooling performance [14–17]. However, durability has always been a concern for any application of bamboo materials. The compromising of mechanical properties caused by continuous exposure to hot water flow in the cooling tower can be problematic. In addition, bamboo is vulnerable to fungal infection because of its richness in nutrients. Fungal infection could be fatal as it decreases the mechanical strength of bamboo and subsequently shortens the BGP's service life. The lack of research in this aspect hinders the development of BGP for industrial application.

To fill this gap, the mechanical properties, such as the modulus of rupture (MOR) and modulus of elasticity (MOE), of BGPs that had been used for nine years in cooling towers were investigated and compared to the properties of unused control samples. Density and crystallinity were also investigated, and samples were observed under environment scanning electron microscope (ESEM) to gain a better understanding of the changes in mechanical properties, as well as BGP's fungal resistance.

2. Materials and Methods

2.1. Materials

Raw materials were obtained from Moso bamboo (*Phyllostachys edulis* (Carrière) J.Houz) grown in Shaowu, Fujian Province, China. Bamboo culms were cut into strips (1200 mm in longitudinal direction and 40 mm in tangential direction). Three holes with a diameter of 10 mm were made on the strips. Round bamboo sticks were inserted into the holes to connect the bamboo strips, as shown in Figure 1. The dimension of one piece of BGP was 1200 mm × 600 mm × 40 mm, and the spacing between the bamboo strips was 50 mm. BGP units were stacked to a height of 1.5 m in a hyperbolic cooling tower (Figure 1). Control samples were collected from the fresh BGP units.

Nine-year-old BGP units were collected from two hyperbolic cooling towers located respectively in Fujian and Shandong Province. The BGP collected from Fujian Province (FJBGP) was used in a hyperbolic cooling tower of a thermal power plant. The one collected from Shandong Province (SDBGP) was used in a hyperbolic cooling tower of a steel mill. In both cooling towers, the inlet water temperature was 45 to 50 °C, and the water mass flux was around 6500 kg/(h·m²). Prior to the experiment, all specimens were conditioned at 21 ± 2 °C, with relative humidity of 65 ± 3%, to reach the equilibrium moisture content (EMC).

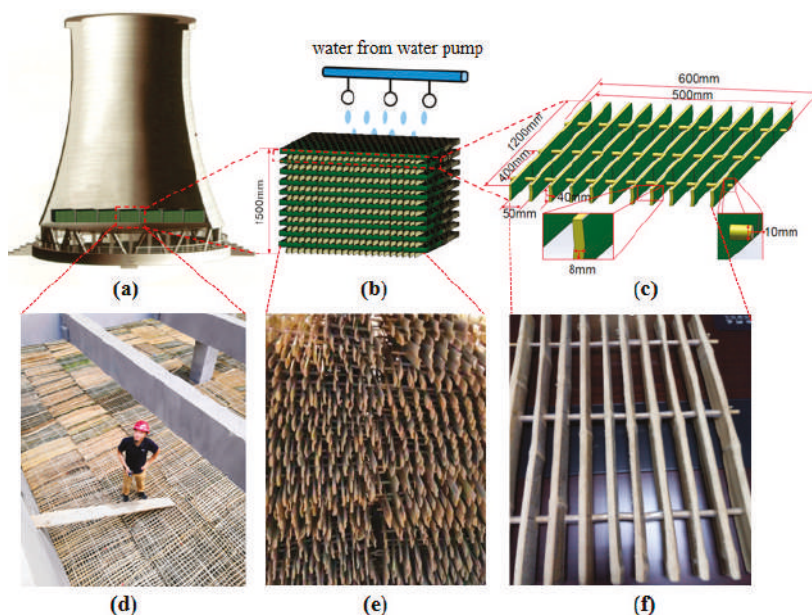


Figure 1. (a,d) Application of bamboo grid packing (BGP) in hyperbolic cooling towers; (b,e) stack of BGP units; (c,f) BGP assembled with bamboo strips.

2.2. Mechanical Properties and Density Test

Three-point static bending tests were performed according to GB/T 15780-1995 to obtain both the MOR and the MOE [18]. Since the load on the BGP is mainly in the tangential direction in the actual working environment of a cooling tower, the bending tests of bamboo strips were also performed in the tangential direction. The dimension of test specimens was 160 mm (longitudinal) \times 10 mm (tangential) \times t (thickness of the bamboo culm wall). Tests were loaded along the tangential direction at a rate of 6 mm/min. The moisture content was measured after the bending tests. The specimen density was measured with the drainage method according to GB/T 1933-2009 [19]. The number of specimens in the control group, the FJBG, and the SDBG for the determination of mechanical properties and density testing were ten, twenty, and sixteen, respectively.

2.3. Crystallinity Test

Eighty mesh bamboo powder was used as the experimental material. Bamboo powder was processed by a mill, which comprised a means of randomly mixing and distributing the small fiber lengths in various directions at surface pressures far below those that would induce crystallite fracture [20]. X-ray diffraction (XRD) measurements were performed to assess the crystalline properties of air-dried bamboo cell walls using an X-ray diffractometer (AV300, Panalytical Co., Amsterdam, The Netherlands) at a wavelength of 0.154 nm. The incident X-ray radiation was measured as the characteristic Cu X-ray passing through a nickel filter with a power of 40 kV and 40 mA. The XRD spectrum of every specimen was recorded in the angles (2θ) of 5–50°. Three replicates were tested in this section. The cellulose crystallinity was calculated by the following Segal method [21]:

$$C_{rl} = \frac{I_{002} - I_{am}}{I_{002}} \times 100\% \quad (1)$$

where C_{rl} represents the crystallinity of cellulose (%), I_{002} represents the reflection intensity of (002) plane diffraction, and I_{am} represents the intensity at the minimum near 18° of 2θ angle.

The Scherrer equation, in X-ray diffraction and crystallography, relates the size of sub-micrometer particles, or crystallites, in a solid to the broadening of a peak in a diffraction pattern [22]. This study used this method to determine the size of crystal particles in cellulose. The Scherrer equation was used to calculate the mean size of ordered (crystalline) domains and can be written as [23]:

$$D = \frac{K\lambda}{\beta \cos \theta} \quad (2)$$

where D represents the mean size of the crystal region (nm), K represents a dimensionless shape factor (0.9), λ represents the X-ray wavelength, β represents the line broadening at half the maximum intensity, and θ represents the scattering angle.

2.4. Microstructure Observation

An environmental scanning electron microscope (ESEM, XL30 FEG, FEI Co., Hillsboro, OR, USA) was used to observe the microstructure of bamboo strips. Cubic specimens (5 mm × 5 mm × 5 mm) were carefully prepared with razor blades and microtome to obtain a neat surface. Then, the surfaces of specimens were coated with elemental gold film (8–10 nm) and observed under the ESEM.

2.5. Statistical Analysis

Multiple comparisons were first subjected to an analysis of variance (ANOVA) using SPSS 19.0 (IBM SPSS Corporation, Chicago, IL, USA), and significant differences between average values of control and used BGP specimens were determined using Duncan's test at 0.05 significance level.

3. Results and Discussion

3.1. Mechanical Properties and Density

The mechanical properties of the BGP strips are presented in Table 1. The MOR of FJBGP and SDBGP were 106.16 MPa and 107.91 MPa, respectively, and the MOE of FJBGP and SDBGP were 8869.66 MPa and 8986.50 MPa. The difference in mechanical properties between FJBGP and SDBGP was not statistically significant. However, the MOE and MOR of both FJBGP and SDBGP were all significantly lower than those of the control samples. These results demonstrated that the hygrothermal conditions in the cooling towers had a negative effect on the BGP's mechanical properties. This might be related to the degradation of bamboo components by the water flow, which decreased its density and crystallinity.

Table 1. The average MOR, MOE, and density of used BGPs and control samples.

Materials	MOR (MPa)	MOE (MPa)	Density (g/cm ³)	Retention of Properties (%)		
				MOR	MOE	Density
Control	143.15 ± 16.68a	10,250.83 ± 1091.67a	0.7165 ± 0.4452a	100	100	100
FJBGP	106.16 ± 19.14b	8869.66 ± 1737.26b	0.6596 ± 0.5839b	74.16	86.53	92.06
SDBGP	107.91 ± 26b	8986.50 ± 2010.31b	0.6531 ± 0.8499b	75.38	87.67	91.15

Note: Standard deviation are presented after ±. The different letters in the same column indicate a significant difference at the 0.05 level.

Compared to the control samples, the MOR retention of FJBGP and SDBGP were 74.16% and 75.38%, respectively, and the MOE retention of FJBGP and SDBGP were 86.53% and 87.67%. The retention of MOE exceeded that of MOR, which could be attributed to the fact that the hemicellulose and cellulose are more susceptible to degradation than lignin in hygrothermal condition [24,25]. Bamboo is mainly composed of cellulose, hemicellulose, and lignin. Cellulose in the cell walls of bamboo acts as a framework that provides both elasticity and strength, while lignin acts as a hard and solid substance that contributes to hardness and rigidity [26]. Hemicellulose acts as a matrix material

that ensures the toughness, hardness, and strength of bamboo [24]. The thermal stability of lignin is better than that of cellulose and hemicellulose [26].

According to the “Technical specifications for bamboo filler of fossil fuel plants cooling tower” [27], the normal requirements for MOR and MOE are 100 MPa and 8500 MPa, respectively. Although the mechanical properties of the used BGP decreased, they still met the requirements despite nine years of use.

The average densities and standard deviations are shown in Table 1. The difference in density between FJBG and SDBG was not statistically significant. The densities of FJBG and SDBG were significantly lower than that of control samples at the 0.05 level. The density retention of FJBG and SDBG were 92.06% and 91.15%, respectively, compared to control samples. The decrease of density could be explained by the degradation of bamboo cell wall components and the loss of water-soluble starch in the cell lumina (see Section 3.3) caused by the circulating hot water. However, the effect of starch loss on the density decrease could be neglected because the percentage of starch content in Moso bamboo is only around 0.1% [28]. The decrease of density could also explain the decrease of mechanical properties of the used BGP, since there was a significant correlation between density and mechanical properties, as presented in Figure 2, which was consistent with previous research [29]. However, the values of used BGPs were lower than those of control samples with similar densities for MORs (see the dotted circle of Figure 2), but not for MOEs. The reason could be the degradation and hydrolysis of hemicellulose and cellulose far exceeded that of lignin, as explained above. In addition, the decrease in cellulose crystallinity may also be an important factor (see Section 3.2).

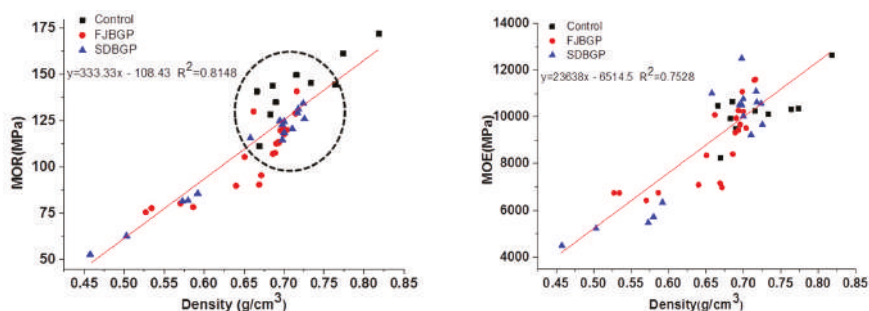


Figure 2. Relationships between MOR/MOE and density. Details of the dotted circles are explained in the text. FJBG: bamboo grid packing collected from Fujian; SDBG: bamboo grid packing collected from Shandong.

3.2. Crystallinity

Cellulose consists of amorphous and crystalline regions. Crystalline cellulose is tightly packed and hard to degrade, while the amorphous region easily decomposes under high temperature [30]. Cellulose crystallinity refers to the percentage of crystalline cellulose in the total cellulose and reflects the degree of crystallization that occurs during cellulose accumulation. The degree of orientation and relative content of the crystalline region have a significant effect on the fracture strength, toughness, and elastic modulus of bamboo [24]. When the cellulose is subjected to external forces, the molecular chains will be aligned along the direction of the external force to produce the preferential orientation, and the interaction between molecules will be greatly enhanced.

The XRD patterns of the three groups of samples are shown in Figure 3. It is clear that there was no change in the position of the cellulose diffraction peak. However, after BGP had been used in the cooling tower for nine years, the intensity of cellulose diffraction peak (002) significantly dropped. The crystallinity and crystal size of samples are as shown in Table 2. Compared to the control samples, the crystallinity retention of FJBG and SDBG were respectively 87.76% and 89.77%, and the crystal size retention of FJBG and SDBG were 85.21% and 86.88%. Hot water in the cooling tower could

degrade the amorphous matrix of the used BGPs, which may increase the C_H . However, in this study, the crystallinity of FHBGP and SDBGP decreased. This could be explained by the following reasons: The hot water cleaved acetyl groups from hemicellulose side chains to yield acetic and uronic acid [31], which catalyzed the hydrolysis of cellulose. Acid degraded not only the amorphous region of cellulose, but also the crystalline region [32], which is consistent with the decrease in crystal size (Table 2). The proportion of the crystalline region in the cell walls was low. When acid cleaved the molecular chain in the crystalline region, part of the crystalline region would be turned into an amorphous region, resulting in lower crystallinity and smaller crystal size of SDBGP and FJBGP.

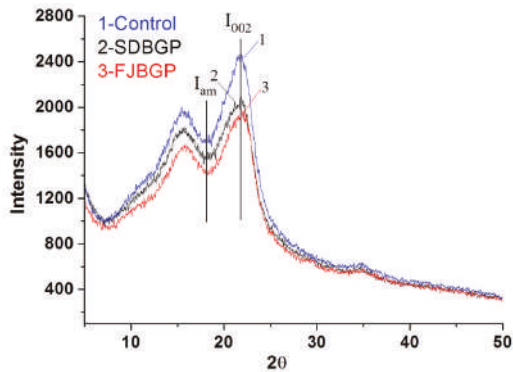


Figure 3. X-ray diffraction (XRD) patterns of the three sample groups.

Table 2. Crystallinity parameters of the three sample groups.

Sample	2θ	C_H	D (nm)	Retention of Properties (%)	
				C_H	D
Control	21.88	0.3276	2.82	100	100
FJBGP	21.76	0.2875	2.4	87.76	85.21
SDBGP	21.83	0.2941	2.45	89.77	86.88

The decrease in crystallinity led to low fracture strength and elastic modulus of the BGP, which can partly account for the decrease of MOR and MOE of used BGPs (Table 1).

3.3. Microstructure Characteristics

Bamboo is susceptible to insect and fungal infestation, which can modify the microstructure and reduce the mechanical properties of bamboo. According to the classification of durability, bamboo belongs to the third grade (non-durable grade). In general, when untreated bamboo is used in the outdoor environment, its service life does not exceed seven years [33]. The poor durability of bamboo is due to its richness in nutrients, which provide a food source for insects and rot fungi. After being infected by rot fungi, the microstructure of the bamboo changes, i.e., holes eroded by rot fungi appear in cell walls and mycelium in the cell cavities.

As shown in Figure 4a,b, the parenchyma cells of the control specimens contained many starch granules—several cells were virtually full of it. Furthermore, the starch granules were big. The inner walls of the cells were smooth. After being subjected to a rotting test for three weeks and 15 weeks, respectively, starch granules in the parenchyma cells disappeared and had been completely digested by rot fungi (Figure 4c,d) [33]. There were a large number of mycelia in the cell cavities, and the inner walls of the cells have formed big holes due to erosion by rot fungi. Noticeably, the following phenomena were observed in this study of both SDBGP and FJBGP: In the parenchyma cells of used BGPs, large-size starch granules disappeared (Figure 4e,f), but a few small-sized granules were still

present. The inner walls of all cells remained smooth, without mycelium. The holes observed in the inner walls of cells were not the result of erosion by rot fungi, but were pits. These phenomena indicated that the BGPs were not attacked by fungi after being used for nine years, which could be explained by the following reasons: Firstly, the surfaces of the bamboo strips were covered with a 0.1–0.5 mm thick water film due to the continuous presence of water flow in the cooling tower [34]. Bamboo decay fungi are mostly aerobic fungi. The water film prevented them from obtaining oxygen. Secondly, the water temperature in the cooling towers generally exceeded 40 °C, which is higher than the suitable temperature for fungal growth (3–38 °C) [33]. Moreover, the starch granules in the bamboo were partially dissolved by the circulating hot water, resulting in the decreased amount and size.

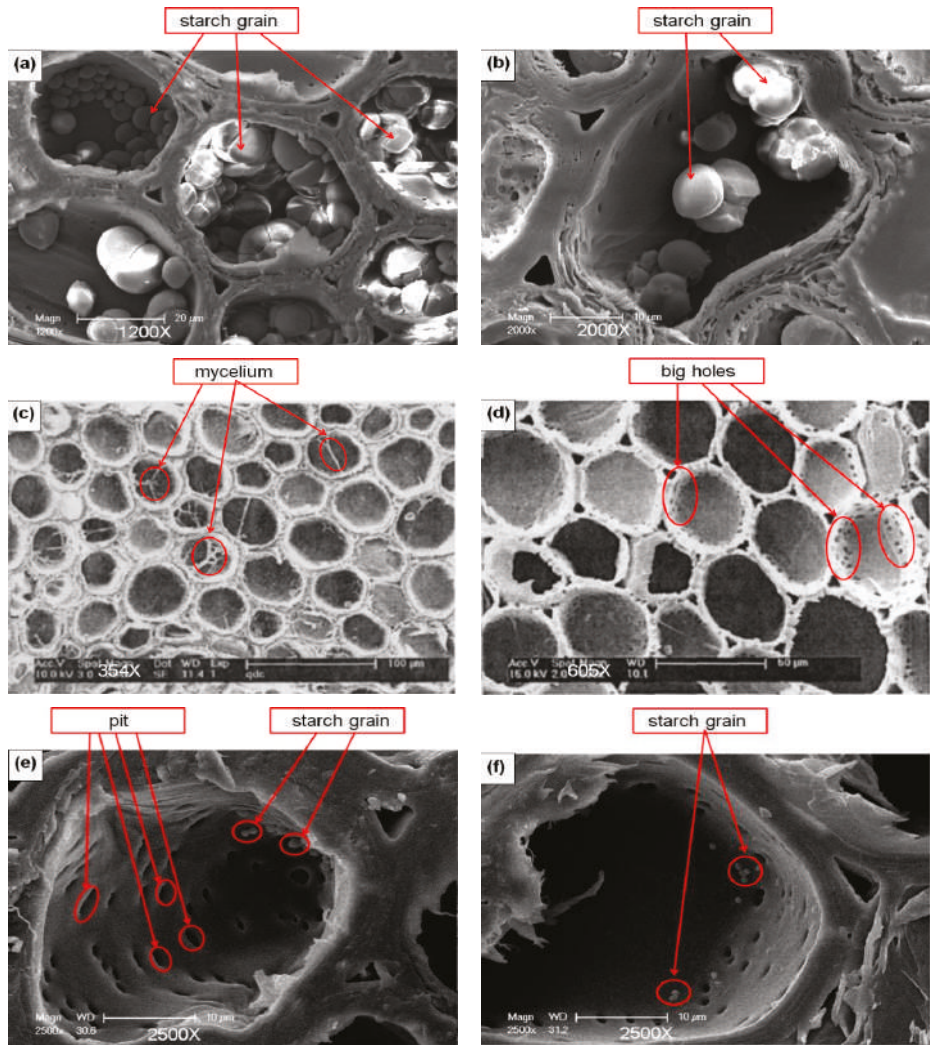


Figure 4. Environment scanning electron microscope (ESEM) images of bamboo cells. (a,b) Control samples; (c,d) specimens after three and 15 weeks of decay, respectively (from Qin [33]); (e,f) specimens of the used BGPs.

Combining all the findings and analyses, it can be concluded that the decreases in the mechanical properties of used BGPs were caused by decreases in density and crystallinity instead of fungal infection, despite that, for most bamboo applications, reduced durability caused by fungal damage is one of the major problems.

4. Conclusions

The properties of BGP that had been in use for nine years in two industrial cooling towers were investigated and compared to those of unused control samples. It was found that the MOR and MOE retentions were around 75% and 87%, respectively, which still met the normal use requirements for cooling towers. The density decreased with retention more than 91%. The crystallinity and crystal size retentions were about 89% and 86%, respectively. Bamboo is vulnerable to fungal infection due to its rich content of nutrients. However, a small amount of small-size starch granules was still present in the cell lumina of used BGP, and bamboo cell walls were also free from mycelia, which indicated that the used BGPs were not infected by fungi. No significant differences in the properties were found for the BGPs collected from the two cooling towers, which had similar conditions.

This study provides primary data for BGP used in industrial cooling towers. Further evaluation of BGP's service life is essential, as it may help promote the application of BGP as one of many uses of the abundant biomass resource of bamboo.

Author Contributions: L.-S.C., C.-H.F., and B.-H.F. conceived and designed the experiments; L.-S.C. performed the experiments; X.-X.M. analyzed the data; J.-P.L. contributed reagents/materials/analysis tools; L.-S.C. wrote the paper, and C.-H.F. revised it.

Funding: This research was funded by the Foundation of International Centre for Bamboo and Rattan (grant number: 1632016015) and the Forestry Patent Industrialization Guidance Project (grant number: Forestry Patent 2017-2).

Acknowledgments: The authors acknowledge the financial supports of the Foundation of International Centre for Bamboo and Rattan (No. 1632016015) and the Forestry Patent Industrialization Guidance Project (Forestry Patent 2017-2).

Conflicts of Interest: The authors declare no conflict of interest.

References

1. Zhao, Z.G. A New Thermo-characteristic Formula for the Packing of Cooling Tower and It's use. *J. Hydrodyn.* **1996**, *11*, 599–605.
2. Chen, J.B.; Wang, Y.H.; Wang, J.; Zhang, P.; De-Xing, L.I. Experimental study on performance of cooling tower packing. *Ind. Water Wastewater* **2010**, *41*, 65–68.
3. Goshayshi, H.R.; Missenden, J.F. The investigation of cooling tower packing in various arrangements. *Appl. Therm. Eng.* **2000**, *20*, 69–80. [[CrossRef](#)]
4. Chen, J.B.; Shi, Y.H.; Wang, Y.H.; Hou, H.L.; Li, D.X. Experimental Study of Cooling Tower Packing and Deduce the New Formula of the NTU. *Adv. Mater. Res.* **2012**, *383–390*, 6134–6138. [[CrossRef](#)]
5. Lemouari, M.; Boumaza, M. Experimental investigation of the performance characteristics of a counterflow wet cooling tower. *Energy* **2010**, *36*, 5815–5823. [[CrossRef](#)]
6. Ma, X.X.; Lu, J.P.; Qin, D.C.; Fei, B.H. Application of bamboo in the circulating water cooling system. *J. For. Eng.* **2016**, *1*, 33–37.
7. Fazita, M.R.N.; Jayaraman, K.; Bhattacharyya, D.; Haafiz, M.K.M.; Saurabh, C.K.; Hussin, M.H.; Abdul, K.H.P.S. Green Composites Made of Bamboo Fabric and Poly (Lactic) Acid for Packaging Applications—A Review. *Materials* **2016**, *9*, 435. [[CrossRef](#)] [[PubMed](#)]
8. Chen, Y.L.; Shi, Y.F.; Xie, D.X. Performance Comparison between Bamboo Grid Packing and PVC Film Packing and its Applications. *Power Stn. Aux. Equip.* **2016**, *37*, 37–41.
9. Lobovikov, M.; Paudel, S.; Piazza, M.; Ren, H.; Wu, J. World bamboo resources. A thematic study prepared in the framework of the Global Forest Resources Assessment 2005. *Non-Wood For. Prod.* **2007**. [[CrossRef](#)]
10. Chirici, G.; Corona, P.; Portoghesi, L. Global forest resources assessment. *Ital. J. For. Mt. Environ.* **2013**, *4*, 269–273.

11. Lima, R.A.F.; Rother, D.C.; Muler, A.E.; Lepsch, I.F.; Rodrigues, R.R. Bamboo overabundance alters forest structure and dynamics in the Atlantic Forest hotspot. *Boil. Conserv.* **2012**, *147*, 32–39. [[CrossRef](#)]
12. Yang, Q.P.; Yang, G.Y.; Song, Q.N.; Shi, J.M.; Ou, Y.M.; Qi, H.Y.; Fang, X.M. Ecological studies on bamboo expansion: Process, consequence and mechanism. *Chin. J. Plant Ecol.* **2015**, *39*, 110–124.
13. Fang, C.H.; Jiang, Z.H.; Sun, Z.J.; Liu, H.R.; Zhang, X.B.; Zhang, R.; Fei, B.H. An overview on bamboo culm flattening. *Constr. Build. Mater.* **2018**, *171*, 65–74. [[CrossRef](#)]
14. Xi, M.J.; Zhang, R.P.; Wang, X.G.; Li, N.; Lu, S.J.; Yu, Z.X. Analysis of Characteristic of Bamboo Grating Filler in Cooling Tower. *Hebei Electr. Power* **2000**, *2*, 42–43.
15. Chu, X.M.; Wu, Y.C. The Cooling Effect is Significant after Cooling Tower Replaces the Bamboo Grid Packing. *Power Stn. Aux. Equip.* **1996**, *2*, 22–23.
16. Wang, Z.Q.; Liang, Q.; Chen, X. Transformation & economic analysis of cooling tower trickling filler in 300 MW unit. *Ningxia Electr. Power* **2005**, *1*, 42–46.
17. Fei, B.H.; Ma, X.X.; Qin, D.C.; Lu, J.P. New Materials for Industrial Cooling Tower: Bamboo Packing. *World Bamboo Rattan* **2016**, *14*, 31–35.
18. GB/T 15780–1995 *Testing Methods for Physical and Mechanical Properties of Bamboos*; General Administration of Quality Supervision, Inspection and Quarantine of the People's Republic of China/Standardization Administration of the People's Republic of China: Beijing, China, 1995.
19. GB/T 1933–2009 *Method for Determination of the Density of Wood*; General Administration of Quality Supervision, Inspection and Quarantine of the People's Republic of China/Standardization Administration of the People's Republic of China: Beijing, China, 2009.
20. Aeo, B.S.; Chaabouni, Y.; Msahli, S.; Sakli, F. Morphological and crystalline characterization of NaOH and NaOCl treated *Agave americana* L. fiber. *Ind. Crops Prod.* **2012**, *36*, 257.
21. Li, J. *Wood Spectroscopy*; Science Press: Beijing, China, 2003.
22. Patterson, A.L. The Scherrer Formula for X-ray Particle Size Determination. *Phys. Rev.* **1939**, *56*, 978–982. [[CrossRef](#)]
23. Chen, M.; Wang, C.; Fei, B.; Ma, X.; Zhang, B.; Zhang, S.; Huang, A. Biological Degradation of Chinese Fir with *Trametes Versicolor* (L.) Lloyd. *Materials* **2017**, *10*, 834. [[CrossRef](#)]
24. Liu, Y.X.; Zhao, G.J. *Wood Resources Materials Science*; China Forestry Publishing House: Beijing, China, 2004.
25. Tjeerdma, B.F.; Militz, H. Chemical changes in hydrothermal treated wood: FTIR analysis of combined hydrothermal and dry heat-treated wood. *Holz Roh-Werkst* **2005**, *63*, 102–111. [[CrossRef](#)]
26. Qin, L. *Effect of Thermo-Treatment on Physical, Mechanical Properties and Durability of Reconstituted Bamboo Lumber*; Chinese Academy of Forestry: Beijing, China, 2010.
27. DL/T 1361–2014 *Technical Specifications for Bamboo Filler of Fossil Fuel Plants Cooling Tower*; National Energy Administration of the People's Republic of China: Beijing, China, 2014.
28. Fan, F.Y. *Seasonal Variation of Starch Content in Dendrocalamus giganteus and Phyllostachys edulis and Its Relationship to Insect Damages*; Southwest Forestry University: Kunming, China, 2010.
29. Xu, Y.M. *Wood Science*; China Forestry Publishing House: Beijing, China, 2006.
30. Bhuiyan, M.T.R.; Hirai, N.; Sobue, N. Changes of crystallinity in wood cellulose by heat treatment under dried and moist conditions. *J. Wood Sci.* **2000**, *46*, 431–436. [[CrossRef](#)]
31. Sattler, C.; Labbé, N.; Harper, D.; Elder, T.; Rials, T. Effects of Hot Water Extraction on Physical and Chemical Characteristics of Oriented Strand Board (OSB) Wood Flakes. *CLEAN-Soil Air Water* **2010**, *36*, 674–681. [[CrossRef](#)]
32. Li, X.J.; Liu, Y.; Gao, J.M.; Wu, Y.Q.; Yi, S.L.; Wu, Z.P. Characteristics of FTIR and XRD for wood with high-temperature heating treatment. *J. Beijing For. Univ.* **2009**, *31*, 104–107.
33. Qin, D.C. *A Fundamental Study on the Application of CuAz Preservatives for Bamboo*; Chinese Academy of Forestry: Beijing, China, 2004.
34. Northwest Electric Power Design Institute. *Power Engineering Water Design Manual*; China Electric Power Press: Beijing, China, 2005.



Article

Effects of Hygrothermal Environment in Cooling Towers on the Chemical Composition of Bamboo Grid Packing

Li-Sheng Chen ^{1,2}, Ben-Hua Fei ^{1,2}, Xin-Xin Ma ^{1,2}, Ji-Ping Lu ³ and Chang-Hua Fang ^{1,2,*}

¹ Department of Biomaterials, International Center for Bamboo and Rattan, Beijing 100102, China; chenlisheng@icbr.ac.cn (L.-S.C.); feibenhua@icbr.ac.cn (B.-H.F.); maxx@icbr.ac.cn (X.-X.M.)

² SFA and Beijing Co-Built Key Laboratory of Bamboo and Rattan Science & Technology, State Forestry Administration, Beijing 100102, China

³ Hengda Bamboo Filler Limited Company, Yixing 214200, China; hdlwz@163.com

* Correspondence: cfang@icbr.ac.cn; Tel.: +86-010-84789842

Received: 28 February 2019; Accepted: 16 March 2019; Published: 19 March 2019

Abstract: Bamboo grid packing (BGP) is a new kind of cooling packing, used in some Chinese hyperbolic cooling towers, which has excellent potential to complement or replace cooling packing made of polyvinyl chloride (PVC), cement, and glass fiber-reinforced plastic. For bamboo applications, mechanical properties and service life are matters of concern; this is strongly associated with bamboo's chemical composition and mass loss. To better understand the mechanics of mechanical property deterioration and service life reduction, this study investigated the effects of hygrothermal environments in cooling towers on the chemical and elemental composition, mass loss, Fourier-transform infrared (FTIR) spectrum, and color changes of BGP. The results showed that BGP that had been in service for nine years in cooling towers exhibited major decreases in content of hemicellulose and benzene-ethanol extractives, as well as a significant increases in the content of α -cellulose and lignin. Exposure to the hygrothermal environment led to a decrease of oxygen content and around 8% mass loss, as well as an increase in carbon content compared to control samples. The hot water flow in cooling towers not only hydrolyzed hemicellulose, but also degraded some functional groups in cellulose and lignin. The lightness (L^*) and chromaticity (a^* and b^*) parameters of the used BGP all decreased, except for the a^* value of the outer skin. The total color change (ΔE^*) of the inner skin of used BGP exceeded that of the outer skin.

Keywords: bamboo grid packing; cooling packing; cooling tower; chemical composition; elemental composition; FTIR; color

1. Introduction

A hyperbolic cooling tower is a device wherein hot water from the system is cooled by the ambient air with the assistance of cooling packing [1], and it is widely used in industries due to its high capacity for heat rejection and energy saving [2]. As the core component of a cooling tower, good cooling packing not only increases effective contact between air and water, which promotes heat and mass transfer, but also provides less resistance to the movement of air to reduce pressure drop [3]. In order to improve heat dissipation efficiency and reduce cost, many different materials have been used as cooling packing, such as polyvinyl chloride (PVC), cement, and glass fiber-reinforced plastic. PVC packing with smooth- and cross-ribbing is the most popular kind due to its outstanding cooling performance and lightness in weight. It is used in 96% of cooling towers [4]. However, PVC packing also has lots of disadvantages, such as short service life, poor anti-fouling properties, environmental burdens, etc. Furthermore, the price of PVC is on the rise. Therefore, many attempts have been made to seek an environmentally-friendly, low cost, and longer-serving alternative to PVC.

Owing to its fast growth speed, short rotation, great mechanical strength, and low energy consumption [5], bamboo, an abundant and sustainable plant resource, has been used as an innovative material for cooling packing. The product, known as bamboo grid packing (BGP), has been used in some hyperbolic cooling towers in China in recent years [6]. BGP has showed good temperature adaptability and anti-fouling properties, and also costs less than its PVC counterpart, which makes it a promising substitute for PVC packing. Mechanical properties and service life are a concern for all bamboo applications; this is strongly associated with its chemical composition and mass loss. The mechanical properties of bamboo were studied in our previous report [2]. However, it is still largely unknown how the hygrothermal environment in cooling towers affects the chemical composition of BGP. The lack of research in this aspect hinders the development of BGP for wider industrial application.

To better understand the reasons of mechanical property deterioration and service life reduction, the effects of hygrothermal environments in cooling towers on the chemical and elemental composition of BGP were investigated. In order to prevent damage to BGP's chemical composition and structure, Fourier-transform infrared (FTIR) spectroscopy was applied in this study. The presence of compounds or functional groups can be determined according to the number, shape, position, and intensity of the spectral bands, thus revealing the structure of the compound and its variation [7,8]. The color changes of BGP were also investigated, as they suggested variation in the chemical composition and structure. This study not only offers a new perspective for understand the changing patterns of the chemical composition, chemical structure, and color of BGP used in cooling towers, but may also contribute to the exploration of new approaches to alleviate hygrothermal aging.

2. Materials and Methods

2.1. Materials

The materials used in this study were identical to those in the previous study [2]. Raw materials were obtained from Moso bamboo (*Phyllostachys edulis* (Carr.) J. Houz), aged for four years, grown in Shaowu, Fujian Province, China. The bamboo culms were sawn into segments 1200 mm long (Figure 1a) and then split longitudinally into several strips (1200 mm in longitudinal direction and 40 mm in tangential direction) (Figure 1b). Three holes with a diameter of 10 mm were made on the strips with a distance about 400 mm between each hole (Figure 1c). As shown in Figure 1e, round bamboo sticks 600 mm in length were inserted into the holes to connect the bamboo strips. The spacing between the strips was 50 mm. The dimensions of one piece of BGP were around 1200 mm × 600 mm × 40 mm. BGP units were stacked to a height of around 1.5 m in hyperbolic cooling towers [2]. BGP that has been in use for nine years was collected from two hyperbolic cooling towers located in Fujian and Shandong Provinces, respectively. The BGP collected from Fujian Province (FJBGP) and Shandong Province (SDBGP) were used in hyperbolic cooling towers of a thermal power plant and a steel mill, respectively. The bamboo materials used to fabricate the BGPs in these two towers were obtained from the same bamboo species and the same place as mentioned above. In both cooling towers, the inlet water temperature was around 45 to 50 °C, and the water mass flux was around 6500 kg/(h·m²). Control samples were collected from unused BGP units. Prior to testing, all specimens were kept in a conditioned room at 21 ± 2 °C and 65 ± 3% relative humidity until their weights stabilized.

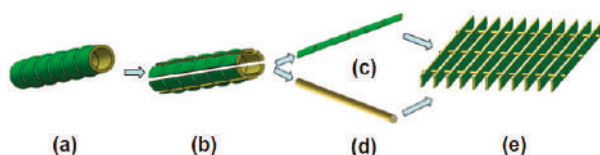


Figure 1. Preparation process of bamboo grid packing (BGP): (a) Raw bamboo; (b) radial splitting; (c) bamboo strip; (d) round bamboo stick; (e) bamboo grid packing.

2.2. Chemical Composition Measurements

Chemical composition of the used BGP and control samples were both measured. Specimen from each experiment was ground to pass a 40-mesh screen. The following contents in the ground meal was measured in accordance with relative standards: Acid-insoluble lignin using GB/T 2677.8-1994 [9], holocellulose content using GB/T 2677.10-1995 [10], α -cellulose content using GB/T 744-2004 [11], and benzene-ethanol extractives using GB/T 2677.6-1994 [12]. The content of hemicellulose is the difference between the content of holocellulose and that of α -cellulose.

2.3. Elemental Composition and Mass Loss

The used BGP and control samples were ground to fine powder and passed through different sieves to obtain a particle size between 0.2 and 0.5 mm. The powder was then conditioned at 103 °C for 24 h and stored in closed bottles before analysis. Elemental analyses were performed using a Thermofinnigan Flash EA1112 micro-analyzer (Sundy Co., Hunan, China). The content of carbon, oxygen, and hydrogen were measured. At least three replicates were tested for each sample. Mass loss due to chemical degradation caused by the hygrothermal environment in cooling towers was calculated according to the following equation:

$$ML(\%) = \frac{m_0 - m_1}{m_0} \times 100\% \quad (1)$$

where m_0 is the initial anhydrous mass of the sample before being put to use in cooling towers, and m_1 is the anhydrous mass of the same sample after nine years of service.

2.4. FTIR Spectroscopy Analysis

Before being ground, the used BGP was gently brushed to remove impurities from the surface. Then all specimens for the FTIR analysis were prepared by being ground in a mill with a 100-mesh screen (FW100, TAISITE Co., Tianjin, China). The FTIR spectra of the samples were obtained in a Nexus 670 spectrometer (Nicolet, WI, USA) within the range of 500–4000 cm^{-1} , with a resolution of 4 cm^{-1} and 64 scans. The KBr pellet, consisting of KBr and randomly-selected bamboo powder with a weight ratio of 100:1, was prepared prior to the measurement. The FTIR analysis for each sample was performed in quintuplicate. For evaluation of the spectra, only the area between wavenumbers 800 and 1800 cm^{-1} will be discussed; this includes the most important values of lignocellulose materials [13].

2.5. Color Measurements

The changes in color of BGP surface due to hygrothermal treatment were measured using a Technibrite Brightmeter micro S-5 colorimeter (Technidyne Corporation, New Albany, IN, USA) with an aperture size of 1 cm^2 . CIELAB (CIEL*a*b*) is a color space that describes all the colors visible to the human eye and it is created to serve as a device-independent model used as a reference [14]. In the CIELAB system, the L^* axis represents the lightness (L^* varies from 100 (for white) to zero (for black)), a^* and b^* describe the chromatic coordinates on the green–red and blue–yellow axis,

respectively (+ a^* is for red, $-a^*$ for green, + b^* for yellow, $-b^*$ for blue) [15]. ΔE^* was calculated using the following equation:

$$\Delta E^* = \sqrt{(\Delta L^*)^2 + (\Delta a^*)^2 + (\Delta b^*)^2} \quad (2)$$

where ΔL^* , Δa^* , and Δb^* are the difference of initial (control samples) and final (used BGP) values of L^* , a^* , and b^* , respectively.

2.6. Statistical Analysis

The effects of hygrothermal environment on the chemical composition and color changes in comparison with control samples were analyzed by analysis of variance (ANOVA) using SPSS 19.0 (IBM SPSS Corporation, Chicago, IL, USA). The significance ($p < 0.05$) between average values of control samples and used BGP specimens was compared using Duncan's test. Different letters given along with the average values of tested parameters indicated a significant difference by Duncan's test.

3. Results and Discussion

3.1. Chemical Composition Analysis

The structure of bamboo is stable because the natural tissues of the cell walls are composed of three bio-based chemicals—cellulose, hemicellulose, and lignin. Cellulose provides structural support in the cell walls. Hemicellulose and lignin are the binding and packing materials for the skeleton structure. The three components are interwoven into thin layers that together form bamboo cell walls [16]. In addition to lignocellulosic structures, bamboo also contains a variety of low molecular weight organic compounds known as extractives—such as terpenes, resins, fatty acids, waxes, and phenols—which can be extracted using solvents [17,18]. The temperature of inlet water in both cooling towers was around 45 to 50 °C, and the effects of hot water flow on the chemical composition of the used BGP are presented in Table 1.

Table 1. Analysis of main chemical composition of the used BGP and control samples.

Sample	Holocellulose (%)	α -Cellulose (%)	Hemicellulose (%)	Lignin (%)	Benzene-Ethanol Extractives (%)
Control	64.08a (1.25)	41.03a (1.94)	23.05c (0.09)	24.37a (2.23)	5.77c (0.86)
FJBGP	66.27ab (2.01)	45.43b (4.08)	20.84b (2.75)	27.68b (2.44)	1.62b (1.33)
SDBGP	67.81b (2.35)	48.35b (2.24)	19.46a (2.65)	26.63b (4.06)	1.15a (1.23)

Note: FJBGP: bamboo grid packing collected from Fujian; SDBGP: bamboo grid packing collected from Shandong. Values in parentheses are coefficient of variation. The different letters in the same column indicate a significant difference at the 0.05 level.

The hemicellulose content of FJBGP and SDBGP were 20.84% and 19.46%, respectively. Both data were significantly lower than those of control samples, which indicates that hot water flow in the cooling towers partially degraded hemicellulose. Hemicellulose is a heterogeneous low molecular weight polysaccharide composed of acetyl groups, aldonic acid groups, and different glycosyl groups, most of which are thermally labile, especially the acetyl groups. Furthermore, because of its branched structure and amorphous tissues, hemicellulose is considerably more susceptible to thermal degradation than other chemical components [19].

The benzene-ethanol extractive contents of FJBGP and SDBGP were 1.62% and 1.15%, respectively, which were also significantly lower than those of control samples. The changes in benzene-ethanol extractive content of the used BGP were not consistent with the results of heat-treated bamboo and wood [20,21]. Changes in extraction content are related to the degradation of hemicellulose and cellulose. Volatiles, extractives, and water are products that result from hemicellulose and cellulose degradation [22]; the phenolic compounds, which can be very soluble in benzene-ethanol mixture, can also be formed in depolymerization reactions [23]. The decrease in the benzene-ethanol extractive

content of the used BGP may be attributed to the dissolution of extractives in hot water flow and the degradation of hemicellulose.

The α -cellulose contents of FJBGP and SDBGP were 45.43% and 48.35%, respectively, and the lignin contents were 27.68% and 26.63%. These numbers were all significantly higher than those of control samples, which indicates that the degradation of α -cellulose and lignin by hot water flow was less significant than that of hemicellulose. α -Cellulose is a homogeneous polysaccharide consisting of the same type of glucosyl groups. It is also a straight-chain structural macromolecule without branched chain, therefore its thermal stability is relatively good. Lignin is a complex phenolic polymer synthesized from three alcohol monomers (namely *p*-coumaryl alcohol, coniferyl alcohol, and sinapyl alcohol) [24]. It has large molecular weight, few lyophilic groups, and is insoluble in water and general solvents. Lignin is the most stable compound for which thermal degradation is observed above 100 °C, although high temperatures can result in cleaved bonds within the lignin [25]. Because cellulose and lignin have fewer lyophilic groups and more stable chemical structures, they are more difficult to hydrolyze by hot water flow than hemicellulose. The increase of α -cellulose and lignin contents in SDBGP and FJBGP may largely be the result of the hydrolysis of benzene-ethanol extractive content and the degradation of hemicellulose.

The effects of hygrothermal environments on the chemical composition of BGP may be less conspicuous in the short term because the highest water temperature is usually below 65 °C. The actual extent of change in the chemical composition of used BGP was due to years of accumulation.

Our previous experiment studied the mechanical properties of used BGP that had been in service for nine years in cooling towers [2]; the reduction in the mechanical properties of SDBGP and FJBGP was mainly caused by the depolymerization reactions of polymers, which led to the reduction in hemicellulose, the most thermochemically sensitive component of bamboo. The degradation of hemicellulose is primarily responsible for initial strength loss [26,27].

3.2. Elemental Composition and Mass Loss

Elemental composition and mass loss of the samples are presented in Table 2. Results indicate that the hygrothermal environment led to a drop in oxygen content and an increase of carbon content of used BGP compared to control samples, which was in line with the results of heat-treated wood [21,28,29]. The decrease of the O/C ratio of used BGP manifested severe dehydration due to higher degradation of amorphous polysaccharides and/or higher amounts of carbonaceous materials within the bamboo structure, as reported for heat-treated wood [30–32]. The degradation of polysaccharides involves depolymerization by transglycosylation and dehydration reactions. As a result, the production of anhydro monosaccharides that could participate in subsequent reactions led to the formation of carbonaceous materials [17,33].

Table 2. Elemental composition and mass loss of used BGP and control samples.

Sample	Carbon (%)	Oxygen (%)	Hydrogen (%)	O/C ^a	Mass Loss ^b (%)
Control	48.68	45.11	6.14	0.695	-
FJBGP	48.95	44.95	6.06	0.689	7.94
SDBGP	49.15	44.73	6.06	0.683	8.85

Note: ^a = atomic ratio; ^b = mass loss due to hygrothermal treatment.

Elaieb et al. reported that the O/C ratio was negatively correlated with mass loss and inferred that the O/C ratio is a good indicator for mass loss of wood after thermo-degradation [34]. Moreover, the O/C ratio is related to the content of hemicellulose [28]. The O/C ratio and hemicellulose contents of FJBGP were 0.689 and 20.84%, respectively, exceeding those of SDBGP, while the mass loss of FJBGP was 7.94%, lower than that of SDBGP. These indicate that hygrothermal degradation of SDBGP was more significant than of FJBGP.

3.3. FTIR Analysis

To investigate the changes of chemical structure that took place in used BGP, FTIR spectroscopy was applied in this study. Spectra of specimens are shown in Figure 2. Bamboo bears basic structural similarities to wood because of the similar chemical constituents. Therefore, characterization and assignment of IR peaks in bamboo was done by reference to wood, as previously described by Wang and Ren [35,36]. The assignments of the peaks to structural components were as follows: 1730 cm^{-1} for unconjugated C=O in xylan (hemicellulose), 1603 cm^{-1} and 1510 cm^{-1} for aromatic skeleton in lignin, 1460 cm^{-1} for CH_3 deformation in lignin and CH_2 bending in xylan, 1425 cm^{-1} for CH_2 scissor vibration in cellulose, 1370 cm^{-1} for C-H deformation in cellulose and hemicellulose, 1330 cm^{-1} for C-H vibration in cellulose and C₁-O vibration in syringyl derivatives, 1240 cm^{-1} for syringyl ring and C-O stretch in lignin and xylan, 1160 cm^{-1} for C-O-C vibration in hemicellulose and cellulose, 1122 cm^{-1} for aromatic skeletal and C-O stretch in lignin and cellulose, 1048 cm^{-1} for C-O stretch in cellulose and hemicellulose, 897 cm^{-1} for C-H deformation in cellulose [37–39].

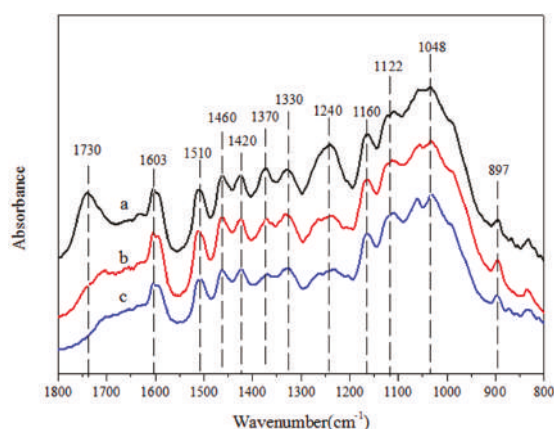


Figure 2. Fourier-transform infrared (FTIR) spectra of used BGP and control samples. (a) Control samples; (b) BGP collected from Fujian Province (FJBGP); (c) BGP collected from Shandong Province (SDBGP).

Hydrothermal treatment seemed to have a significant impact on the chemical structure of used BGP (Figure 2). Peaks at 1730 , 1370 , 1240 , and 1048 cm^{-1} for used BGP decreased compared to control samples. The intensity of the unconjugated C=O peak at 1730 cm^{-1} , often used as an important baseline for the degradation of hemicellulose [25], experienced a dramatic decrease, indicating that hemicellulose was degraded most severely. The degradation of unconjugated C=O was caused by deacetylation that occurred during hydrothermal treatment, which was a result of the cleavage of acetyl groups linked as ester groups to the hemicellulose [40]. The hydrothermal treatment caused a marked reduction in the 1370 cm^{-1} peak in used BGP due to damage of C-H bonds in hemicellulose and cellulose. The peak intensity of 1240 cm^{-1} of used BGP was lower than that of control samples owing to the degradation of syringyl ring and C-O bonds in lignin and xylan. The decrease in intensities of absorption bands at 1048 cm^{-1} indicates the loss of C-O in cellulose and hemicellulose. The difference in FTIR spectra between FJBGP and SDBGP was rather slight, except for the absorption bands at 1048 cm^{-1} . The intensities of absorption bands at 1048 cm^{-1} in SDBGP was lower than that of FJBGP, and the absorption peak at 1048 cm^{-1} in SDBGP was split into two small peaks, which showed the degradation of C-O bonds in SDBGP was more noticeable than that of FJBGP. Although the content of cellulose and lignin increased, the C-H and C-O bonds in cellulose and syringyl ring in lignin were both partially degraded.

The intensity of the remaining bands for used BGP were almost the same with control samples, which indicates that functional groups corresponding to these peaks were relatively unaffected by hot water flow.

3.4. Color Changes

The color of lignocellulosic material is related to its chemical composition. Since the main chemical composition and structure of bamboo is similar to wood, the theory and method of analyzing color changes of wood can be applied to analyze bamboo. The effects of hygrothermal environment on color changes of the outer and inner skin of all samples are shown in Table 3. Control samples were light-colored. L^* values of the outer and inner skin were 66.27 and 74.03, respectively. The surface color grew significantly darker after nine years of use. In terms of the outer and inner skin, the L^* value of FJBG decreased from 66.27 to 40.95 and from 74.03 to 36.30, respectively, and that of SDBG decreased from 66.27 to 50.85 and from 74.03 to 41.95. Changes in color reflected alteration in the chemical composition and structure of BGP during hygrothermal treatment. Some studies reported that a decrease in L^* caused by a loss of lightness was possibly due to a degradation of hemicellulose and an increase in lignin content [41,42], as well as the degradation of oxygen-containing groups such as carboxyl groups and acetyl groups [19]. The darkening of used BGP may mainly be attributable to the degradation of acetyl groups in hemicellulose and oxidation of lignin.

Table 3. Color changes of used BGP and control samples.

Samples		CIELAB			
		L^*	a^*	b^*	ΔE^*
Outer skin	Control	66.27c (5.08)	1.70a (3.23)	14.34c (12.48)	—
	FJBG	40.95a (4.91)	3.40b (9.12)	11.69a (4.19)	25.51
	SDBG	50.85b (5.68)	4.44c (7.21)	13.61b (3.38)	15.68
Inner skin	Control	74.03c (2.34)	5.16c (8.91)	19.91c (4.82)	—
	FJBG	36.30a (3.5)	2.87a (7.77)	9.99a (8.51)	39.08
	SDBG	41.95b (12.35)	3.84b (6.14)	13.32b (9.67)	32.78

Note: Values in parentheses are coefficient of variation. The different letters in the same column indicate a significant difference at the 0.05 level.

The a^* value of FJBG and SDBG outer skin increased from 1.7 to 3.4 and from 1.7 to 4.44, respectively. However, the changes in the inner skin demonstrated an opposite trend, decreasing from 5.16 to 2.87 (FJBG) and from 5.16 to 3.84 (SDBG), respectively. The original brightly-colored lignocellulosic material turned dark and reddish under the hygrothermal environment, as a result of the volatilization of a large amount of colored extracts. However, the color indices of lignocellulosic material (near neutral color) only increase slightly due to the “darkening” effect caused by the rapid oxidation of the chemical composition [43]. Naturally, the original color of bamboo outer skin is green, while the inner skin is mostly red-brownish. After most of the extractives and chromophores in used BGP were hydrolyzed by hot water flow and some chemical composition were oxidized, the color of the outer and inner skin of used BGP become somewhat alike. In other words, the outer skin reddened while the inner skin grew comparatively green.

For the b^* value, FJBG decreased from 14.34 to 11.69 and from 19.91 to 9.99 for the outer and inner skin, respectively, and SDBG dropped from 14.34 to 13.61 and from 19.91 to 13.32. The lower b^* values of used BGP indicates that it became bluer compared to control samples. This specific change was induced by the modification of hemicellulose following hygrothermal treatment [15]. The total color difference (ΔE^*) of used BGP’s inner skin was greater compared to the outer skin

because the inner skin underwent a greater change in terms of lightness. The ΔE^* was caused by the volatilization of color extracts and the oxidation, degradation and polymerization of the chemical composition, which also had a significant correlation with the content of holocellulose, α -cellulose, and acid insoluble lignin [44].

4. Conclusions

The results of this study confirmed that the hygrothermal environment in cooling towers influenced the chemical and elemental composition, mass loss, chemical structure, and color changes of BGP. Statistically significant differences were observed in the content of hemicellulose, benzene-ethanol extractives, α -cellulose, and lignin between used BGP and control samples. Specifically, there was a decrease of hemicellulose and benzene-ethanol extractive content in used BGP and an increase in α -cellulose and lignin content. The O/C ratio of used BGP decreased in general, but it was higher in FJBGP than in SDBGP with less mass loss. The FTIR spectra showed the unconjugated C=O, C-H, and C-O bonds in hemicellulose; C-H and C-O bonds in cellulose; and the syringyl ring in lignin were partially degraded. However, the peak intensities and positions of the rest of the functional groups remained mostly unchanged. Color parameters such as lightness (L^*) and chromatic coordinates a^* and b^* of used BGP surface all decreased due to the hygrothermal environment's influence, with the exception of the a^* value of the outer skin. The total color difference (ΔE^*) of used BGP's inner skin was more substantial than that of the outer skin.

This study provides primary data for BGP used in industrial cooling towers. Still more work needs to be done in order to promote the application of BGP, such as optimizing its design, evaluating its service life, devising appropriate methods to alleviate the effects of hygrothermal aging, etc.

Author Contributions: L.-S.C., X.-X.M., and B.-H.F. conceived and designed the experiments; L.-S.C. performed the experiments; C.-H.F. analyzed the data; J.-P.L. contributed reagents/materials/analysis tools; L.-S.C. wrote the paper, and C.-H.F. revised it.

Funding: This research was funded by Foundation of International Centre for Bamboo and Rattan (grant numbers: 1632016015) and the Forestry Patent Industrialization Guidance Project (grant numbers: Forestry Patent 2017-2).

Acknowledgments: The authors acknowledge the financial supports of the Foundation of International Centre for Bamboo and Rattan (No. 1632019002) and the Forestry Patent Industrialization Guidance Project (Forestry Patent 2017-2).

Conflicts of Interest: The authors declare no conflict of interest.

References

- Seetharamu, K.N.; Swaroop, S. The effect of size on the performance of a fluidized bed cooling tower. *Wärme-und Stoffübertragung* **1991**, *26*, 17–21. [[CrossRef](#)]
- Chen, L.S.; Fei, B.H.; Ma, X.X.; Lu, J.P.; Fang, C.H. Investigation of Bamboo Grid Packing Properties Used in Cooling Tower. *Forests* **2018**, *9*, 762. [[CrossRef](#)]
- Lemouari, M.; Boumaza, M. Experimental investigation of the performance characteristics of a counterflow wet cooling tower. *Int. J. Therm. Sci.* **2010**, *49*, 2049–2056. [[CrossRef](#)]
- Goshayshi, H.R.; Missenden, J.F. The investigation of cooling tower packing in various arrangements. *Appl. Therm. Eng.* **2000**, *20*, 69–80. [[CrossRef](#)]
- Fang, C.H.; Jiang, Z.H.; Sun, Z.J.; Liu, H.R.; Zhang, X.B.; Zhang, R.; Fei, B.H. An overview on bamboo culm flattening. *Constr. Build. Mater.* **2018**, *171*, 65–74. [[CrossRef](#)]
- Chen, Y.L.; Shi, Y.F.; Xie, D.X. Performance Comparison between Bamboo Grid Packing and PVC Film Packing and its Applications. *Power Stn. Aux. Equip.* **2016**, *37*, 37–41.
- Slahor, J.J.; Hassler, C.C.; Degroot, R.C.; Gardner, D.J. Preservative Treatment Evaluation of Red Maple and Yellow-Poplar with ACQ-B. *For. Prod. J.* **1997**, *47*, 50–54.
- Deng, Q.P.; Li, D.G.; Zhang, J.P. FTIR Analysis on Changes of Chemical Structure and Compositions of Waterlogged Archaeological Wood. *J. Northwest For. Univ.* **2008**, *23*, 149–153.

9. GB/T 2677.8-1994 *Fibrous Raw Material-Determination of Acid-insoluble Lignin*; General Administration of Quality Supervision, Inspection and Quarantine of the People's Republic of China; Standardization Administration of the People's Republic of China: Beijing, China, 1994.
10. GB/T 2677.10-1995 *Fibrous Raw Material-Determination of Holocellulose*; General Administration of Quality Supervision, Inspection and Quarantine of the People's Republic of China; Standardization Administration of the People's Republic of China: Beijing, China, 1995.
11. GB/T 744-2004 *Pulps-Determination of Alkali Resistance*; General Administration of Quality Supervision, Inspection and Quarantine of the People's Republic of China; Standardization Administration of the People's Republic of China: Beijing, China, 2004.
12. GB/T 2677.6-1994 *Fibrous Raw Material-Determination of Solvent Extractives*; General Administration of Quality Supervision, Inspection and Quarantine of the People's Republic of China; Standardization Administration of the People's Republic of China: Beijing, China, 1994.
13. Gelbrich, J.; Mai, C.; Militz, H. Evaluation of bacterial wood degradation by Fourier Transform Infrared (FTIR) measurements. *J. Cult. Herit.* **2012**, *13*, S135–S138. [[CrossRef](#)]
14. Schimleck, L.R.; Espey, C.; Mora, C.R.; Evans, R.; Taylor, A.; Muniz, G. Characterization of the wood quality of pernambuco (*Caesalpinia echinata* Lam) by measurements of density, extractives content, microfibril angle, stiffness, color, and NIR spectroscopy. *Holzforschung* **2009**, *63*, 457–463. [[CrossRef](#)]
15. Pandey, K.K. Study of the effect of photo-irradiation on the surface chemistry of wood. *Polym. Degrad. Stab.* **2005**, *90*, 9–20. [[CrossRef](#)]
16. Xu, Y.M. *Wood Science*; China Forestry Publishing House: Beijing, China, 2006.
17. Rowell, R.M. *Handbook of Wood Chemistry & Wood Composites*; CRC Press: Boca Raton, FL, USA, 2005.
18. Ma, Q.Z. *The Research on Utilization Approaches of High-Grade Resource Recovering of Bamboo Resources*; Central South University of Forestry and Technology: Changsha, China, 2011.
19. Windeisen, E.; Strobel, C.; Wegener, G. Chemical changes during the production of thermo-treated beech wood. *Wood Sci. Technol.* **2007**, *41*, 523–536. [[CrossRef](#)]
20. Meng, F.D.; Yu, Y.L.; Zhang, Y.M.; Yu, W.J.; Gao, J.M. Surface chemical composition analysis of heat-treated bamboo. *Appl. Surf. Sci.* **2016**, *371*, 383–390. [[CrossRef](#)]
21. Mohareb, A.; Sirmah, P.; Pétrissans, M.; Gérardin, P. Effect of heat treatment intensity on wood chemical composition and decay durability of *Pinus patula*. *Eur. J. Wood Wood Prod.* **2012**, *70*, 519–524. [[CrossRef](#)]
22. Hill, C.A.S. *Wood Modification: Chemical, Thermal and Other Processes*; John Wiley and Sons: Hoboken, NJ, USA, 2006.
23. Herrera, R.; Erdocia, X.; Llano-Ponte, R.; Labidi, J. Characterization of hydrothermally treated wood in relation to changes on its chemical composition and physical properties. *J. Anal. Appl. Pyrolysis* **2014**, *107*, 256–266. [[CrossRef](#)]
24. Yang, S.M.; Jiang, Z.H.; Ren, H.Q.; Fei, B.H.; Yao, W.B. Study status and development tendency of bamboo lignin. *Wood Process. Mach.* **2008**, *19*, 23–33.
25. Tjeerdsmä, B.F.; Militz, H. Chemical changes in hydrothermal treated wood: FTIR analysis of combined hydrothermal and dry heat-treated wood. *Holz Roh-Werkst.* **2005**, *63*, 102–111. [[CrossRef](#)]
26. Levan, S.L.; Ross, R.J.; Winandy, J.E. *Effects of Fire Retardant Chemicals on the Bending Properties of Wood at Elevated Temperatures*; U.S. Department of Agriculture, Forest Service, Forest Products Laboratory: Madison, WI, USA, 1990.
27. Winandy, J.E. *Effects of Fire Retardant Treatments After 18 Months of Exposure at 150 °F (66 °C)*; Res. Note FPL-RN-0264; U.S. Department of Agriculture, Forest Service, Forest Products Laboratory: Madison, WI, USA, 1995.
28. Inari, G.N.; Pétrissans, M.; Pétrissans, A.; Gérardin, P. Elemental composition of wood as a potential marker to evaluate heat treatment intensity. *Polym. Degrad. Stab.* **2009**, *94*, 365–368. [[CrossRef](#)]
29. Candelier, K.; Dumarcay, S.; Petrisans, A.; Desharnais, L.; Gerardin, P. Comparison of chemical composition and decay durability of heat treated;wood cured under different inert atmospheres: Nitrogen or vacuum. *Polym. Degrad. Stab.* **2013**, *98*, 677–681. [[CrossRef](#)]
30. Alén, R.; Kotilainen, R.; Zaman, A. Thermochemical behavior of Norway spruce (*Picea abies*) at 180–225 °C. *Wood Sci. Technol.* **2002**, *36*, 163–171. [[CrossRef](#)]
31. Inari, G.N.N.; Petrisans, M.; Lambert, J.; Ehrhardt, J.J.; Gérardin, P. XPS characterization of wood chemical composition after heat-treatment. *Surf. Interface Anal.* **2010**, *38*, 1336–1342. [[CrossRef](#)]

32. Nguila, I.G.; Steeve, M.; Stéphane, D.; Mathieu, P.; Philippe, G. Evidence of char formation during wood heat treatment by mild pyrolysis. *Polym. Degrad. Stab.* **2007**, *92*, 997–1002.
33. Fabbri, D.; Chiavari, G.; Prati, S.; Vassura, I.; Vangelista, M. Gas chromatography/mass spectrometric characterisation of pyrolysis/silylation products of glucose and cellulose. *Rapid Commun. Mass Spectrom.* **2010**, *16*, 2349–2355. [[CrossRef](#)]
34. Elaieb, M.; Candelier, K.; Pétrissans, A.; Dumarçay, S.; Gérardin, P.; Pétrissans, M. Heat treatment of Tunisian soft wood species: Effect on the durability, chemical modifications and mechanical properties. *Maderas Cienc. Tecnol.* **2015**, *17*, 699–710. [[CrossRef](#)]
35. Wang, X.; Ren, H. Comparative study of the photo-discoloration of moso bamboo (*Phyllostachys pubescens* Mazel) and two wood species. *Appl. Surf. Sci.* **2008**, *254*, 7029–7034. [[CrossRef](#)]
36. Wang, X.Q.; Ren, H.Q. Surface deterioration of moso bamboo (*Phyllostachys pubescens*) induced by exposure to artificial sunlight. *J. Wood Sci.* **2009**, *55*, 47–52. [[CrossRef](#)]
37. Pandey, K.K.; Pitman, A.J. FTIR studies of the changes in wood chemistry following decay by brown-rot and white-rot fungi. *Int. Biodeterior. Biodegrad.* **2003**, *52*, 151–160. [[CrossRef](#)]
38. Sun, B.; Liu, J.; Liu, S.; Yang, Q. Application of FT-NIR-DR and FT-IR-ATR spectroscopy to estimate the chemical composition of bamboo (*Neosinocalamus affinis* Keng). *Holzforschung* **2011**, *65*, 689–696. [[CrossRef](#)]
39. Tomak, E.D.; Topaloglu, E.; Gumuskaya, E.; Yildiz, U.C.; Ay, N. An FT-IR study of the changes in chemical composition of bamboo degraded by brown-rot fungi. *Int. Biodeterior. Biodegrad.* **2013**, *85*, 131–138. [[CrossRef](#)]
40. Carrasco, F.; Roy, C. Kinetic study of dilute-acid prehydrolysis of xylan-containing biomass. *Wood Sci. Technol.* **1992**, *26*, 189–208. [[CrossRef](#)]
41. Shangguan, W.; Gong, Y.; Zhao, R.; Ren, H. Effects of heat treatment on the properties of bamboo scrimber. *J. Wood Sci.* **2016**, *62*, 383–391. [[CrossRef](#)]
42. Bekhta, P.; Proszkyk, S.; Krystofia, T. Colour in short-term thermo-mechanically densified veneer of various wood species. *Eur. J. Wood Wood Prod.* **2014**, *72*, 785–797. [[CrossRef](#)]
43. Zhang, S.J.; Zhang, S.C.; Zhang, S.H. Effect of hot treatment on wood color of different treespecies. *For. Technol.* **1996**, *21*, 44–46.
44. Zhang, Y.M. *Study on the Effect of Color and Physical-Mechanical Properties for Heat-Treated Bamboo*; Chinese Academy of Forestry: Beijing, China, 2010.



© 2019 by the authors. Licensee MDPI, Basel, Switzerland. This article is an open access article distributed under the terms and conditions of the Creative Commons Attribution (CC BY) license (<http://creativecommons.org/licenses/by/4.0/>).

MDPI
St. Alban-Anlage 66
4052 Basel
Switzerland
Tel. +41 61 683 77 34
Fax +41 61 302 89 18
www.mdpi.com

Forests Editorial Office
E-mail: forests@mdpi.com
www.mdpi.com/journal/forests



MDPI
St. Alban-Anlage 66
4052 Basel
Switzerland

Tel: +41 61 683 77 34
Fax: +41 61 302 89 18

www.mdpi.com



ISBN 978-3-03928-822-9